Neural correlates of
perceptual decision and categorization:
Implications for basic science and clinical research

I
50 µV

Correlatos neuronais da decisão
percetual e categorização de estímulos visuais:
Implicações para a ciência básica e aplicação clínica

José Eduardo de Figueiredo Lima Rebola

2012

· U C ·

UNIVERSIDADE DE COIMBRA

Neural correlates of perceptual decision and categorization:

Implications for basic science and clinical research

Correlatos neuronais da decisão percetual e categorização de estímulos visuais:

Implicações para a ciência básica e aplicação clínica

José Eduardo de Figueiredo Lima Rebola

2012

Neural correlates of perceptual decision and categorization:

Implications for basic science and clinical research

Correlatos neuronais da decisão percetual e categorização de estímulos visuais:

Implicações para a ciência básica e aplicação clínica

José Eduardo de Figueiredo Lima Rebola

2012

Cover Design: José Rebola

Universidade de Coimbra

Faculdade de Medicina

Neural correlates of perceptual decision and categorization:

Implications for basic science and clinical research

Dissertation presented to obtain a Ph.D. degree in Biomedical Sciences at the
Faculty of Medicine of the University of Coimbra

Dissertação de Doutoramento apresentada à Faculdade de Medicina da Universidade de
Coimbra, para prestação de provas de Doutoramento em Ciências Biomédicas

José Eduardo de Figueiredo Lima Rebola

2012

Supervised by:

Miguel Castelo-Branco, Ph.D.
Jorge Manuel Miranda Dias, Ph.D.

Para a Gracinda , a Margarida, a Joana, a Lena, o Hildebrando e o Zé

"…e se aprendo sinto-me gente, que só é gente quem consegue ser assim."

in *Lídia*, Anaquim

Contents

Summary

Basic and Clinical Neuroscience are two mutually dependent multidisciplinary fields and it is the flow of information and knowledge between both that stimulates scientific advance. The work compiled in this thesis is yet another contribution for this intertwining, by mainly studying perceptual decision and visual categorization in the human brain while focusing on possible implications for the treatment of patients with Temporal Lobe Epilepsy or TLE.

However, the path here travelled starts with a pure methodological study that aims at improving the mapping of interictal spikes in TLE. In fact, it is only by understanding the limitations of currently available methodology that one can address the basic science questions which answers may also help circumvent clinical problems. We approach the mapping of interictal epileptiform discharges (IEDs), abnormal electrical events that happen between epileptic seizures, not by the development of a new tool but by the optimization and combination of the existent ones. The mapping of interictal spikes in epilepsy is an especially difficult topic because these events are comprised of fast propagating and non-independent activity. In the tested framework, we combined a blind source separation technique named Independent Component Analysis (ICA) with a source localization algorithm that retains advantages of both high and low-resolution current density reconstructions. In addition to simulated data through which we validated the approach, we investigated the clinical question of confirming the involvement of the frontal lobe in the TLE epileptic network. We obtained promising results. First, by successfully localizing and extracting the timecourse of activation for the simulated sources. Then, by confirming our clinical hypothesis.

The contribution of neuroimaging techniques in the field of epilepsy is not restricted to the mapping of interictal events, which is a crucial step in the

pre-operative work for epilepsy surgery. Another important application that bloomed in recent years is that of functional brain mapping. In short, a subject is placed inside a Magnetic Resonance Imaging (MRI) scanner, and performs a sequence of tasks while data is being collected. Functional Magnetic Resonance Imaging (fMRI) is a neuroimaging technique that explores magnetic properties of the changes in cerebral blood flow that indirectly accompanies neuronal activation. By statistically correlating these changes with task times, fMRI is able to identify the brain areas that underlie the execution of a given task, thereby, in its simplest version, assigning function to location. Thus, this technique has been used in epileptic patients mainly to map language, motor and memory functions in each individual, for a better planning of resection areas and projection of the post-operative impairment.

In this thesis, we propose that these mapping batteries should be augmented to include the mapping of high-level visual networks, namely category-preferring networks (face, body, object and place-preferring networks). This procedure can be particularly informative in posterior brain epilepsies, in which mapping the epileptic foci remains a difficult exercise because none of the available methods (reports of clinical manifestations, neurological examination, EEG assessment and neuropsychological evaluations) provides sufficient information about the area of onset, and the fast spread of paroxysms often produces mixed features of occipital, temporal and parietal related symptoms. Epileptic foci mapping has already been shown to benefit from such characterization using category-selective visual evoked potentials (the N170, elicited by face stimuli). Therefore it is natural to foresee the benefit of assessing this topic with the flexibility and improved spatial resolution of fMRI.

Despite almost two decades of fMRI studies concerning category-preferring visual networks, a standard methodology for their reliable and robust definition in each individual has not yet been obtained. The work here presented thus turns to cognitive neuroscience, hoping to contribute to a more thorough understanding of category-preferring networks which will allow

maximizing the benefit of using visual localizers in the pre-operative mapping of epilepsy.

A number of authors have already explored the impact of changing the stimuli, the duration, the contrasts and the statistical thresholds used in visual localizer studies. We opted for an emerging complementary approach, which attempts to integrate anatomical information with the consistent spatial relations to other category-preferring visual areas of different categories. We used anatomical information, spatial relations and response profiles across categories to disentangle face-preferring patches in the lateral occipitotemporal cortex, a region where many selective patches co-exist and inconsistent results have been reported. We identified a patch on the posterior continuation of the Superior Temporal Sulcus (STS) that is dissociable from the classically reported STS activation to faces.

Yet another way to build on the current knowledge concerning category-preferring networks is by assessing their modulation with endogenous decision-related rather than exogenous factors, i.e., manipulating task-goals and perceptual demands arising from top-down processes rather than relying on passive responses to changes in the simple features extracted by bottom-up processing. To this end, we designed visually ambiguous long-trial perceptual decision-making paradigms through the use of impoverished images. Our paradigm was based on the slow rotation of these images until the subject suddenly perceived the content occluded in it, allowing us to compare pre-perceptual and post-perceptual states on these networks. Furthermore, other features of experimental design (see Chapter 5) allowed us to separate sensory, decision-making and motor response processes.

Prior to the intended characterization of visual category-preferring networks with these tasks, and in order to establish parallels to other perceptual decision-making areas, we used the paradigms to clarify the neural correlates of the decision-making architecture. We mainly focused on the insular/frontal operculum complex, to which many different roles have been assigned. This is not without due cause. We managed to prove the existence of multiple sub-divisions inside this complex, with the anterior insula being related to evidence

accumulation, mid-insula/operculum being linked to decision-signaling and posterior insula participating in response execution.

The modulations of selectivity and other properties of category-preferring visual networks are reported in our last study (Chapter 6). We concluded that category-preferring networks also participate in the perception of their non-preferred categories, with the notable exceptions of the STS and the parahippocampal place area, which is selective for places and scenes. We functionally dissociated the Fusiform Face Area and Occipital Face Area, two of the most important nodes in the face-network, by evidencing a coupling of the latter to demanding visual search computations while the former had no such link, being involved in post-perception analysis.

Overall, we believe that this thesis, by exploring methodological, basic cognitive neuroscience, and brain mapping issues with a potential for clinical application in epilepsy, has contributed to shorten the gap that still exists between fundamental and applied biomedical science.

Resumo

As neurociências básica e clínica são dois campos multidisciplinares em que a troca recíproca de informação e conhecimento estimula o avanço científico. Ao estudar os correlatos neuronais da decisão percetual e categorização visual ao mesmo tempo que se foca em possíveis aplicações na epilepsia do lobo temporal, o trabalho compilado nesta tese contribui para o reforçar desta ligação entre os dois tópicos.

No entanto, o caminho aqui percorrido começa com um estudo essencialmente metodológico que visa melhorar o mapeamento das descargas interictais na epilepsia do lobo temporal. Na verdade, só através do entendimento das limitações da metodologia atual poderemos avaliar as questões de neurociência básica cujas respostas podem também contribuir para a resolução de problemas clínicos.

Abordamos o mapeamento das descargas interictais epileptiformes, descargas elétricas anormais que ocorrem entre crises epiléticas, não através do desenvolvimento de uma nova ferramenta mas sim pela combinação e otimização de duas já existentes.

Este mapeamento é particularmente difícil uma vez que os eventos interictais se caracterizam por atividade que se propaga rapidamente entre diferentes focos, gerando manifestações neuroelétricas no escalpe que não são independentes. Na abordagem testada, combinámos uma técnica de separação de fontes chamada Análise por Componentes Independentes com um algoritmo de localização de fontes que reúne as vantagens das reconstruções de densidade de corrente de alta e baixa resolução. Para além de simulações através das quais validámos a nossa abordagem, investigámos também como questão clínica o envolvimento do lobo frontal na rede epilética da epilepsia de lobo temporal. Os resultados obtidos foram prometedores: primeiro, pelo sucesso na localização e extração da trajetória temporal das fontes simuladas. Depois, pela confirmação da hipótese clínica em análise.

A contribuição das técnicas de neuroimagem no campo da epilepsia não se limita ao mapeamento das descargas interictais, um dos passos cruciais no trabalho que precede a intervenção cirúrgica. Outra aplicação essencial que tem florescido nos anos mais recentes diz respeito ao mapeamento cerebral funcional. Em resumo, neste procedimento o paciente é colocado num scanner de ressonância magnética e executa uma sequência de tarefas ao mesmo tempo que se recolhem dados. A ressonância magnética funcional é uma técnica de neuroimagem que explora as diferentes propriedades magnéticas do fluxo sanguíneo cerebral indiretamente ligado à atividade neuronal. Pela correlação estatística das diferenças nestes dados com os tempos de execução das tarefas, a ressonância magnética funcional consegue, na sua forma mais simples, identificar as áreas responsáveis pelas ditas tarefas, estabelecendo uma correspondência entre anatomia e função. Assim sendo, esta técnica é usada nos pacientes com epilepsia primariamente como forma de mapear as redes neuronais que estão na base de funções de linguagem, motoras e de memória, com vista a excluí-las se possível das áreas de ressecção e perceber realisticamente o impacto pós-operatório no perfil cognitivo do doente. Nesta tese, propomos que esta bateria de testes deveria ser aumentada pela inclusão do mapeamento das redes visuais de alto-nível, nomeadamente redes de processamento visual preferencial de categorias específicas, como caras, corpos, objetos e locais. A informação daqui proveniente será particularmente benéfica para a avaliação de epilepsias do córtex posterior, nas quais o mapeamento dos focos é ainda uma tarefa difícil dado que nenhum dos métodos disponíveis (relatórios de manifestações clínicas, exames neurológicos, avaliação neuropsicológica e EEG) proporciona informação suficiente acerca da zona de início, e a rápida propagação dos paroxismos frequentemente produz sintomas relacionados com os lobos temporal, occipital e parietal. Alguns autores reportaram já melhorias na localização do mapeamento dos focos epiléticos conseguidas através do uso de potenciais evocados específicos de uma categoria (N170, potencial evocado por faces). Deste modo, os benefícios associados ao uso destes paradigmas numa técnica de maior flexibilidade e superior resolução espacial como é o caso da ressonância magnética funcional são fáceis de prever.

Apesar de quase duas décadas de estudos de ressonância magnética funcional sobre as redes visuais que privilegiam o processamento de uma categoria principal, ainda não se estabeleceu uma metodologia comum para a sua definição fiável e robusta em cada pessoa. O trabalho aqui reportado debruça-se desta forma na neurociência cognitiva, na esperança de contribuir para um entendimento mais profundo de tais redes que permita maximizar o benefício associado ao uso de localizadores visuais na avaliação pré-operatória em pacientes com epilepsia.

O impacto de alterar os estímulos, a duração, o contraste e os limites estatísticos associados aos localizadores visuais já foi alvo de avaliação por outros grupos de investigação. Aqui, optámos por uma abordagem complementar, emergente na literatura, que se propõe a integrar a informação anatómica com as relações espaciais consistentes a outras áreas do mesmo foro visual de alto nível mas com respostas preferenciais para outras categorias.

Juntámos ainda a esta informação a caracterização dos perfis de resposta de cada região a várias categorias com vista à separação das áreas corticais preferenciais para faces que se incluem no cortex lateral occipitotemporal, uma região na qual se verifica uma multiplicidade de áreas com processamento preferencial e alguma inconsistência de resultados. Esta estratégia permitiu-nos identificar uma região na continuação do sulco temporal superior (STS) dissociável da zona de ativação para faces classicamente associada ao STS.

Uma outra maneira de expandir a caracterização das redes visuais preferenciais é pela modulação da sua atividade por fatores endógenos em oposição aos exógenos, i.e., pela manipulação das tarefas e requisitos percetuais em vez da simples quantificação do incremento ou decremento na atividade das regiões por reação passiva às mudanças nas propriedades básicas dos estímulos.

Com este intuito, construímos paradigmas de longa duração que induzem ambiguidade percetual por meio de imagens com informação limitada, como é o caso das imagens Mooney, constituídas por jogos de sombras a preto e branco. O nosso paradigma baseia-se na rotação lenta destas imagens até que o observador subitamente percebe o seu conteúdo. Este procedimento permite-nos a comparação dos períodos pré e pós-percetuais nestas redes visuais. Para

além disso, outras propriedades do nosso paradigma experimental (ver Capítulo 5) permitiram-nos separar os processos sensoriais e motores dos de pura decisão.

Previamente à caracterização pretendida das redes visuais preferenciais para categorias específicas, e para que se pudessem estabelecer paralelos com as restantes áreas envolvidas na decisão, usámos estes paradigmas para clarificar os correlatos neuronais da arquitetura cerebral para a tomada de decisões percetuais. O foco deste estudo foi no complexo insula/opérculo frontal, um dos módulos menos compreendidos, uma vez que já lhe foram afetas várias funções neste contexto. A origem desta variabilidade ficou patente nos nossos resultados, ao provarmos a existência de várias subdivisões neste complexo. Estabelecemos uma ligação da ínsula anterior à função de acumulador, enquanto que o opérculo frontal e a porção da ínsula que lhe é adjacente se relacionam com mecanismos mais puros de decisão e da sua sinalização à restante rede. A ínsula posterior acarreta funções relacionadas com a execução das respostas associadas à decisão.

A modulação da seletividade e outras propriedades dinâmicas das redes visuais preferenciais são reportadas no nosso último estudo (Capítulo 6). Concluímos que as redes preferenciais para categorias específicas também participam na perceção das suas categorias não-preferidas, com as importantes exceções do STS e da região do giro parahipocamapal preferencial para locais e cenas. Obtivemos também uma dissociação funcional entre dois dos nós mais importantes da rede de processamento de faces, a área de faces fusiforme e a área de faces occipital. Conseguimo-lo ao mostrar que esta última está particularmente envolvida em computações de busca visual em condições adversas e exigentes, enquanto que a primeira não é envolvida neste tipo processamento, favorecendo análises pós-percetuais.

Em suma, acreditamos que esta tese, por exploração da metodologia de EEG, neurociência cognitiva e tópicos de mapeamento cerebral com vista à aplicação clínica na epilepsia do lobo temporal, contribuiu para encurtar a distância que ainda existe entre a ciência biomédica aplicada e fundamental.

Agradecimentos

Um trabalho de doutoramento, por mais valioso que seja o doutorando, nunca é trabalho de uma pessoa só.

Mesmo que o fosse no percurso académico, não o seria no percurso de vida. Gostaria assim de expressar os meus sinceros agradecimentos a todas as pessoas que fizeram este percurso comigo.

O meu primeiro agradecimento vai naturalmente para o Professor Doutor Miguel Castelo-Branco. Expresso aqui a minha admiração e o meu reconhecimento por toda a sua trajetória e trabalho realizado. Sublinho de uma forma mais particular a sua sabedoria sem limites, visão, e perseguição apaixonada das questões científicas que lhe surgem tão naturalmente como o discurso. Por fim um sentido obrigado por ter sempre uma palavra nos momentos mais complicados.

Para o Professor Doutor Jorge Manuel Miranda Dias vai a minha elevada gratidão, admiração e estima. Sempre disponível e com um entusiasmo contagiante, sinto que a forma como a sua reputação precede a sua presença ilustra a tão almejada universalidade da universidade naquilo que ela tem de melhor.

Ao Doutor Francisco Sales, que embora não fazendo parte da orientação formal deste trabalho foi um dos grandes responsáveis para que ele acontecesse. Com ele percebi a real dimensão do estudo da epilepsia, e do impacto que ela tem no mundo real. Mais, aprendi-o num contexto no qual a competência, preocupação e dedicação são pedras basilares.

Ao Doutor José Pedro Marques, que foi o meu primeiro elo de ligação ao IBILI ainda enquanto bolseiro. Dos escassos meses de convivência tentei copiar-lhe o dinamismo, a seriedade na execução e a jovialidade no trato.

Os meus agradecimentos seguintes vão para os meus colegas de trabalho, a quem tenho a sorte de poder chamar amigos. Se houve uma rede que sempre me amparou em alguns desequilíbrios foi sem dúvida a teia de amizade que encontro diariamente quando chego ao IBILI e que ao longo destes seis anos se foi tornando sempre mais resistente.

Felizmente, são demasiados para que os possa enumerar aqui, mas devo uma palavra de redobrado apreço à Inês Almeida, Inês Bernardino, João Castelhano (companheiro na construção de estímulos Mooney), Filipa Júlio e Ana Pina.

Destaco com especial carinho as minhas duas cúmplices no Gabinete 72. Primeiro a Joana Sampaio, curiosamente com a mesma formação que eu, que me recebeu de sorriso rasgado e com quem um espaço de trabalho se transformou também num espaço de debate, discussão e cooperação. Dela herdei por osmose o pragmatismo, o entusiasmo e a coragem que sendo mais dela ia dando para os dois.

Depois, a Inês Violante, bioquímica por diploma e cativante por Natureza. As inúmeras horas passadas no gabinete pareceram mais leves graças ao seu companheirismo e mais produtivas graças ao seu exemplo. Posso hoje dizer com orgulho que sou melhor cientista e pessoa do que quando se juntou ao grupo.

Ao Carlos Ferreira, João Marques e Alda Pinto, pela simpatia e ajuda na recolha dos dados de ressonância, quer nas primeiras horas da manhã quer nas últimas da noite.

Finalmente, um especial obrigado a todos os meus amigos, pela alegria e partilha nos momentos bons, e apoio nos momentos menos bons. Se eu podia concluir o doutoramento sem vocês? Podia… mas não era a mesma coisa.

Por último, um imenso obrigado à minha família, omnipresente no meu bem-estar e a quem devo tudo ao longo de todos estes anos, não cinco mas trinta. De vocês herdei os valores e a tenacidade que fazem de mim o que sou.

Obrigado,

José Rebola

Foreword

The bridge between basic and clinical neuroscience has always been bidirectional. Since the early days of brain studies that patients with disorders and lesions have been a window to the understanding of brain complexity and functioning, as in the famous case of Phineas Gage in 1848. Complementarily, adding to the knowledge we have of mankind, one of the primary purposes of clinical neuroscience is the opportunity to help people with such disorders. The repeated crossing of this link between basic knowledge and potential clinical application earned it its name: translational neuroscience.

The work compiled in this thesis walks on both sides of this bridge, and advances on both ends strengthen the possibility that the bridge is crossed either way. One such way, moving from the clinical research to basic science is through the use of implanted electrodes or subdural grids and strips on epileptic patients. The primary use of this technique, known as electrocorticography, is the localization of epileptic foci. However, the possibility of using such a powerful tool for cognitive purposes provides an insight into temporal lobe organization that circumvents the current spatial and temporal limitations of brain imaging. A different way to cross the bridge, in the opposite direction, is that by taking advantage of the gathered knowledge on the organization and functional properties of the temporal lobe, using functional brain imaging, one can ultimately provide a less invasive mapping of the epileptic circuits, pre-operative planning and assessment of post-operative impairment for certain types of epilepsies.

The work here reported is an example of the growing intertwining between basic and clinical neuroscience, hoping that each day the sides grow closer and the bridge runs shorter.

Chapter 1

Introduction

The goal of this thesis is to advance in our understanding of perceptual decision and high level visual categorization in the human brain, exploring the relationships between fundamental cognitive neuroscience and potential application to clinical research with a focus on epilepsy.

This issue was approached from both the clinical and basic science sides so that ultimately the knowledge about category-selective processing and organization in the human temporal lobe may be used in the future to provide more reliable non-invasive mapping of epileptic foci, and help alleviate post-operative impact on cognitive functions. Such an ambitious long-term goal requires the integration of many fields of research and the achievement of numerous "checkpoints" in between.

In sum, the main goals of this thesis were two-fold:

- mapping of epileptic foci and sources in EEG, based on clinical physiological events such as abnormal interictal activity.

- functional mapping of category-processing networks within and beyond the temporal lobe, using decision based paradigms. The use of decision based paradigms emphasizes the parsing of cognitive components in categorization tasks and provides a basic science framework to understand neural mechanisms of perception and closure well beyond the visual cortex.

Due to this multidisciplinary and parallel nature of the herein proposed work, it is adequate, for sake of clarity, to provide an independent context to the basic and applied objectives of this thesis.

1.1 Clinical methodology: a new approach to interictal spike localization in epilepsy and the importance of localizers in post-operative assessment

Epilepsy is a common chronic neurological disorder that affects about 50 million people worldwide (Ngugi, Bottomley, Kleinschmidt, Sander, & Newton,

2010). It is characterized by recurrent seizures - which are a series of physiological and behavioural events in response to sudden, usually brief, excessive electrical discharges in a group of brain cells. Such seizures can vary from the briefest lapses of attention or muscle jerks, to severe and prolonged convulsions.

Usually, epilepsy is controlled, but not cured, with medication. However, over 30% of people with this disorder do not have seizure control even with the best available medications (Sander, 1993). Surgery is then one of the few options for people with focal epileptic seizures that remain resistant to treatment. The goal for these procedures is total control of epileptic seizures, although anticonvulsant medications may still be required.

Currently, the evaluation of candidates for epilepsy surgery is still a highly invasive procedure representing discomfort and even risk for the patients. However, the advances in neuroimaging, particularly electroencephalography (EEG) and functional magnetic resonance imaging (fMRI), paved the way for a more straightforward pre-surgical process, both on the localization of the epileptic foci and on the prediction of post-operative implications. In fact, neuroimaging has become mandatory in the work-up of epilepsy localization and the lateralization of seizure foci (Lai, Mak, Yung, Ho, & Hung, 2010), which should be stable and unilateral. For a review of the importance of EEG in epilepsy see (Noachtar & Rémi, 2009). The first step into such a localization procedure is usually the EEG, by assessing which electrode locations, and hence brain regions, show some electrical pattern of interest (Gotman, Kobayashi, Bagshaw, Bénar, & Dubeau, 2006).

A common next step (regarding localization) is invasive intracranial EEG usually by means of a strip or grid of electrodes on the putative foci region that record activity directly from the brain surface. This step aims to establish the precise location of the foci as well as to plan which areas of the brain are up for resection. One of the drawbacks of such an approach is the evident increased risk of turning one surgical procedure into two. Another disadvantage is the discomfort and limitations that patients experience during the twenty-four or

forty-eight hours bearing with intracranial electrodes. The third possible downside of this *modus operandi* is that the coverage of the implanted strip is limited (Zijlmans et al., 2007), and its location is naturally very dependent on the optimization of the first-step of the approach, the scalp EEG. In this manner, misplacement of the intracranial grid will yield only partial information, leaving possibly relevant brain sites of epileptic foci unrecorded.

Functional magnetic resonance imaging is a tool that can help overcome some of these problems. The advent of simultaneous EEG-fMRI recordings has made it possible to visualize the BOLD signal related to the interictal spikes. The combination of the superior temporal resolution of the EEG with the cubic millimetre spatial resolution of the fMRI circumvents their individual limitations. Naturally, being indirect measures of neuronal activity, the localization results of both techniques may not always coincide, and must still be interpreted with care. The pruning of methods of the interictal EEG analysis for improved epileptic source localization is the contribution of this thesis in the field of epilepsy. Following Chapter 2 that reviews the tools used, this work is presented in Chapter 3.

On the long run, the technical advances in EEG and fMRI will hopefully allow these techniques to replace the pre-operative invasive approach (Babiloni, 2003) and provide a detailed characterization of an individual's abnormal brain activity. In the meanwhile, it already provides a much more precise and robust planning of where to place the subdural strips or grids. Additionally, there are other important contributions of fMRI to the epilepsy surgery planning process. Sets of "localizers", which are cognitive tasks design to locate and isolate brain areas underlying the execution of a given task, can be used to map the individual's brain regions, by identifying and delineating areas that carry out language, motor and reading functions, as well as memory formation and recollection (Tharin & Golby, 2007). The more information is acquired on the functional divisions and boundaries of the subject's cortex, the more carefully surgeons can plan the areas to resect and realistically assess the post-operative implications of surgery, making sure which crucial areas for normal brain function will or not be affected. This procedure is surpassing the older Wada

test in many ways, which in a invasive manner practically shuts down a whole hemisphere in the brain in order to evaluate the other hemisphere (Baxendale, 2009; Pelletier, Sauerwein, Lepore, Saint-Amour, & Lassonde, 2007), with all the risks to the patient that such a procedure implies.

Current fMRI mapping approaches are basically used routinely for language and motor functions, but for other functions such as memory, despite promising results at a group level mapping is still hard to obtain reliable single subject level maps (Figueiredo et al., 2008). To circumvent these difficulties of achieving a robust mapping at the individual level therefore requires a prior focus on basic cognitive neuroscience.

In this thesis, we propose the extension of the existent localizer sets, as to include the evaluation of high-level visual networks, which are known to play a key role in the organization of the temporal lobe. As such, one of the goals of this thesis is to advance in the anatomical and functional characterization of neocortical visual category-preferring processing networks within and beyond the temporal lobe. Needless to say, the optimization of these localizers will lead to more robust delineation of the areas relevant to its associated tasks.

The herein presented work regarding localizer optimization and category-selective network topography is summarized in Chapter 4, with a specific focus on faces, bodies, places and general object categories.

Using visual localizers as a starting point, we moved on to study the way in which high-level categorization influences and is influenced by processes of perceptual decision-making.

1.2 Challenges in cognitive neuroscience: categorization and perceptual decision-making in the human brain

The topic of brain organization and specialization has both fascinated and divided neuroscientists for quite a long time, since the era of phrenology. The hypothesis that specific areas in the brain are devoted to specific processes was then proved for several tasks, from among which language and motor processes are the most historically striking (see (Feindel, 1982; Lazar & Mohr, 2011) for an excellent review of the work of Paul Broca and Wilder Penfield).

In the nineteen seventies and eighties the work of Damasio was important in highlighting visual areas involved in some forms of neurological agnosias, such as prosopagonosia, the inability to recognize faces (Damasio & Tranel, 1986; Tranel & Damasio, 1988; Tranel, Damasio, & Damasio, 1988). This agnosia was mostly present in patients with right hemispheric damage to the fusiform gyrus, lesional evidence that suggested the presence of face-selective regions in occipitotemporal cortex. In 1997, with the advent of fMRI, this hypothesis was confirmed and the issue of visual processing dedicated to specific categories was once again boosted by the identification of the Fusiform Face Area (FFA), an area seemingly dedicated to the processing of faces (Kanwisher, McDermott, & Chun, 1997). The following years were prolific on the investigation of brain areas devoted to the dominant processing of a single category, attempting to find the anatomical boundaries and functional divisions between areas processing these privileged categories. Our current understanding of visual processes shows that there are indeed specific networks (not merely areas) (Epstein, Parker, & Feiler, 2007; Hodzic, Kaas, Muckli, Stirn, & Singer, 2009; Ishai, Schmidt, & Boesiger, 2005) devoted to the processing of human faces, bodies, places and general objects. This doesn't go without controversy, with authors suggesting expertise in contrast to innate specialization (Gauthier & Bukach, 2007).

Such controversy can only be tackled by a detailed characterization of the functional properties of the nodes that build the category-selective networks. As mentioned earlier, by studying the contribution of specific areas to the process of visual categorization, we explore the organization of the visual areas within and beyond the temporal lobe. We may then integrate our knowledge with information on how the brain evolves from integrating points to bars, bars to contours, contours to shapes, shapes to objects, in sum, all the stages of visual processing (Kitcher, 1988; Marr, 1978).

In this work we provide a characterization of category-selective areas that minimizes dependency on low-level stimuli properties. This is a tenable strategy due to the invariance property, by which high level categorical selectivity is independent from low level stimulus properties. By developing paradigms of visual categorization under ambiguous conditions the impact of high-level endogenous factors such as selectivity, perceptual closure and holistic processing is favoured over low-level exogenous factors. Accordingly, the structure of this thesis also moves from top-down to bottom-up processing mechanisms.

In Chapter 5 we dissect current models of the decision architecture in the brain. A recent review (Heekeren, Marrett, & Ungerleider, 2008) defined perceptual decision-making as the process through which "humans effortlessly gather sensory evidence around them, interpret such evidence and choose adequate behaviour". As a corollary, it is also the process through which a subject, influenced by mood, assumptions or motivations can misperceive a stimulus as being another. Thus, only by placing category-selective visual processing within the ranks of the overall perception and decision-making architectures can one understand the special place category-selective areas have on the visual hierarchy, merging the low-level inputs of contour and shape analysis with the high-level influences of task goals, motivation, template generation and error assessment.

The deconstruction of perceptual closure beyond the temporal lobe, as well as the parsing of a complex cognitive operation into its components, are the topics of this chapter.

The following characterization of the functional properties of category-dedicated visual networks using ambiguous images is detailed in Chapter 6.

Finally, a summarized discussion and conclusions is presented in Chapter 7. At the light of these findings, the basic and clinical science links between the topics in the different chapters are revisited and future work and directions are pointed.

References

Babiloni, F. (2003). "The stone of madness" and the search for the cortical sources of brain diseases with non-invasive EEG techniques. *Clinical Neurophysiology*, *114*(10), 1775–1780.

Baxendale, S. (2009). The Wada test. *Current opinion in neurology*, *22*(2), 185–9.

Damasio, A. R., & Tranel, D. (1986). Disorders of recognition. In W. G. Bradley, R. B. Daroff, G. M. Fenichel, & C. D. Marsden (Eds.), *Neurology in clinical practice Vol 1 Principles of diagnosis and management* (pp. 179–187). Butterworth Heinemann Publishers, Boston, MA, US.

Epstein, R. a, Parker, W. E., & Feiler, A. M. (2007). Where am I now? Distinct roles for parahippocampal and retrosplenial cortices in place recognition. *The Journal of neuroscience: the official journal of the Society for Neuroscience*, *27*(23), 6141–9.

Feindel, W. (1982). The contributions of Wilder Penfield to the functional anatomy of the human brain. *Human Neurobiology*, *1*(4), 231–234.

Figueiredo, P., Santana, I., Teixeira, J., Cunha, C., Machado, E., Sales, F., Almeida, E., et al. (2008). Adaptive visual memory reorganization in right medial temporal lobe epilepsy. *Epilepsia*, *49*(8), 1395–408.

Gauthier, I., & Bukach, C. (2007). Should we reject the expertise hypothesis? *Cognition*, *103*(2), 322–30.

Gotman, J., Kobayashi, E., Bagshaw, A. P., Bénar, C.-G., & Dubeau, F. (2006). Combining EEG and fMRI: a multimodal tool for epilepsy research. *Journal of magnetic resonance imaging: JMRI*, *23*(6), 906–20.

Heekeren, H. R., Marrett, S., & Ungerleider, L. G. (2008). The neural systems that mediate human perceptual decision making. *Nature reviews. Neuroscience*, *9*(6), 467–79.

Hodzic, A., Kaas, A., Muckli, L., Stirn, A., & Singer, W. (2009). Distinct cortical networks for the detection and identification of human body. *NeuroImage*, *45*(4), 1264–71.

Ishai, A., Schmidt, C. F., & Boesiger, P. (2005). Face perception is mediated by a distributed cortical network. *Brain research bulletin*, *67*(1-2), 87–93.

Kanwisher, N., McDermott, J., & Chun, M. M. (1997). The fusiform face area: a module in human extrastriate cortex specialized for face perception. *The Journal of neuroscience: the official journal of the Society for Neuroscience*, *17*(11), 4302–11.

Kitcher, P. (1988). Marr's computational theory of vision. *Philosophy of Science*, *55*(1), 1–24.

Lai, V., Mak, H. K., Yung, A. W. Y., Ho, W. Y., & Hung, K. N. (2010). Neuroimaging techniques in epilepsy. *Hong Kong medical journal / Hong Kong Academy of Medicine*, *16*(4), 292–8.

Lazar, R. M., & Mohr, J. P. (2011). Revisiting the contributions of paul broca to the study of aphasia. *Neuropsychology Review*, *21*(3), 236–239.

Marr, D. (1978). Representing Visual Information - a computational approach. *Lectures on Mathematics in the Life Sciences*, *10*, 61–80.

Ngugi, A. K., Bottomley, C., Kleinschmidt, I., Sander, J. W., & Newton, C. R. (2010). Estimation of the burden of active and life-time epilepsy: a meta-analytic approach. *Epilepsia*, *51*(5), 883–90.

Noachtar, S., & Rémi, J. (2009). The role of EEG in epilepsy: a critical review. *Epilepsy & behavior: E&B*, *15*(1), 22–33.

Pelletier, I., Sauerwein, H. C., Lepore, F., Saint-Amour, D., & Lassonde, M. (2007). Non-invasive alternatives to the Wada test in the presurgical evaluation of language and memory functions in epilepsy patients. *Epileptic disorders: international epilepsy journal with videotape*, *9*(2), 111–26.

Sander, J. W. (1993). Some aspects of prognosis in the epilepsies: a review. *Epilepsia*, *34*(6), 1007–1016.

Tharin, S., & Golby, A. (2007). Functional brain mapping and its applications to neurosurgery. *Neurosurgery*, *60*(4 Suppl 2), 185–202.

Tranel, D., & Damasio, A. R. (1988). Non-conscious face recognition in patients with face agnosia. *Behavioural Brain Research*, *30*(3), 235–249.

Tranel, D., Damasio, A. R., & Damasio, H. (1988). Intact recognition of facial expression, gender, and age in patients with impaired recognition of face identity. *Neurology*. Lippincott Williams & Wilkins.

Zijlmans, M., Huiskamp, G., Hersevoort, M., Seppenwoolde, J.-H., van Huffelen, A. C., & Leijten, F. S. S. (2007). EEG-fMRI in the preoperative work-up for epilepsy surgery. *Brain: a journal of neurology*, *130*(Pt 9), 2343–53.

Chapter 2

Neuroscientific tools for brain mapping

This chapter briefly reviews the two main brain imaging tools used in this work: EEG and fMRI. This section is not meant as an extensive description of the methodology involved in these tools and their output data. Instead, it focuses primarily on the coupling between the neurophysiological properties of brain signals and the technology that enables their recording and analysis.

2.1 Electroencephalography (EEG)

Information transfer in the brain along axons and neurons occurs by electrical conduction of generated action potentials. Chemical mechanisms, in turn, allow the release of neurotransmissors that enable communication between neurons. These mechanisms rely on the balancing and unbalancing of ionic concentrations, and thus generate electrical currents (Schomer & Silva, 2010). If a large number of neurons in a given area are simultaneously active and communicating, then the generated electrical currents can combine and achieve dimensions that allow voltage fluctuations to be detectable at the skin surface (Olejniczak, 2006). The EEG is the brain electrical activity measured and recorded at the scalp by surface electrodes (see Figure 2.1).

In short, EEG activity therefore always reflects the summation of the synchronous activity of thousands or millions of neurons that have similar spatial orientation. Pyramidal neurons of the cortex are thought to produce most EEG signal because they are well-aligned and tend to fire together (Schomer & Silva, 2010). Because voltage fields fall off with the square of the distance, activity from deep sources is more difficult to detect than currents near the skull.

It must be emphasized that electrical activity picked up at the skin surface does not mimic the electrical fluctuations around the active neurons. Blur distortion occurs as electrical potentials generated in the brain are volume

conducted through brain, cerebral spinal fluid, the low-conductivity skull, and the scalp to the recording surface electrodes. In this manner, the surface EEG signal is a heavily spatially filtered version of the original signals (see Figure 2.2), which results in its chief disadvantage: poor spatial resolution (Le & Gevins, 1993). However, its temporal resolution is still unsurpassed, with current equipments capable of delivering samples faster than 5Khz and even up to 20Khz.
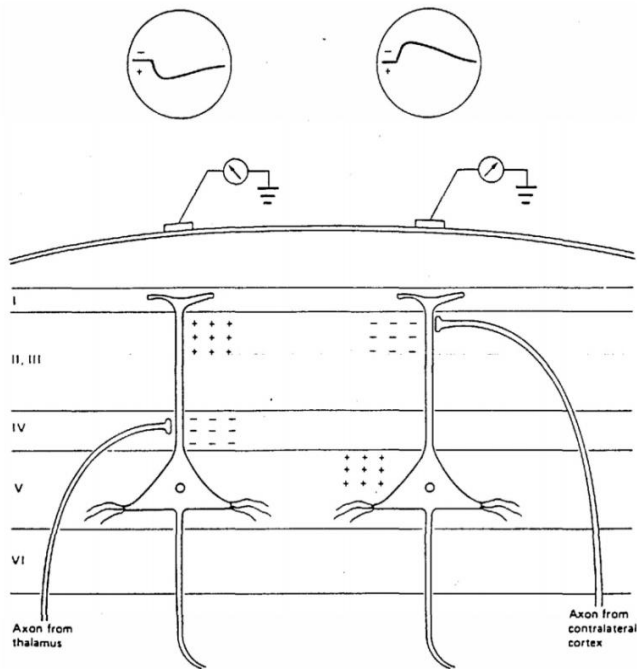

Figure 2.1 - Generation of extracellular voltage fields from graded synaptic activity. Relationship between polarity of surface potentials and site of dendritic postsynaptic potentials. Reproduced from (Olejniczak, 2006)

This trade-off of excellent temporal resolution vs poor spatial resolution makes the EEG a perfect tool to analyse the dynamics of neuronal activity or detecting changes and abnormal electrical patterns, albeit unable to precisely pinpoint where in the cortex are the sources that generate this activity.

This problem of finding the cortical location of a recorded electrical scalp signal is called source localization or inverse problem. Such type of problem is called an ill-posed problem, which means that for the same recorded activity there is an infinite combination of electrical sources that could have generated it (Lopes, 2010). A similar problem would be trying to perform a scene reconstruction form a single photo. These problems can only be solved with additional information, assumptions or constraints. In EEG, these are still open issues to which this work hopes to contribute in the particular field of epilepsy.

Since its first days, EEG has revolutionized and remained an invaluable tool on the diagnosis and understanding of epilepsy (Wiedemann, 1941). In a condition which hallmarks are abnormal electric discharges in the brain, this technique emerges naturally for the characterization of the dynamics, propagation and even attempted prediction of ictal (seizures) and interictal (between seizures) events. The clinical evaluation of a presumed epileptic individual without the use of the EEG is almost unthinkable (Schomer & Silva, 2010).
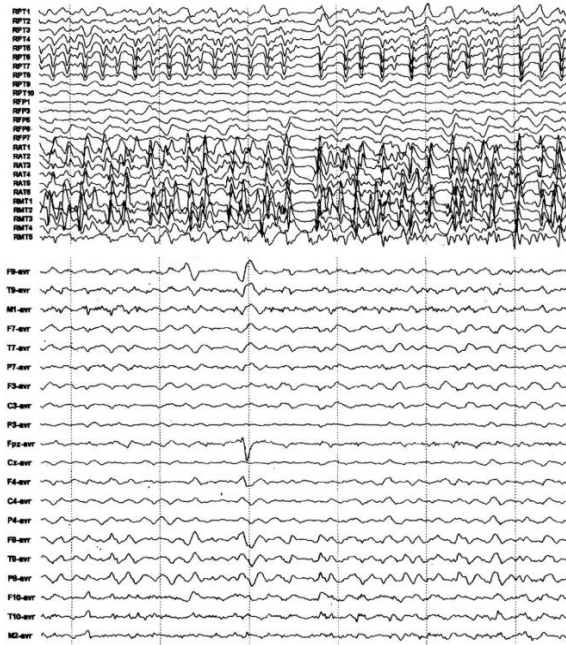
Figure 2.2 - Simultaneous intracranial and scalp EEG recording of a temporal lobe seizure. The channels in the upper third of the picture represent intracranial contacts, whereas the ones in the lower part represent the scalp contacts. The intracranial recording appears to be generally more regular and of higher amplitude then the scalp one, which appears to be attenuated. Reproduced from (Olejniczak, 2006)

However, not every problem is solved by the use of EEG. The need to establish the precise foci of the paroxysmal epileptic activity, combined with the unpredictable and unreplicable nature of ictal or interictal EEG recordings makes the evaluation very dependent on the quality of EEG source localization and rejection of artifacts. The work described in Chapter 3 is centered on these two sensitive matters.

2.2 Functional Magnetic Resonance Imaging (fMRI)

Functional magnetic resonance imaging (fMRI), just like the EEG, is a technique that indirectly measures brain **activity** and should not be confused with standard MRI, which is a technique tailored for the study and assessment of brain **structure.**
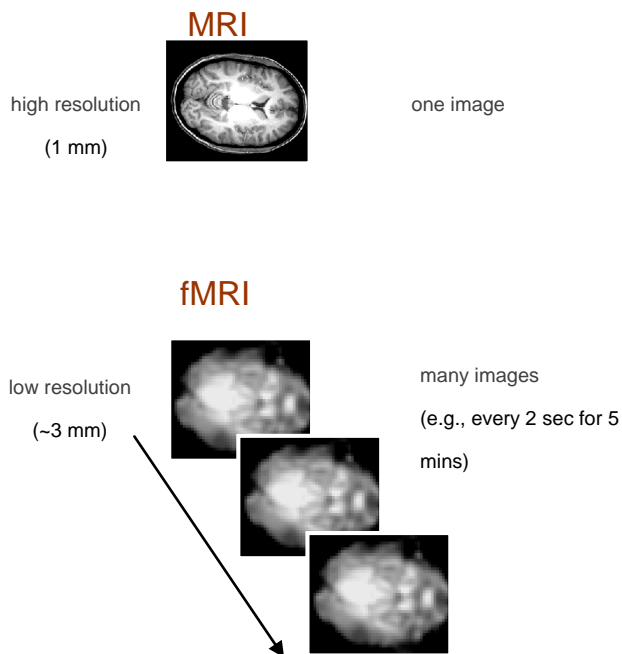
MRI

high resolution

(1 mm)

one image

fMRI

low resolution

(~3 mm)

many images

(e.g., every 2 sec for 5

mins)

Figure 2.3 – Comparison between structural MRI and fMRI data. While MRI provides a single "static" output with high-resolution information on brain structures and tissue types, fMRI consists of a sequence of lower-resolution volumes (sets of images) acquired across time. Changes between these volumes in brain regions relate to the blood flow that accompanies neuronal activation and thus can be related to the tasks being executed.

Briefly, the so-called Blood Oxygen Level Dependent (BOLD) signal that allows this imaging explores neuronal properties other than electrical currents,

and was described in the seminal publication of Ogawa in 1990 (Ogawa, Lee, Kay, & Tank, 1990) . The principle behind it can be roughly summarized as follows:

Neuronal activity in the brain and the consequent metabolic changes in neurones and glia that accompany neurotransmitter release are energy-requiring.

To meet this increased metabolic demand, neuronal activation is accompanied by increased blood flow (Roy & Sherrington, 1890). This was demonstrated in 1890 by physiologist Charles Sherrington, who also observed that the increase in total oxygen delivery exceeded the increase in oxygen utilization.

Thus, a surplus of oxygenated blood surrounds the active areas of the brain some seconds after its activation. The time between the consumption of energy due to neuronal activation and this surplus of oxygen is called the haemodynamic delay.

The key factor behind this technique is that oxygenated and deoxygenated haemoglobin have different magnetic properties, the latter being paramagnetic and contributing to a quicker loss of transversal magnetization (T2). The particular type of incremental signal loss due to increase in local field heterogeneity is called the T2*. This is reflected in the acquired fMRI signal, which is lower for desoxyhemoglobin (Ogawa & Lee, 1990; Ogawa, Lee, Nayak, & Glynn, 1990). Thus, by repeatedly scanning the brain of a subject performing a task, and inspecting changes in the signal that are correlated with task times (taking into account the haemodynamic delay), one can identify the areas responsible for executing such a task. Figure 2.4 illustrates this summary.
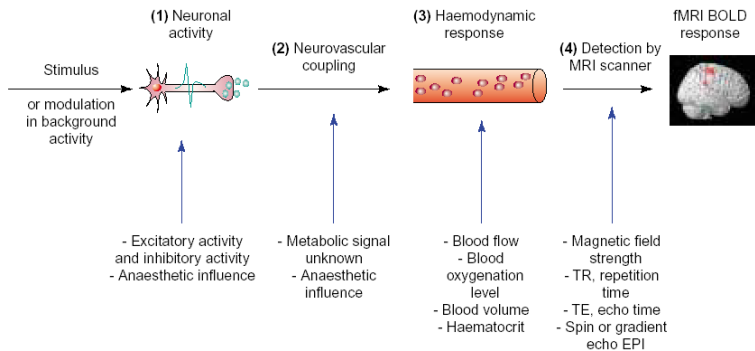
Figure 2.4 - The BOLD signal has several constituents: (1) the neuronal response to a stimulus or background modulation; (2) the complex relationship between neuronal activity and triggering a haemodynamic response (termed neurovascular coupling); (3) the haemodynamic response itself; and (4) the way in which this response is detected by an MRI scanner.
Reproduced from (Arthurs & Boniface, 2002)

The temporal resolution of fMRI is inherently limited by the slow blood flow response it depends on. Unlike EEG, fMRI cannot uncover the dynamics of mental activity on the sub-millisecond timescale on which neurons operate. However, relative to other brain imaging techniques, fMRI has unequalled spatial resolution – using 7 Tesla scanners activity can be mapped down to 1mm. fMRI is therefore suited to answer questions on which areas perform a cognitive, sensory or motor task, pinpointing their location but falling short on the subtle temporal dynamics of their activations.
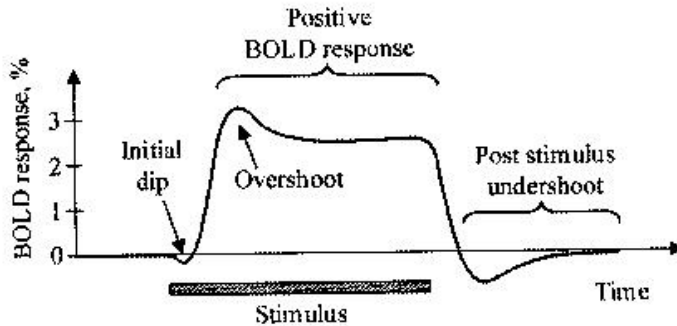
Figure 2.5 - Schematic representation of the common features of the fMRI BOLD response to a period of neuronal stimulation. During the first epoch a small negative 'initial dip' may be observed. Subsequently, a more robust 'positive BOLD response' is observed. Following cessation of the stimulus a return to baseline accompanied by a 'post-stimulus undershoot' is often seen. Taken from (Hoge & Pike, 2004)

A multitude of paradigms has been used in fMRI, which reflects the flexibility in defining stimulus presentation protocols and analysis pipelines for this technique.

The most fundamental paradigms in experimental design explored in this thesis are the block and event-related designs.

Blocked paradigms employ time-integrated averaging procedures and were the first approach to be employed in fMRI studies (Bandettini, Wong, Hinks, Tikofsky, & Hyde, 1992; Kwong et al., 1992). In this approach a series of trials in one condition is presented during a discrete epoch of time that typically ranges from 16s to a minute, which generates a sustained BOLD response. The signal acquired during one condition is then compared to other blocks involving different task conditions, which are typically 'tightly' matched, differing only on the factor of interest. Such a comparison is called a contrast. For example, regarding localizers, to study visual face processing and isolate the areas specifically active for faces, one compares (contrasts) the viewing of face

images with the viewing of objects or landscapes, thereby eliminating all response components related to common visual processing.

The use of 'loose' task comparisons (e.g., task against rest or fixation) is also often used to assess overall quality and identifying entire networks of regions underlying a given task (Donaldson & Buckner, 2004).

One can also study with fMRI the activation elicited by a task by measuring single events rather than 'blocked ones' (that have in general multiple associated events), in what is commonly known as event-related paradigms. It has been shown that even events as brief as 34 ms elicits a measurable fMRI response (Rosen, Buckner, & Dale, 1998). If events are widely spaced in time then the BOLD signal can rise and recover to baseline without interference from the following or previous event.

Event-related paradigms are especially useful when the condition is user-defined (by a self driven response, for instance) or when the events are unpredictable such as in simultaneous EEG-fMRI for the study of interictal epileptic events. In this latter case, the EEG spike times are the model that is then used to look for meaningful related activations in the fMRI data. Another advantage of the event related paradigm is that one can study isolated trials and the cognitive/motor responses for each event.
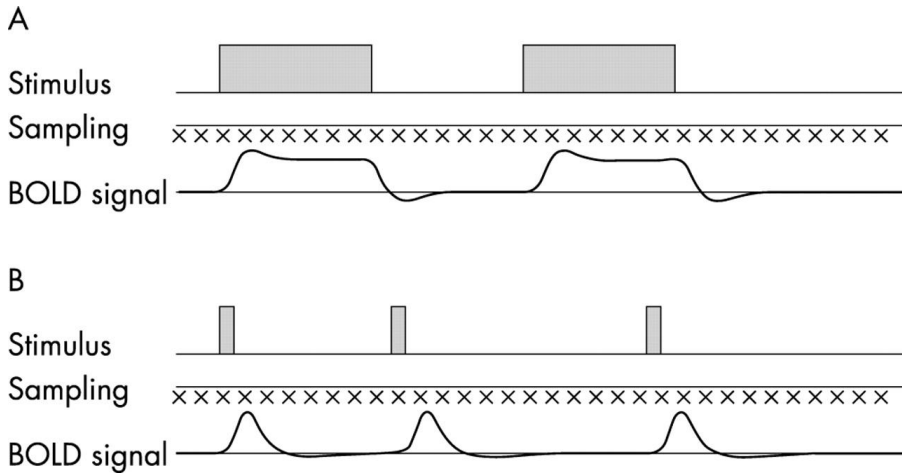
A

Stimulus

Sampling ×××××××××××××××××××××××××××××××××××××××

BOLD signal

B

Stimulus

Sampling ×××××××××××××××××××××××××××××××××××××××

BOLD signal

Figure 2.6 - Schematic representation of a block design functional magnetic resonance imaging (fMRI) paradigm (A) and an event related fMRI paradigm (B). For the block design a relatively long (30 second) stimulation period is alternated with a control period. For the event related design a brief stimulus period is used, which can either be periodic or randomized. In both cases volumes of data (indicated by the crosses) are collected continuously, typically with a repeat time of three to five seconds.
Reproduced from (Matthews & Jezzard, 2004)

Due to the use of both blocked and event-related designs in this thesis, the singularities of the chosen methods are further detailed in the chapters that use fMRI for data collection.

References

Arthurs, O. J., & Boniface, S. (2002). How well do we understand the neural origins of the fMRI BOLD signal? *Trends in neurosciences*, *25*(1), 27–31.

Bandettini, P. A., Wong, E. C., Hinks, R. S., Tikofsky, R. S., & Hyde, J. S. (1992). Time course of EPI of human brain function during task activation. *Magnetic Resonance in Medicine*, *25*(2), 390–397.

Donaldson, D. I., Buckner, R. L., Effective paradigm design. In Jezzard, P., Matthews, P. M., Smith, S. M., Functional MRI: an introduction to methods. New York: Oxford University Press, 2004 177-196.

Hoge, R. D., Pike, B. G., Quantitative measurement using fMRI. In Jezzard, P., Matthews, P. M., Smith, S. M., Functional MRI: an introduction to methods. New York: Oxford University Press, 2004 159-176.

Kwong, K. K., Belliveau, J. W., Chesler, D. A., Goldberg, I. E., Weisskoff, R. M., Poncelet, B. P., Kennedy, D. N., et al. (1992). Dynamic magnetic resonance imaging of human brain activity during primary sensory stimulation. *Proceedings of the National Academy of Sciences of the United States of America*, *89*(12), 5675–5679.

Le, J., & Gevins, a. (1993). Method to reduce blur distortion from EEG's using a realistic head model. *IEEE transactions on bio-medical engineering*, *40*(6), 517–28.

Lopes, F. (2010). *EEG - fMRI*. (C. Mulert & L. Lemieux, Eds.) (pp. 19–39). Berlin, Heidelberg: Springer Berlin Heidelberg.

Matthews, P. M., & Jezzard, P. (2004). Functional magnetic resonance imaging. *Journal of neurology, neurosurgery, and psychiatry*, *75*(1), 6–12.

Ogawa, S., & Lee, T. M. (1990). Magnetic resonance imaging of blood vessels at high fields: in vivo and in vitro measurements and image simulation. *Magnetic Resonance in Medicine*, *16*(1), 9–18.

Ogawa, S., Lee, T. M., Kay, a R., & Tank, D. W. (1990). Brain magnetic resonance imaging with contrast dependent on blood oxygenation. *Proceedings of the National Academy of Sciences of the United States of America*, *87*(24), 9868–72.

Ogawa, S., Lee, T. M., Nayak, A. S., & Glynn, P. (1990). Oxygenation-sensitive contrast in magnetic resonance image of rodent brain at high magnetic fields. *Magnetic Resonance in Medicine*, *14*(1), 68–78.

Olejniczak, P. (2006). Neurophysiologic basis of EEG. *Journal of clinical neurophysiology: official publication of the American Electroencephalographic Society*, *23*(3), 186–9.

Rosen, B. R., Buckner, R. L., & Dale, a M. (1998). Event-related functional MRI: past, present, and future. *Proceedings of the National Academy of Sciences of the United States of America*, *95*(3), 773–80.

Roy, C. S., & Sherrington, C. S., (1890). On the regulation of the blood supply of the brain. *Journal of Physiology*, 11(1-2), 85-108

Schomer, D. L., & Silva, F. L. D. (2010). *Niedermeyer's Electroencephalography: Basic Principles, Clinical Applications, and Related Fields.* (Donald L Schomer & Fernando Lopes Da Silva, Eds.)*Book* (Vol. 1, p. 1296). Lippincott Williams & Wilkins.

Wiedemann, H. R. (1941). HANS BERGER. *The Lancet*, *153*(6171), 705.

Chapter 3

A new approach to interictal spike localization in epilepsy

3.1 Open issues and motivation for the study

EEG source localization (ESL) is a discipline that aims to localize the sources of electric currents within the brain that give rise to the recorded potential fields at the scalp (Plummer, Harvey, & Cook, 2008). It is almost as old as the science of EEG itself (Jayakar, Duchowny, Resnick, & Alvarez, 1991) but has been "geared up" in the last few decades by computer-assisted source modelling techniques on the back of digital EEG technology.

One of the goals of this thesis is a new approach to the mapping of epileptic foci and sources in EEG, based on clinical physiological events such as abnormal interictal activity.

Our approach is not so much concerned with the development of new tools as it is with the optimization and innovative use of the existent ones. Specifically, we combine Independent Component Analysis, a tool initially used as an artifact rejection technique, with a source localization algorithm based on the principle of Current Density Reconstruction (see 3.2-Methods).

We used this methodological framework not only as a proof of concept but also to confirm the clinical hypothesis that frontal lobe areas are, among others, included in the network of the Temporal Lobe epilepsy (TLE) (Spencer, 2002; Takaya et al., 2006). This involvement of the frontal lobe in TLE was suggested in the literature (Adam, Saint-Hilaire, & Richer, 1994; Lieb, Dasheiff, Engel, & Genton, 1991; Shin, Hong, Tae, & Kim, 2002) and further supported by unpublished data at our local Epilepsy Monitoring Unit by some patients' performance patterns on neuropsychological assessment tests such as WCST and Stroop tests, seizure semiological analyses and SPECT / PET studies.

As mentioned in Chapter 1, the first and crucial step in epilepsy surgery planning is to pinpoint the epileptic foci. Thus, achieving the best possible result in ESL is of particular importance when dealing with epilepsy. To this end, validation of our approach with clinical data in addition to prior guiding simulations is of utmost relevance.

One should note that although history has proven electroencephalography to be the most important tool in the surgical planning of medically refractive epilepsy so far, this by no means implies that all problems in the field of epilepsy are currently solved. In fact, our current pathophysiological understanding of the cellular, molecular and systems level mechanisms by which abnormal activity patterns develop and propagate in epilepsy is largely incomplete (Chang & Lowenstein, 2003).

Epileptic seizures are of unpredictable nature and are comprised of very complex patterns which still elude the most experienced researchers/clinicians in this area. Therefore, a common informative alternative to characterize epileptic patterns is the topography of interictal epileptiform discharges (IEDs), electrical abnormalities or paroxysms which are likely to occur between seizures in a routine EEG examination of a potential epileptic patient given a sufficient but not excessively prolonged time window (e.g. thirty minutes).
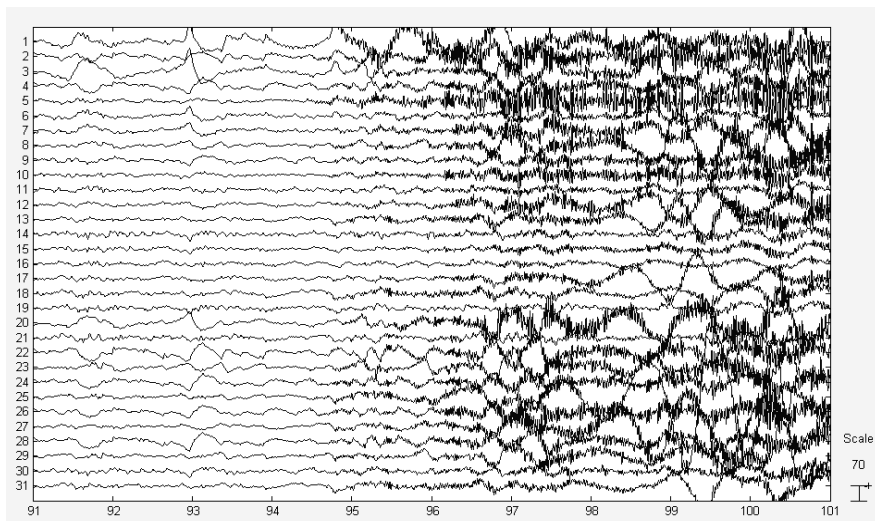

Figure 3.1 - EEG recording of a patient with Temporal Lobe Epilepsy. Note the pronounced increase in activity and complexity after seizure onset and its erratic (lack of) pattern

IEDs are often evaluated for the identification and classification of epileptic syndromes (Torre et al., 1999), since they not share the severity of seizures but are nonetheless distinguishable from background activity. Furthermore, IEDs and seizures seem to share at least in part the same networks and circuitry (Dzhala & Staley, 2003), which sets the grounds for mapping and studying their dynamics.
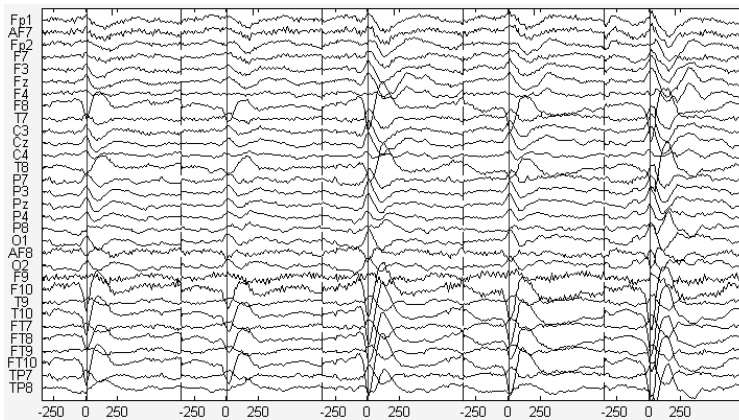

Figure 3.2 – Epoched (segmented) interictal electric discharges (IED) of a patient with Temporal Lobe Epilepsy. The topographic consistent pattern (albeit different amplitudes) of the recorded paroxysms, in addition to being contained events in time separable from the background activity, make them an easier subject of analysis than the ictal EEG.

Simpler than seizures, IEDs nonetheless have a quite complex spatiotemporal pattern. As previous findings suggest that IEDs consist most likely of cortical and subcortical network joint activations rather than local events restricted to one area (Spencer, 2002), some approximations in source localization algorithms that have been used to characterize these events in the

past (Merlet & Gotman, 1999; Pataraia, Lindinger, Deecke, Mayer, & Baumgartner, 2005) may not be correctly applied.

Taking these premises together, and given the lack of a single flawless tool for source localization and/or EEG analysis which presents robust and valid results under all circumstances, we propose here a new methodological framework to analyse the problem of characterizing complex and propagating IED patterns. Our proposed approach attempts to take the best out of two powerful EEG analysis tools and combine them for improved reliability of the results. Those tools are Independent Component Analysis (ICA) (Comon, 1994) and a Current Density Reconstruction algorithm called Standardized Shrinking Loreta Focuss (SSLOFO) (Liu et al., 2005). The combination of ICA with other techniques has been a successfully employed strategy in the past (Jung, Kim, Kim, & Chung, 2005; Kobayashi, Akiyama, Nakahori, Yoshinaga, & Gotman, 2002a, 2002b).

We tested our framework by validating it with simulations and then applied it to clinical data. With the simulations, we meet our goal of improving the methods of source localization in EEG, particularly in these disadvantageous conditions of contaminated recordings and the inability to systematically reproduce the events of interest as in evoked or event-related potentials. Also, through the use of real clinical data, we answer the specific clinical neuroscience question of assessing the involvement of the Frontal Lobe in TLE.

3.2 Methods

3.2.1 Standard Shrinking Loreta Focuss – SSLOFO

Two fundamental problems exist in the practice of EEG source localization (ESL)—forward and inverse. The forward problem is the problem of calculating the potentials at the skin surface, with the sources known, by

modelling the compartments through which the electrical activity propagates. Forward models range from simple (a single spherical shell models the brain surface) to complex (a four-layered realistic model, its compartments segmented from the patient's MRI scan, modelling the brain, cerebrospinal fluid, skull, and scalp surfaces) (Darvas, Pantazis, Kucukaltun-Yildirim, & Leahy, 2004). Thus, for a specific electrical source, the forward model will enable the computation of a specific potential field at its surface (Wilson & Bayley, 1950) and will provide a "unique" solution. The inverse problem, by contrast, has no unique solution. That is, an infinite number of source permutations can, in theory, explain a specific potential field recorded at the surface (Helmholtz, 1853). The inverse problem is made soluble by the incorporation of mathematical constraints into inverse modelling algorithms. The two major inverse modelling alternatives are the dipolar approach and current density reconstruction methods.

In the dipolar approach to the inverse problem, the researcher assumes a priori that the features in the EEG or evoked potential are generated by one or a small number of intracranial dipole sources, following the principle that a coherent activation of a large number of pyramidal cells in a small area of cortex can be modelled as an equivalent current dipole. The current dipole is therefore the basic element used to represent neural activation in these EEG-based inverse methods (Darvas et al., 2004). However, the simplifications that enable the dipolar approach are often not valid. For instance, one must know the number of active areas *a priori* to effectively represent them through dipole approximations, which is not always the case. Furthermore, if the active area is too large, then the validity of the dipolar approach is compromised.
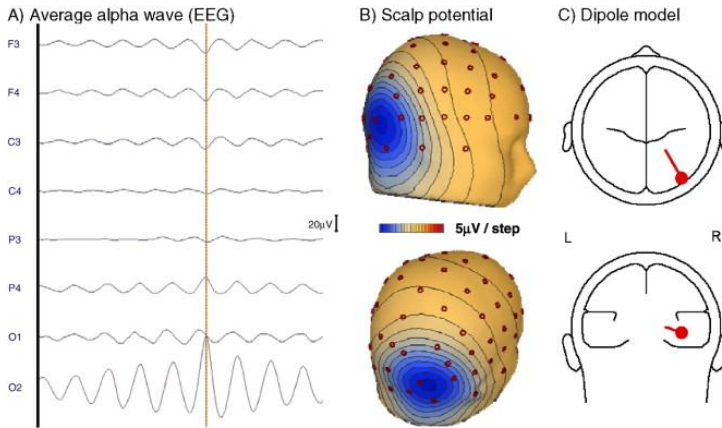
Figure 3.3 - An example of the equivalent dipole approach. In A) we can see the vertical line signalling the sample chosen for source localization (in this case the authors intended to map the generators of the alpha rhythm). The image in B) depicts the scalp potential across electrodes. Finally, C) illustrates the equivalent dipole solution, showing the location and direction that maximally explains the topography on the scalp with one source only. As a downside, if the number of assumed active regions does not correspond to the real number of active regions then this solution may be very inaccurate.
Taken from (Mandelkow et al., 2007)

In contrast to dipole modelling strategies, Current Density Reconstruction (CDR) methods make no assumptions on the number of dipoles used to solve the inverse problem. Instead, the working premise is that multiple sources may be simultaneously active across multiple locations at a given instant in time. The predefined solution space (be it the whole brain volume or just the cortical volume) is split into multiple points, each point representing a "minidipole," fixed in space but free to assume any orientation and strength. Due to the enormous number of permutations that stem from such mini-dipole networks, all offering a theoretically plausible explanation for the measured EEG signal, constraints need to be applied to achieve a unique solution. Just as volume compartment and boundary conditions distinguish one forward model from the next, constraint conditions distinguish one inverse model from the next.
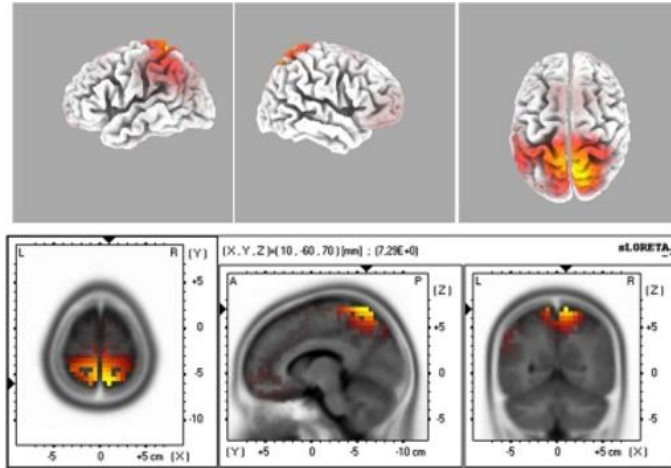
Figure 3.4 – Source localization output for the sLORETA, one of the best-known current density reconstruction algorithms. It is readily seen that the solution is not consisted of a single source. Instead, each point in the source space has a weighted contribution to the measured potential across the electrodes, higher (warmer colors) for the regions that are thought to contribute the most. With this approach the number of active areas does not need to be defined *a priori*.
Taken from (Ozgoren, Bayazit, Gokmen, & Oniz, 2010)

One possible way to divide CDR methods is through the resolution of the source space. Both high and low-resolution methods have their individual strengths and weaknesses. However, SSLOFO emerged as a novel current distribution reconstruction algorithm that combines the advantages of both low and high-resolution methods in an automated fashion. Low-resolution methods such as LORETA (Pascual-Marqui, Michel, & Lehmann, 1994) and sLORETA (Pascual-Marqui, 2002) can estimate the area of primary activity but suffer from poor spatial resolution. These inverse methods are useful in reconstructing some simple source configurations but become inefficient for large numbers of sources not restricted to a given area. The large point spread functions of these

techniques can make it difficult to discern multiple active regions. On the other end, high-resolution methods such as FOCUSS (Gorodnitsky & Rao, 1997) are able to localize focal sources which relate to some specific diseases or functions of the brain, but these methods are not generally robust to distributed activity and may generate "over-focal" results.

Starting from a very smooth estimate, given by sLORETA, SSLOFO improves the spatial resolution using the recursive strategy of FOCUSS. Standardization is applied in order to keep the estimate localized on regions with significant activity, although multiple regions may emerge and the source space is automatically adjusted every iteration. This somewhat adaptive feature extracts regions of dominant activity while simultaneously localizing multiple sources within those regions. For complete details on this method please refer to Liu et al (Liu et al., 2005).

3.2.2 Independent Component Analysis – ICA

It is well known that the scalp EEG is the sum of different activities arising from their respective neural generators in the brain. Furthermore, some weak or deeper sources might be masked by stronger or more superficial activity, making the EEG 'blind' to the aforementioned sources. As such, rather than carrying out an analysis on the sum of all these ongoing activities, the ideal first step would be the decomposition of the EEG into its separate components in order to carry out a singular analysis for each of the components. This can be done with ICA, a methodology of Blind Source Separation, originally proposed by Pierre Comon in 1994 (Comon, 1994). ICA decomposes a linear mixture of independent signals into its original signals, given there are more sensors than sources and that the sources have non-Gaussian distributions (which are plausible assumptions for most of the events under study (Makeig, Bell, Jung, & Sejnowski, 1996)).

A typical comparison used to understand the reasoning behind ICA is to imagine ten people (sources) speaking at the same time in different places inside

a room, the so-called cocktail-party problem (Brown, Yamada, & Sejnowski, 2001). Providing that the people stand still and that there are at least ten recorders (sensors) in the room walls, what the algorithm CAN do is to isolate the speech of each person. What the algorithm CANNOT do is tell us where the people are inside the room. However, it will output the weight of each person's voice in each of the sensors, an important starting point for the subsequent location purposes.
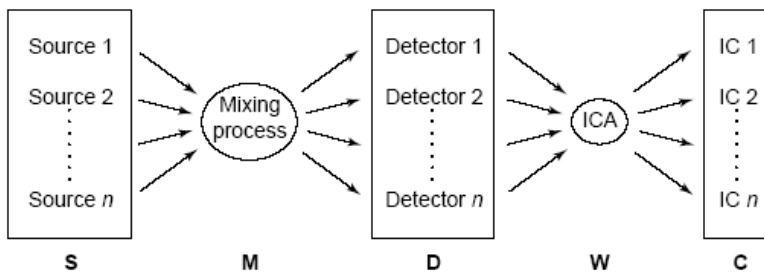

Figure 3.5 The independent component analysis model. *n* hypothetical source signals (S) are mixed linearly and instantaneously by an unknown mixing process (M). Mixed sources are recorded by a set of detectors (D). Independent component analysis (ICA) (W) transforms the detected signals into independent components (IC) (C). If the assumptions of the model are not violated, the independent components will be the original sources except that scale, sign, and order will not be preserved. The number of sources is assumed to be equal to or less than the number of detectors. Taken from (Brown et al., 2001)

Moving back to the EEG real-life situation, once the ICA algorithm is run, a number (typically the number of sensors) of scalp maps or patterns along with its corresponding time courses are obtained. Once again, ICA does not perform source localization. It simple yields a number of scalp maps, where each map is the projection into the scalp of the active cortical patches that build each component. Thus, each component is not necessarily comprised of a

single generator. If two (or more) distinct cortical areas share the same temporal activation they will build up one component and therefore one spatial map. (This would be equivalent to having two people in the room reading exactly the same speech. They would be indistinguishable to the algorithm because these two people are not "independent").

ICA has proven to perform well at separating signals arising from different brain processes, artifacts and noise (Onton, Westerfield, Townsend, & Makeig, 2006). However, IEDs are a very particular kind of events, since they are likely to involve different cortical areas with overlapping or coherent activations and similar waveforms. Thus, an important question arises: how will ICA behave when the required assumptions do not hold true, i.e., when the signals have similar waveforms and are not truly independent? Both spatial and temporal information will be affected: (*i*) the topographies of the components will be a mixture of two or more topographies generated by each of the involved sources; (*ii*) the time courses will be unreliable (some are related to the overlap between signals whilst others relate to the difference of the individual time courses).

The problem is better understood with the help of the following example:

Consider three clearly spaced dipolar sources with the same waveform, the only difference being a temporal delay between them (Figure 3.6a and 3.6b).

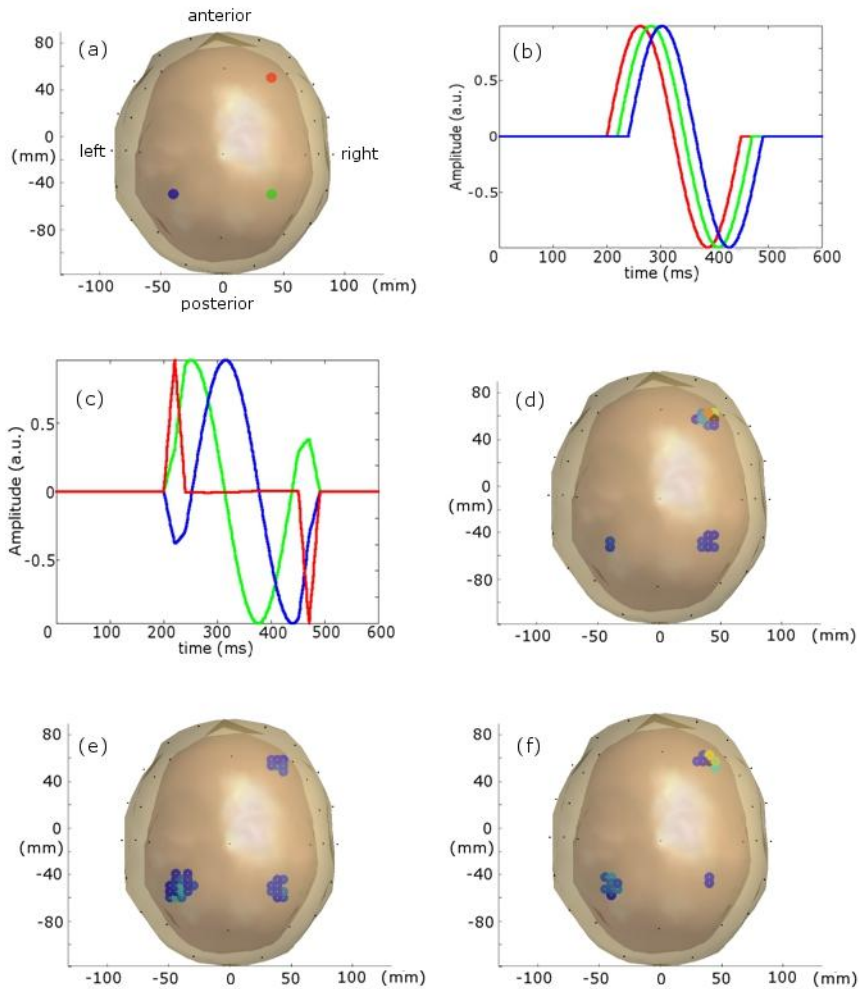**Figure 3.6** - a) Locations of the simulated sources in a top view of a model brain. b) Timecourse of the simulated sources; c) Timecourses of the components extracted by ICA. Comparison of these courses with the original ones readily shows the temporal unreliability of the extraction; d-e) SSLOFO cortical maps of the components 1 to 3. It is clear that source separation was not achieved, even in the absence of noise.

After running ICA, the timecourses assigned to each of the components, are depicted on Figure 3.6c. It becomes clear that there are many differences between the sources and the components' courses. Also, if one runs the SSLOFO algorithm on the components' maps, they will all yield 3 activated patches corresponding to the sources (Figures 3.6d, 3.6e and 3.6f)), which clearly shows that sources' separation was not achieved.

It's important to notice, however, that the activated patches are correctly locating the sources, and no spurious sources arise.

The same behaviour is to be expected with the real clinical data, since IEDs may propagate fast with the same paroxysmal properties. This will lead to electric signals arising from different spatial sources, sharing many temporal properties in their activations, with only small delays between them.

3.2.3 Framework for a new mapping approach:

To solve this problem of signal dependence in IED characterization and mapping, a multi-step algorithm was developed and is proposed here:

1-Decomposition of the epoched EEG signal into independent components using Infomax ICA (Bell & Sejnowski, 1995) as implemented in Matlab (The Mathworks, Inc.).

Regarding clinical data, the epochs ranged from the 400ms prior to the spike peak to 600ms after. The output of this step is a number of independent components equal to the number of sensors, each component with an associated scalp map and ERPimage (examples on Figures 3.7a and 3.7b). From this point onwards, all figures referring to clinical data are depicted for a representative patient AL;
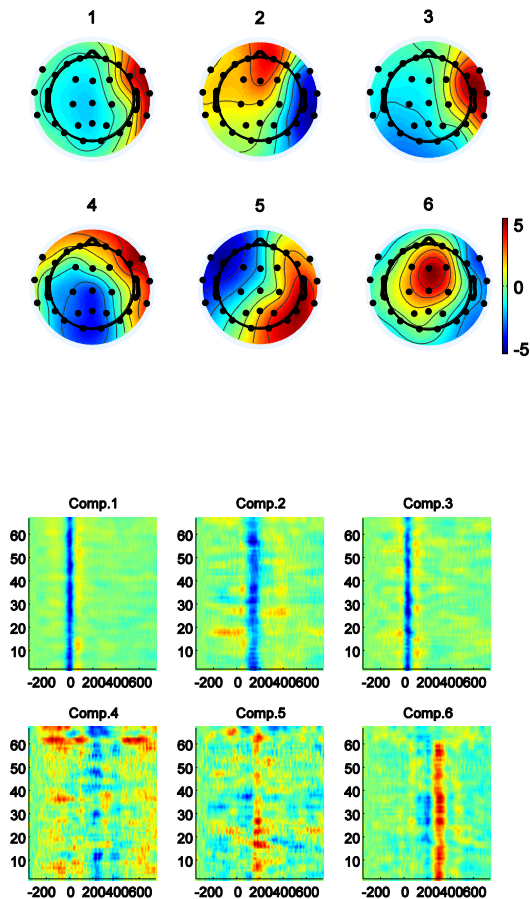
Figure 3.7 - **Top**) Example of component scalp maps for the first six components of patient AL as output in EEGLAB. Black dots denote the position of the electrodes. **Bottom**) ERP images corresponding to the components with scalp maps on Top. ERP images are color-coded 2D matrices with the horizontal axis being time, the vertical axis being the trials and the colors being the intensity of the components' activations. Brighter colors (red) correspond to higher values and darker colors (blue) relate to lower (negative) values. The intensity scale is set to cover the whole range of intensities obtained for the specific ICA decomposition. One should keep in mind that both the absolute values of the component scalp maps and activations do not have meaning *per se* but only when multiplied.

2- Selection of the top M components which are coherently active through the different epochs, i.e., components for which the activations are fairly similar across all trials and therefore their ERP image (see example above) appears closest to vertical bars. However, though a visually empirical concept, the closeness to a vertical structure is a subjective and ambiguous definition. Therefore, an automatic algorithm was used to rank the components.

First of all, there was the need to translate "vertical structure" into mathematical or computational language. Since an ERP image is an intensity-coded 2D matrix with the horizontal axis being time, the vertical axis being the trials and the image itself being the components' activations, a vertical structure is a relation, for a given time sample, between the values of the component activation for all trials, or simply the low variability between such values. The intuitive way to evaluate such measure would be to perform a Fast Fourier Transform along the trial dimension, and check the portion of energy due to the lowest frequency bin when compared to the overall energy. However, time intervals or components with good vertical structure but non-significant values of activation are also not of interest. Thus, the low-frequency portion was multiplied by the overall sum of the component's activations for all trials in the time sample of analysis. In this manner, preference is given to high-energy segments, as it is in these segments that the vertical coherence is of interest. Mathematically, these can be written as

$$Score(i) = \max\left[\left(\frac{\left(\sum_{k=1}^{Ntrials} Icaact(i,t,k) / Ntrials \right)^2}{\sum_{k=1}^{Ntrials} Icaact(i,t,k)^2} * \left| \sum_{k=1}^{Ntrials} Icaact(i,t,k) \right| \right), t \right] \quad \text{(Eq. 1)}$$

Icaact is a three-dimensional matrix where in which first two dimensions represent the component number and time and the last dimension represents the trial number. The notation $\max(f(i,t),t)$ means that the maximum is taken

along the time dimension. Note that the ratio in Eq. 1 is equivalent to taking the ratio of the first bin of the FFT to the overall power. To conclude, normalization is carried out. The component with the greatest score, *Score(i)*, is used to create a normalised score.

$$Norm\_Score(i) = \frac{Score(i)}{\max(Score(i))} \qquad \text{(Eq. 3)}$$

Components were ranked according to the normalized score, and kept as relevant until more than 85% of the data's variance was accounted for.

3- Application of SSLOFO to the M component maps selected in point 2.

The output of this step yields, for each component, the current distribution in the source space that originates the scalp map of the component. This solution has no constraints on the number of active patches, and an example with two active regions is shown in Figure 3.8.
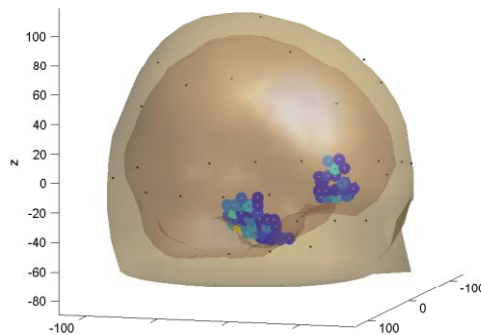

Figure 3.8 – Example of an SSLOFO cortical map for the most coherent component of patient AL. This pattern of activity involving a unilateral lower

lateral temporal lobe and the ipsilateral frontal lobe was seen on most of the patients for the highest ranked components.

4- Recombination of clusters. Because of the imperfect ICA source separation, the maps returned by SSLOFO will show activation of approximately the same cortical regions in more than one component. Thus, each region obtained by SSLOFO is represented by its centroid, and centroids from regions on different components which dist less than 3 cm are clustered together (a new weighted centroid is calculated). Figure 3.9 illustrates a set of final clusters for regions activated on the subset of relevant components (centroids are not shown);
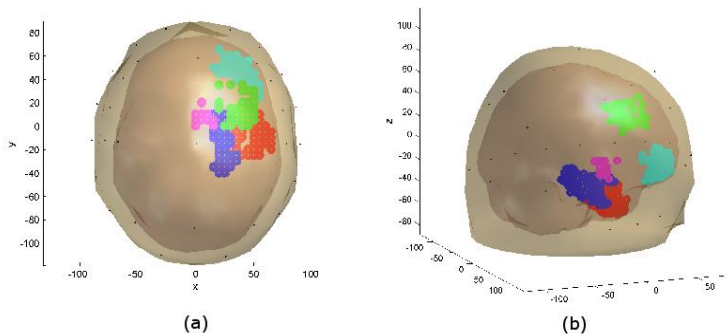

Figure 3.9 – Final cluster for patient AL, built with the maps of the most relevant components. Once this final clustering is achieved, the original data will then be projected into the centroids of the activated patches of cortex.

5- Back-projection of the original data into leadfields generated by three orthogonal dipoles at each of the N centroids. These leadfields are simply the

manifestation of the activity generated by each of such dipoles in the Nbchan channels, and is achieved by solving the forward problem.

All computations involving leadfields and projections were carried out using the Fieldtrip software (http://www.ru.nl/fcdonders/fieldtrip).

Finally, for each of the dipoles, the direction with the greatest power is taken and used to reduce the leadfield matrix to the dimensions of NxNbchan instead of 3NxNbchan. The projection into this new subspace is then computed, resulting on fixed single dipoles at the sources' centroids, each with a corresponding timecourse. Figure 3.10 shows an example of the quality of the projection.

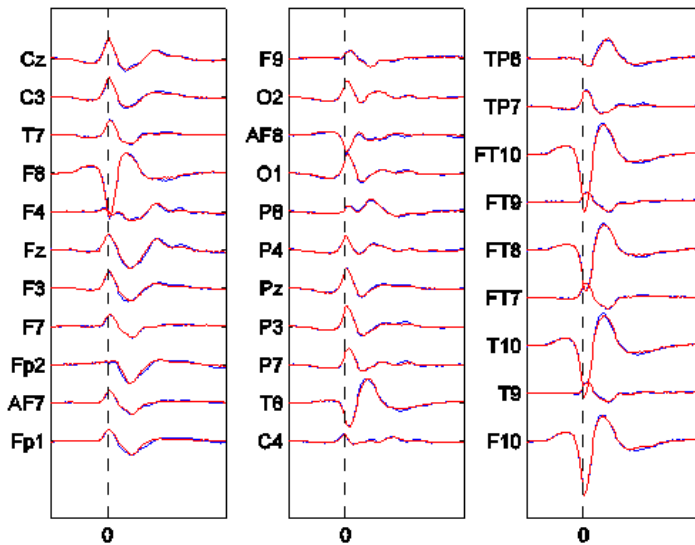**Figure 3.10** - Plot of the original data (blue) versus the final projected data (red) for patient AL along the electrodes. The variance explained was of 98.09% (mean 96.16% across all patients) and is indicative of the goodness-of-fit of the projection

In short, our framework extracts and identifies the components consistently related to the IED by investigating its temporal profile across trials.

Next, source localization of the components' scalp maps is performed. Overlapping patches arising from different components are then clustered, and each cluster is represented by its centroid. The overall EEG activity is then projected into the sub-space generated by the leadfields of dipoles located at these centroids, after taking the direction that accounts for maximum variance, as if the whole activity was solely generated at these sites. The timecourse of activity for each of these sites is finally obtained.

3.2.4 Simulations

The method we propose was tested and validated through the following simulations:

6 randomly located dipolar sources (with 3cm as the minimum distance between them) were simulated. The sources' activations were chosen to be those depicted in Figure 3.11.
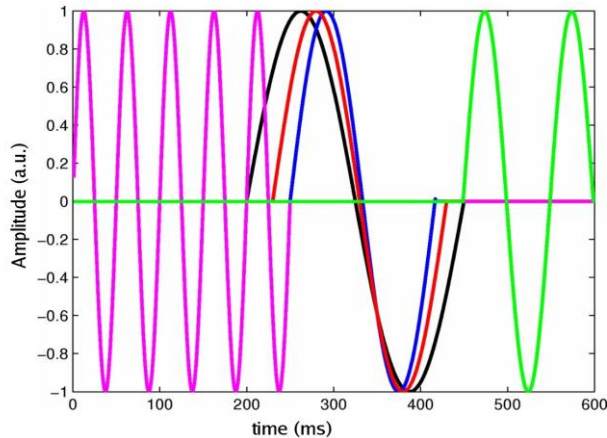

Figure 3.11 – Timecourse of the simulated sources. There are only five plots because two of the sources have purposefully the same activation. This

particular choice of activations allows testing the method's response to non-overlapping, partially overlapping and exactly coherent sources.

There are only five plots because two of the sources have purposefully the same activation. The closely spaced plots have frequencies of 4, 5 and 6 Hz and their start is delayed 20 samples from source 2(black) to 3 (and 4)(red), and 30 samples from source 3 (and 4) to 5(blue). This particular choice of activations allowed us to test the method on the localization accuracy and timecourse reconstruction abilities of coherent, overlapping and non-overlapping sources. Ideally, the method should be capable of keeping the order of activation of sources in the reconstructed waveforms. The simulation's sampling rate was 1KHz. Background physiological noise was added at 3 dB. The overall procedure was repeated 100 times. The datasets were subsequently processed using the proposed method in 3.2.3.

3.2.5 Patients

Recordings were obtained from 10 patients (5 males, 5 females) suffering from medically refractory TLE due to mesial sclerosis. For each of the patients, EEG data was collected with the commercially available Micromed system by means of electrodes AF7, AF8, Fp1, Fp2,F9, F7, F3, Fz, F4, F8, F10, FT9, FT7, FT8, FT10, T9, T7, C3, Cz, C4, T8, T10, TP7, TP8, P7, P3, Pz, P4, P8, O1, O2 placed according to the 10% system.. This configuration was used for special coverage of the low temporal regions. The signal was amplified, digitized at 256Hz and band-pass filtered between 1 and 30 Hz.

Written informed consent was obtained from all participants, and the protocol followed the guidelines approved by our local Ethics Committee.

After epoch extraction and removal of the most artifact contaminated ones, datasets with over 100 IEDs were available for each patient. These datasets were subsequently processed using the method proposed. The

sLORETA source space, consisting of 6239 sources spaced 5mm on grey matter locations, was used as the source space in SSLOFO, for comparison purposes.

Since electrocorticographic data cannot be obtained across the whole brain and, to the best of our knowledge, there is no other *in vivo* method for assessing the number of active dipoles, our results were validated through the following non-parametric approach to understand the null hypothesis distribution: Step five of the proposed framework (see above) was repeated 7500 times for N randomly positioned dipoles. Squared difference to the original data was used for comparison purposes between the random configurations and the algorithmic solution.

3.3 Results

3.3.1 Simulations

For the simulation data, Figure 3.12 shows the components extracted by the ICA and reinforces the notion that components' activations are not representative of the simulated waveforms in the case of overlapping waveforms.
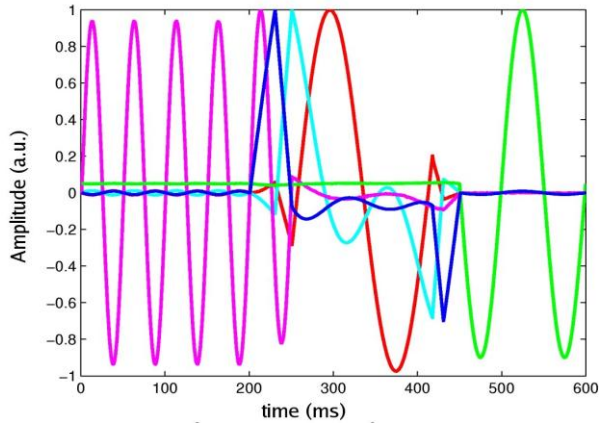
Figure 3.12 – Timecourses of the components of interest for one of the sets of simulated data. The courses corresponding to the non-overlapping sources could be extracted correctly; however, the components that involve the temporally overlapping sources have timecourses that do not resemble the original ones.

On the other hand, after the complete application of the proposed method it was possible to correctly extract the timecourses along with the sources' positions (Figs 3.13 and 3.14). As expected, the amplitudes, frequency and phase was kept among the overlapping sources, thus preserving the necessary information for a study on dynamics. The mean and maximum distance to the simulated sources were respectively 3 and 10mm and the mean explained variance by the reconstructed timecourses was 98.5%.
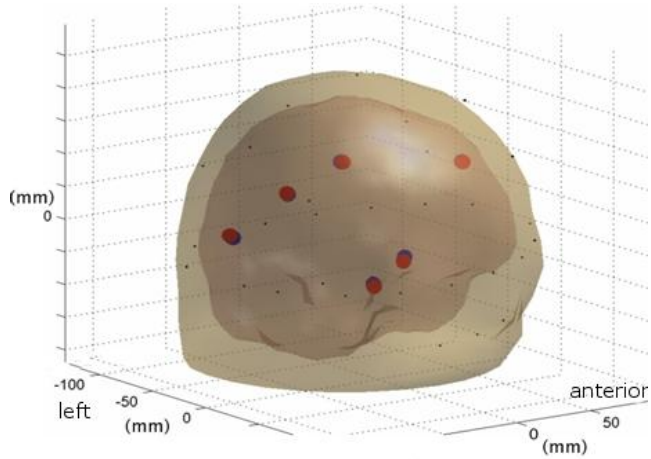
Figure 3.13 – Matching between the simulated (blue) and detected (red) sources for one of the simulations. When only one color is visible, exact localization was achieved. The mean and maximum distances between simulated and real sources in all simulations were 3 and 10 mm respectively.
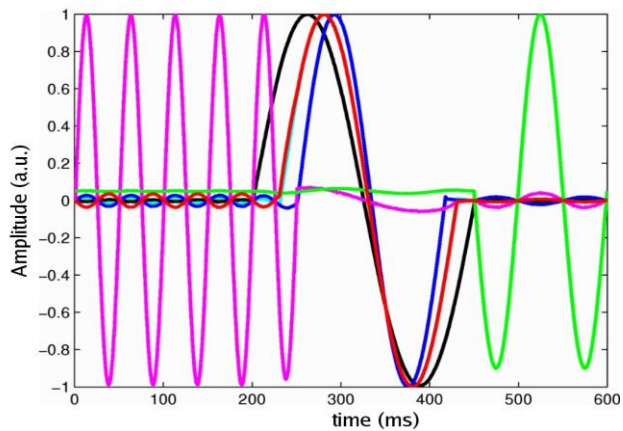
Figure 3.14 – Reconstructed timecourses of the detected sources. It can be seen that both overlapping and non-overlapping courses could be reliably extracted and that the amplitudes, frequency and phase was kept among the overlapping

sources. In this example, the variance explained by the reconstructed courses was of 98.95%.

3.3.2 Patient data:

Concerning the clinical data, the yielded source configurations confirm the activation of areas beyond the temporal lobe with a predominance of the ipsilateral orbitofrontal cortex (Figure 3.15), where activations were found for 9 out of 10 of the studied patients.
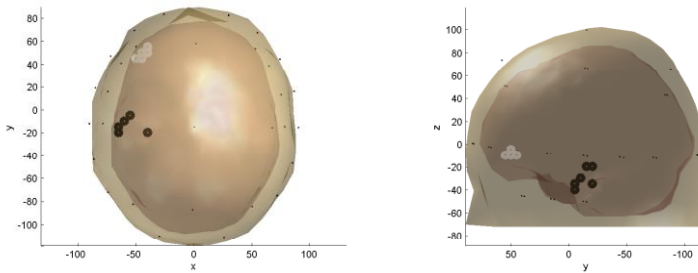
Figure 3.15 – SSLOFO representation of the most consistent pattern of activation: unilateral lower temporal lobe and ipsilateral orbitofrontal lobe. This pattern was present in 9 out of 10 patients, always in the highest ranking components, which is a very interesting result on its own since it was seen on simulations that spurious sources do not usually arise.

Involvement of these areas was much more consistent than detected activation of mesial structures or dipoles in other locations. It should be noted, however, that detection of mesial activity is severely hampered due to its deep locations and weak projection in the scalp. The findings are summarized in Table 3.1 for each individual recording.

Patient	1	2	3	4	5	6	7	8	9	10	Mean
N dipoles	6	6	5	3	5	3	4	3	4	2	-
Lateral temporal Dipoles	Yes	Yes	Yes	Yes	Yes	Yes	Yes	No	Yes	Yes	-
Ipsilateral Frontal Dipoles	Yes	Yes	Yes	Yes	Yes	Yes	Yes	No	Yes	Yes	-
Mesial temporal Dipoles	No	Yes	No	No	No	No	Yes	Yes	No	No	-
Other dipoles	No	Yes	No	No	No	No	No	Yes	Yes	No	-
Rotating Dipole Results	0.00	0.01	0.00	0.00	0.33	0.04	0.05	0.08	0.02	0.05	0.06
Fixed Dipole Results	2.26	0.00	0.01	0.16	2.27	0.01	1.16	0.12	0.76	0.01	0.73

Table 3.1 – Summarized results for the studied patients. The values shown in the two last lines refer to the percentage of random results performing better than the proposed method when considering rotating and fixed dipoles.

Regarding the goodness-of-fit of the proposed source configurations, when compared in terms of squared differences to the original data, the results obtained score better than 99.27% of the random dipole configurations for the same number of dipoles. When only the locations are taken (i.e., 3 orthogonal dipoles per location) the results climb up to 99.94%. Full results are given in Table 3.1.

Also, contrary to what ICA may primarily suggest (note ERP image of component 1, peaking around 0 ms, and component 6, peaking around 300 ms in Figure 3.7), timecourse reconstruction of the found sources (Figure 3.16) reveals a consistent pattern in which the sources share similar activations, with only minor delays and morphology changes.
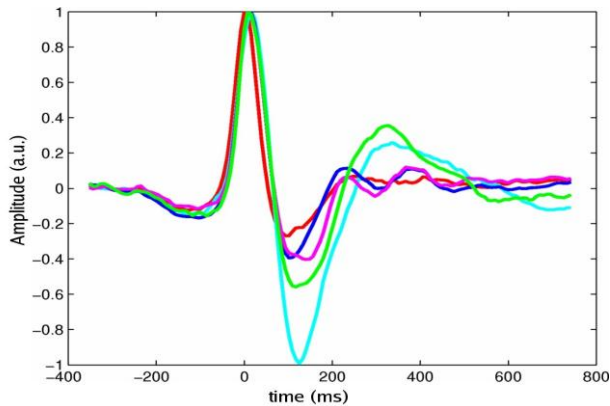
Figure 3.16 – Reconstructed timecourses of the centroids' activity for patient AL. Apart from slight morphology changes and very small delays, the sources share similar activations, which is a plausible model of an IED, contrasting with the differences seen between the courses of components 6 and 1 on Figure 3.7 for the same patient.

This pattern seems to reflect a much more plausible model of an interictal discharge than the one that would be achieved by means of simple ICA decomposition, for the latter suggests at times the presence of a slow-wave in

frontal areas with apparently no preceding spike. However, despite the improvement on timecourse extraction, to infer propagation patterns from the yielded solutions would be over-interpreting since the delays involved are typically of one or two samples and therefore sensitive to the slightest errors. Furthermore, no dominating propagation pattern (frontal to lateral 4/10, lateral to frontal 4/10,) was evident. This is not surprising and is due to the high variability of signals found on TLE IEDs (Alarcon et al., 1997).

3.4 Discussion and Conclusions

We proposed and tested a new approach for the mapping of interictal discharges in epilepsy by combining two tools: ICA and SSLOFO.

From the results presented above, we can conclude that the developed method helps in surpassing some of the shortcomings of single-tool based EEG procedures. The algorithm leads to reliable results as proved by the simulations' excellent localizing accuracy and robust timecourse extraction. When applied to clinical data in TLE, it supports the involvement of the frontal lobe in this kind of epilepsy, and favours theories regarding cortical networks in TLE with activated areas outside the temporal lobe. Indeed, Lieb et al (Lieb et al., 1991) had noted (i) a clear tendency for mesial temporal seizure discharges initially to invade orbitofrontal cortex and (ii) the emergence of a period of clear asymmetry in the frontal lobes during which high-amplitude, rapid discharges were present on the side ipsilateral to the initiating temporal lobe. Our results extend this notion also to IEDs, by suggesting that the frontal region, especially the orbitofrontal cortex, is strongly influenced by mesial temporal activity. It also encourages the assumption that functional cortical network studies in epilepsy can be based on IEDs.

Our results were only possible to obtain due to the improved localization and reduced smearing of the found sources, an important aspect which is related to the focal nature of SSLOFO.

In fact, for completeness sake and comparison purposes, mapping of the components to the cortex with sLORETA and equivalent dipole methods was evaluated. In both simulations and patients, sLORETA provided smooth solutions that did not allow for separation between sources located close to each other. The maps that in SSLOFO had clearly visible separation between temporal and frontal lobe sources were commonly mapped by sLORETA as a single activated area with maxima somewhere in between the sources yielded by SSLOFO. While in clinical data it could be arguable which of the solutions would be closer to the real activity, the same cannot be said about simulations for which the solutions were verifiable. As for equivalent dipole methods, two-dipole modelling with no initialization bias (EEGLAB's DIPFIT) was in consistent agreement with the SSLOFO regions' centroids for maps where only two areas were active.

Despite its very good performance, our experience revealed that when applying SSLOFO one must be alert to the fact that the chosen value for the signal-to-noise ratio (SNR), a required input, influences the output of the algorithm, and future work should focus on an optimal automatic method for assessing the SNR of a component map. This is certainly an issue worth studying since component topographies are much more "noise-free" than individual samples and it is this feature that greatly improves localization accuracy which might not be achieved on the data samples or for deep sources.

On the other hand, some caution must be taken when interpreting the results. 31 EEG channels and a head model with only 6239 possible sources may not be enough for adequate modelling of all brain areas. For instance, one important issue is that epileptiform discharges in temporal lobe epilepsy often show the largest amplitude at the inferior frontal electrode, which is located closer to frontal than to temporal structures. This could be explained by a significant proportion of the signal reaching the scalp through pathways of higher conductivity located anteriorly due to holes in the skull (optic foramen, foramen ovale, and the superior orbital fissure (Torre *et al*, 1999) In this manner, if the head model is not taking into account such subtleties, incorrect mapping of the sources could be taking place. We do however believe that

these are unlikely explanations for our results given the advantages of the SSLOFO methods proven above, and converging evidence from PET/SPECT, neuropsychology, and previous studies on ictal propagation. Studies with denser arrays and realistic head models should nevertheless be a goal.

In the future, further validation of the method can be carried out by comparing the results of this method with simultaneous EEG and fMRI recordings of IEDs. The role of missing, spurious or mislocalized sources will also be of study. Further optimization of the method can be achieved by allowing the dipoles to vary slightly around the position of the clustered centroids. Other adaptations should concern the continuous nature of the IED propagation rather than the discretization assumed here.

Generalization of this methodology to other experimental settings may prove useful to test emerging theories regarding cortical networks and their dynamics in epilepsy.

The assessment of this new methodological framework for improved mapping of the epileptic foci is the contribution of this work to the first step of epilepsy surgery planning. The better is the non-invasive estimate of the epileptic foci, the more accurate will be the proper placement of the subdural strips and/or depth electrodes.

However, another crucial step is the functional characterization of the patient's affected and spared areas through the use of neuroimaging. These brain mapping procedures help planning the extent and boundaries of the resected areas. Furthermore, by knowing the realistic implications of the surgery outcome regarding impaired function, both surgeons and patients can take informed decisions and consent on the surgical procedure.

While current brain mapping procedures for epilepsy focus primarily on language, memory and motor functions, in this thesis we propose the use of visual localizers as a valid step in brain mapping for epilepsy surgery. This discussion is presented in Chapter 4.

References

Adam, C., Saint-Hilaire, J. M., & Richer, F. (1994). Temporal and spatial characteristics of intracerebral seizure propagation: predictive value in surgery for temporal lobe epilepsy. *Epilepsia*, *35*(5), 1065–1072.

Alarcon, G., Garcia Seoane, J. J., Binnie, C. D., Martin Miguel, M. C., Juler, J., Polkey, C. E., Elwes, R. D., et al. (1997). Origin and propagation of interictal discharges in the acute electrocorticogram. Implications for pathophysiology and surgical treatment of temporal lobe epilepsy. *Brain: a journal of neurology*, *120 (Pt 1)*, 2259–82.

Bell, A. J., & Sejnowski, T. J. (1995). An information maximisation approach to blind separation and blind deconvolution. *Neural Computation*, *7*(6), 1129–1159.

Brown, G. D., Yamada, S., & Sejnowski, T. J. (2001). Independent component analysis at the neural cocktail party. *Trends in neurosciences*, *24*(1), 54–63.

Chang, B. S., & Lowenstein, D. H. (2003). Epilepsy. Mechanisms of disease. *The New England Journal of Medicine*, *349*(13), 1257–1266.

Comon, P. (1994). Independent component analysis, A new concept? *Signal Processing*, *36*(3), 287–314.

Darvas, F., Pantazis, D., Kucukaltun-Yildirim, E., & Leahy, R. M. (2004). Mapping human brain function with MEG and EEG: methods and validation. *NeuroImage*, *23 Suppl 1*, S289–99.

Dzhala, V. I., & Staley, K. J. (2003). Transition from interictal to ictal activity in limbic networks in vitro. *The Journal of neuroscience: the official journal of the Society for Neuroscience*, *23*(21), 7873–80.

Gorodnitsky, I. F., & Rao, B. D. (1997). Sparse signal reconstruction from limited data using FOCUSS: a re-weighted minimum norm algorithm. *IEEE Transactions on Signal Processing*, *45*(3), 600–616.

Helmholtz, H. (1853). Ueber einige Gesetze der Vertheilung elektrischer Ströme in körperlichen Leitern mit Anwendung auf die thierisch-elektrischen Versuche. *Annalen der Physik und Chemie*, *165*(6), 211–233.

Jayakar, P., Duchowny, M., Resnick, T. J., & Alvarez, L. A. (1991). Localization of seizure foci: pitfalls and caveats. *Journal of clinical neurophysiology: official publication of the American Electroencephalographic Society*, *8*(4), 414–31.

Jung, K.-Y., Kim, J.-M., Kim, D. W., & Chung, C.-S. (2005). Independent component analysis of generalized spike-and-wave discharges: primary versus secondary bilateral synchrony. *Clinical neurophysiology: official journal of the International Federation of Clinical Neurophysiology*, *116*(4), 913–9.

Kobayashi, K., Akiyama, T., Nakahori, T., Yoshinaga, H., & Gotman, J. (2002a). Systematic source estimation of spikes by a combination of independent component analysis and RAP-MUSIC. I: Principles and simulation study. *Clinical neurophysiology: official journal of the International Federation of Clinical Neurophysiology*, *113*(5), 713–24.

Kobayashi, K., Akiyama, T., Nakahori, T., Yoshinaga, H., & Gotman, J. (2002b). Systematic source estimation of spikes by a combination of independent component analysis and RAP-MUSIC. II: Preliminary clinical application. *Clinical neurophysiology: official journal of the International Federation of Clinical Neurophysiology*, *113*(5), 725–34.

Lieb, J. P., Dasheiff, R. M., Engel, J., & Genton, (P. (1991). Role of the Frontal Lobes in the Propagation of Mesial Temporal Lobe Seizures. *Epilepsia*, *32*(6), 822–837.

Liu, H., Schimpf, P. H., Dong, G., Gao, X., Yang, F., & Gao, S. (2005). Standardized shrinking LORETA-FOCUSS (SSLOFO): a new algorithm for spatio-temporal EEG source reconstruction. *IEEE transactions on bio-medical engineering*, *52*(10), 1681–91.

Makeig, Bell, Jung, & Sejnowski. (1996). Independent Component Analysis of Electroencephalographic Data. (D. Touretzky, M. Mozer, & M. Hasselmo, Eds.)*Methods*, *8*(3), 145–151.

Mandelkow, H., Halder, P., Brandeis, D., Soellinger, M., de Zanche, N., Luechinger, R., & Boesiger, P. (2007). Heart beats brain: The problem of detecting alpha waves by neuronal current imaging in joint EEG-MRI experiments. *NeuroImage*, *37*(1), 149–63.

Merlet, I., & Gotman, J. (1999). Reliability of dipole models of epileptic spikes. *Clinical neurophysiology: official journal of the International Federation of Clinical Neurophysiology*, *110*(6), 1013–28.

Onton, J., Westerfield, M., Townsend, J., & Makeig, S. (2006). Imaging human EEG dynamics using independent component analysis. *Neuroscience and biobehavioral reviews*, *30*(6), 808–22.

Ozgoren, M., Bayazit, O., Gokmen, N., & Oniz, A. (2010). Spectral pattern analysis of propofol induced spindle oscillations in the presence of auditory stimulations. *The open neuroimaging journal*, *4*, 121–9.

Pascual-Marqui, R. D. (2002). Standardized low-resolution brain electromagnetic tomography (sLORETA): technical details. *Methods and findings in experimental and clinical pharmacology*, *24 Suppl D*, 5–12.

Pascual-Marqui, R. D., Michel, C. M., & Lehmann, D. (1994). *Low resolution electromagnetic tomography: a new method for localizing electrical activity in the brain. International Journal of Psychophysiology*, 18, 49–65.

Pataraia, E., Lindinger, G., Deecke, L., Mayer, D., & Baumgartner, C. (2005). Combined MEG/EEG analysis of the interictal spike complex in mesial temporal lobe epilepsy. *NeuroImage*, *24*(3), 607–14.

Plummer, C., Harvey, a S., & Cook, M. (2008). EEG source localization in focal epilepsy: where are we now? *Epilepsia*, *49*(2), 201–18.

Shin, W. C., Hong, S. B., Tae, W. S., & Kim, S. E. (2002). Ictal hyperperfusion patterns according to the progression of temporal lobe seizures. *Neurology*, *58*(3), 373–380.

Spencer, S. S. (2002). Neural networks in human epilepsy: evidence of and implications for treatment. *Epilepsia*, *43*(3), 219–27.

Takaya, S., Hanakawa, T., Hashikawa, K., Ikeda, A., Sawamoto, N., Nagamine, T., Ishizu, K., et al. (2006). Prefrontal hypofunction in patients with intractable mesial temporal lobe epilepsy. *Neurology*, *67*(9), 1674–1676.

Fernández Torre, J. L., Alarcón, G., Binnie, C. D., Seoane, J. J., Juler, J., Guy, C. N., & Polkey, C. E. (1999). Generation of scalp discharges in temporal lobe epilepsy as suggested by intraoperative electrocorticographic recordings. *Journal of neurology neurosurgery and psychiatry*, *67*(1), 51–58.

Wilson, F. N., & Bayley, R. H. (1950). The Electric Field of an Eccentric Dipole in a Homogeneous Spherical Conducting Medium. *Circulation*, *1*(1), 84–92.

Chapter 4

Functional localizers as a brain mapping tool: implications for clinical research and cognitive neuroscience

4.1 Specialized visual processing in the brain: historical milestones

Throughout the years, neuroscience has undisputedly identified a number of regions of the human cortex that are functionally devoted to specific tasks. Starting with the early work of Gall, Broca, Ferriet and Jackson in the 19th century, examples of these span the primary motor cortex, language areas, memory structures, but also extend into the visual domain.

The cortex devoted to visual processing occupies roughly one third of the entire cortical surface and is made up, at least in part, of specialized interconnected modules and maps (Wandell, Dumoulin, & Brewer, 2007).Although the anatomical and functional organization of the visual cortex is quite complex, two main principles of organization have been suggested: hierarchical processing and functional specialization (Kalanit Grill-Spector & Malach, 2004).

In this hierarchical view of the visual brain (Felleman & Van Essen, 1991), each specialized module extracts some characteristics of the viewed images, which are then fed-forward to the next level in the hierarchy. In the bottom levels of the hierarchy the extracted features start with simple bar or line orientation (Hubel & Wiesel, 1968), which then are integrated into contours, which then are integrated into shapes (Zoe Kourtzi, Tolias, Altmann, Augath, & Logothetis, 2003; Maunsell & Newsome, 1987) . Visual input undergoes this common processing, before it is directed towards higher-level visual areas, located anteriorly within the hierarchy.

As features are integrated they represent more global information and thus increase in "meaning", in terms of a semantic or conceptual representation level (Caramazza & Mahon, 2003; Mahon & Caramazza, 2009; Martin, 2007) . The most striking evidence for the existence of these categorical representations in the brain arose from focal brain lesions that led to categorical memory-deficits,

selective agnosias and semantic related syndromes (Brambati et al., 2006; Damasio, Grabowski, Tranel, Hichwa, & Damasio, 1996; Gainotti, 2000; Lyons, Kay, Hanley, & Haslam, 2006). The bi-directional link between category-related representations and the impairment of temporal lobe structures can be further understood by studying TLE patients and has in fact been recently reviewed in (Drane et al., 2008).

However, although the anterior Temporal Lobe plays a major role in binding sensory information into conceptual percepts, in some cases category-selective deficits occur with lesions restricted to the ventral temporal and occipital cortex (De Renzi, 2000; Goodale, Milner, Jakobson, & Carey, 1991; Humphreys & Riddoch, 1984), suggesting dedicated processing in visual regions.

In 1995, with the advent of functional imaging, Rafael Malach and colleagues used fMRI to explore the stages of integration leading from local feature analysis to object recognition in the healthy human brain (R Malach et al., 1995). They reported evidence for object-related activation at the lateral-posterior aspect of the occipital lobe in a region termed the lateral occipital complex (LO). LO showed preferential activation to images of objects, compared to a wide range of texture patterns. Their manipulations of the stimuli suggested that the enhanced responses to objects were not a manifestation of low-level visual processing but instead was uniquely correlated to object detectability. Despite the preferential activation to objects, LO did not seem to be involved in the final, "semantic," stages of the recognition process. These results are thus evidence for the high-level visual cortex to be an intermediate link in the chain of processing stages leading to object recognition.
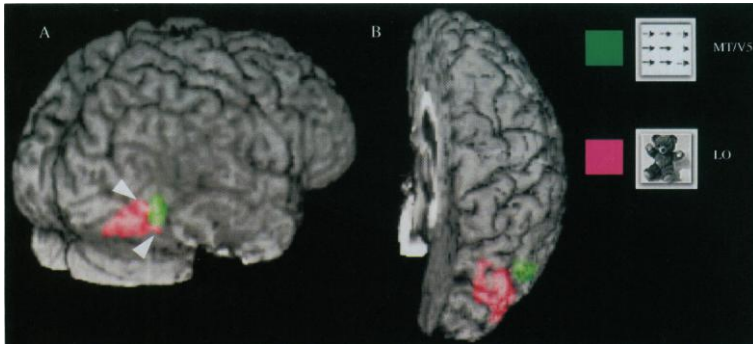
Figure 4.1 - 3D rendering of functional specialization in human occipital lobe. fMRI data in the right hemisphere, superimposed on high-resolution Tl-weighted anatomical data. Pink depicts LO, lateral occipital complex, selective for objects vs. textures. Green represents MT/V5, a cortical region selective for motion. (A) Posterolateral view of the right hemisphere. (B) Top view. Reproduced from (R Malach et al., 1995)

In 1997, Nancy Kanwisher and colleagues went a step further, building on evidence from other modalities, to report an area in the fusiform gyrus that consistently activated more in response to viewing faces than when subjects viewed assorted common objects (Kanwisher, McDermott, & Chun, 1997). They named it Fusiform Face Area (FFA) and went on to study its response properties.

The striking finding with the FFA was the notion that, instead of a general area for the processing of images with increased meaning or coherent shape, such as the LOC, there was evidence for a module dedicated to the processing of a single category, in this case faces. This finding immediately elicited two important questions:
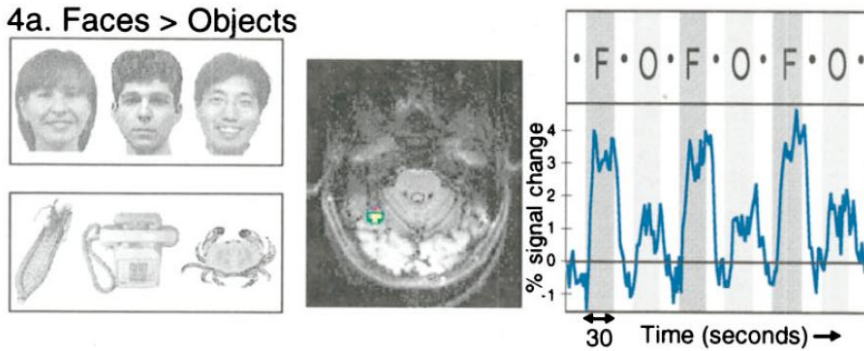
Figure 4.2 - Left: sample stimuli used in the localization procedure. Middle: MRI slice with statistical overlay for one subject, representing the area in the right fusiform gyrus (radiological convention) with increased activation to faces in relation to assorted objects. This area was consistently found across subjects and was named the Fusiform Face Area (FFA) Right: BOLD signal timecourse for the FFA. Note the block design and the striking difference in BOLD magnitude during the blocks presenting images of faces.
Reproduced from (Kanwisher et al., 1997)

1) Why are faces special? (This question can be especially interesting also from the behavioral perspective interest since face processing is highly relevant for social interactions)

2) Are there any other categories that deserve privileged processing?

The following year saw at least one of these questions answered.

The work of Epstein et al showed a particular area within human parahippocampal cortex which is involved in a critical component of navigation: perceiving the local visual environment (R Epstein & Kanwisher, 1998). This region, which was named the 'parahippocampal place area' (PPA), responded selectively and automatically in fMRI to passively viewed scenes.
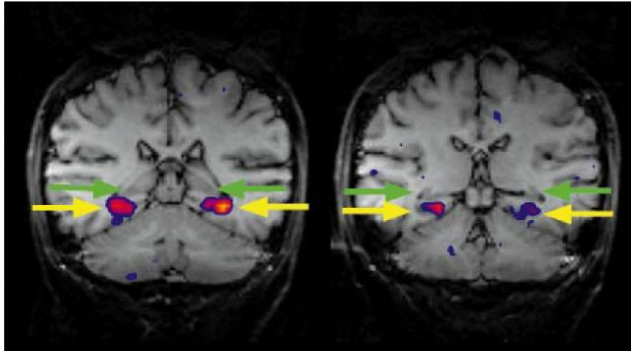
Figure 4.3 - Two adjacent slices from a single subject demonstrating the anatomical location of the PPA. Functional data is overlaid on high-resolution T1-weighted anatomical images of the same slices. Right hemisphere appears on the left. Color-coded significance levels reflect the results of a Kolmogorov–Smirnov test comparing the MR signal intensity during viewing of intact scenes to signal intensity during viewing of intact objects and faces. Note that the PPA (yellow arrows) does not overlap with the posterior part of the hippocampus (green arrows). Posterior slice appears on the left. Talairach coordinates of PPA activation for this subject are −6, 18, −39 and −6, −34, 30.
Reproduced from (R Epstein & Kanwisher, 1998)

The critical factor for this activation appears to be the presence in the stimulus of information about the layout of local space. The response in the PPA to scenes with spatial layout but no discrete objects (empty rooms) is as strong as the response to complex meaningful scenes containing multiple objects (the same rooms furnished) and over twice as strong as the response to arrays of multiple objects without three-dimensional spatial context (the furniture from these rooms on a blank background).

With the turn of the twenty-first century, yet another privileged category was found. Downing and colleagues presented a series of functional magnetic resonance imaging (fMRI) studies revealing substantial evidence for a distinct cortical region in humans, which they named Extrastriate Body Area (EBA) that responds selectively to images of the human body, as compared with a wide range of control stimuli (Downing, Jiang, Shuman, & Kanwisher, 2001). This region was found in the lateral occipitotemporal cortex in all subjects

tested and apparently reflected a specialized neural system for the visual perception of the human body.
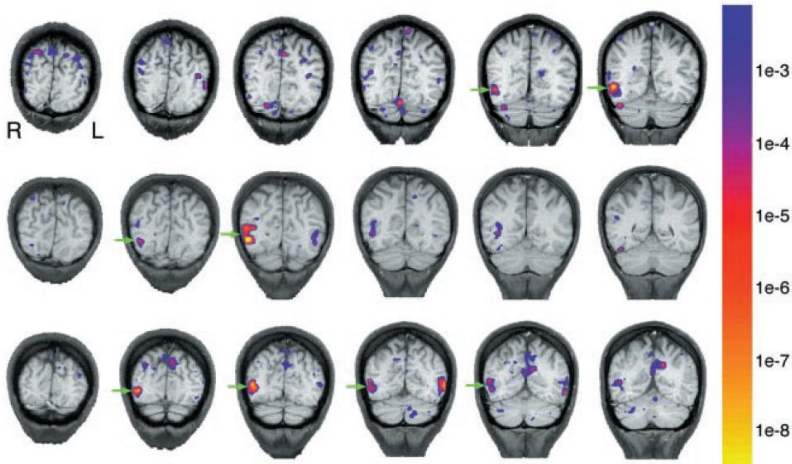
Figure 4.4 - EBA activations in three individual subjects. Each row shows coronal anatomical slices from a single subject, arranged from posterior (left) to anterior (right), overlaid with a statistical map showing voxels that were significantly more active for human bodies and body parts than for objects and object parts. The EBA is visible in the right occipitotemporal cortex of each subject (arrows); in some subjects activation was also observed in the left hemisphere. Scale indicates P value of activations in colored regions. Reproduced from (Downing et al., 2001)

Studies devoted to the finding of other categories worth specialized brain processing found that tools (objects prone to be manipulated) and chairs might also have corresponding functional modules in the brain. However, whether regions that show preference for an object category should be treated as an independent module for processing that category is still an unanswered question (Kalanit Grill-Spector & Malach, 2004).

4.2 Category preferring modules and networks: where are we at?

As a follow up of the aforementioned seminal studies, the fMRI literature witnessed a boost of studies that aimed at characterizing the special processing of objects, faces, places and bodies in the human brain (for reviews see (Gerlach, 2007; Spiridon, Fischl, & Kanwisher, 2006). For most of these categories, it was found that the specialized processing consisted not of a single area or module but an entire network. Also, selectivity became again a disputed concept. The response of these networks (significantly above baseline) for more than one category suggested that these are actually category-preferring networks instead of being truly selective (Downing et al., 2006; Tarr & Gauthier, 2000; Xu, 2005). Indeed, there is still an ongoing debate regarding modularized vs distributed processing, since activity within category-preferring regions can also be used to discriminate between their non-preferred categories (Hanson, Matsuka, & Haxby, 2004), an issue we'll get back to in Chapter 6.

4.2.1   The face-preferring network

The face-preferring network has been the most extensively studied of the category-preferring networks. The attention devoted to face-processing studies is such that the network has been split into a core and extended networks (Haxby, Hoffman, & Gobbini, 2000). The core network is comprised of the Fusiform Face Area (FFA) (Kanwisher et al., 1997), the Occipital Face Area (OFA) (Gauthier et al., 2000), and a region on the posterior bank of the Superior Temporal Sulcus (pSTS) (Puce, Allison, Bentin, Gore, & McCarthy, 1998). The FFA is thought to be involved in the perception of invariant aspects of faces, such as identity, gender and other holistic processing. In turn, the pSTS activates when judgment about the changeable and social aspects of a face is required, such as lip-reading (Calvert et al., 1997) and eye gaze direction (Puce, Allison, Bentin, Gore, & McCarthy, 1998). The OFA is regarded in

many studies as the entry-level of the face-processing network, processing lower-level aspects of faces and face parts, and feeding this information to the rest of the core regions. There is fMRI evidence that inferior occipital gyrus or OFA is involved in processing second-order relational or configural cues (the metric distances between features), but not first-order configural cues (which encode the relative positions of facial features) (Atkinson & Adolphs, 2011).
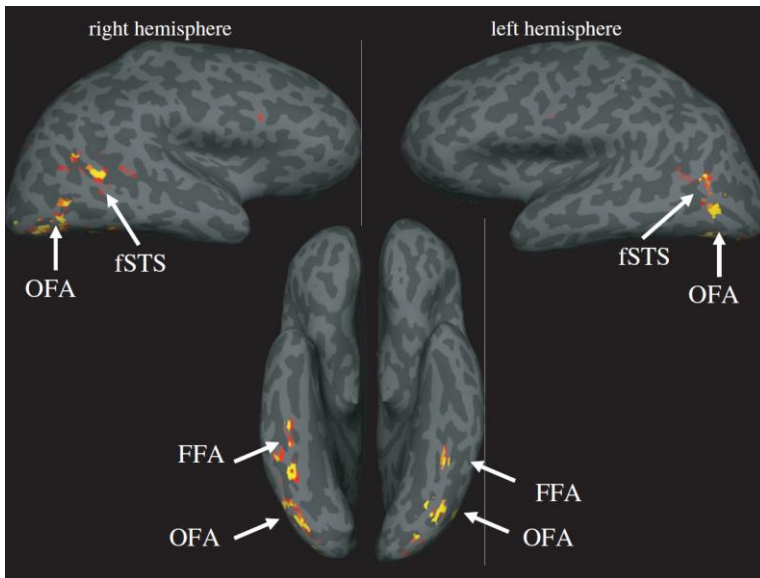
Figure 4.5 - Face-selective activation (faces > objects, p<0.0001) on an inflated brain of one subject, shown from lateral and ventral views of the right and left hemispheres. Three face-selective regions are typically found: the FFA in the fusiform gyrus along the ventral part of the brain, the OFA in the lateral occipital area and the fSTS in the posterior region of the superior temporal Sulcus Reproduced from (Kanwisher & Yovel, 2006)
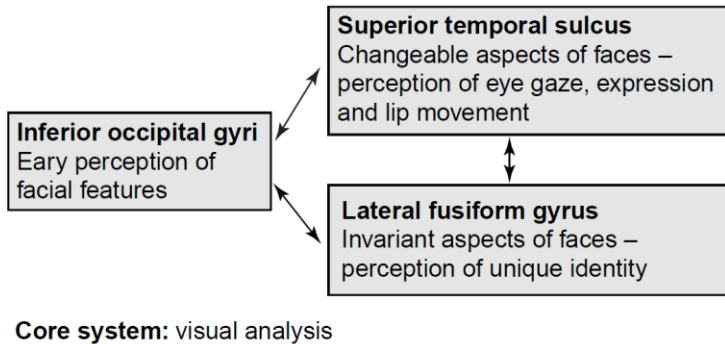
Figure 4.6 - Location and proposed function of the core nodes of the face-preferring network. Adapted from (Haxby et al., 2000)

The extended system includes areas not exclusive to the processing of faces, which work in concert with other neural systems. These include the amygdala, concerning emotional processing, the intraparietal sulcus, regarding spatially directed attention, and statistically more liberal reviews (Ishai, Schmidt, & Boesiger, 2005) also include the inferior frontal gyrus and the orbitofrontal cortex, responsible for assessing attractiveness, familiarity and other subjective judgments on faces.

4.2.2   The scene-preferring network

As for scenes, areas in this dedicated network involve the parahippocampal place area (PPA) (R Epstein & Kanwisher, 1998) and the retrosplenial cortex (RSC) (Maguire, 2001). These two areas perform complementary functions in place recognition (Russell a Epstein, Parker, & Feiler, 2007; Park & Chun, 2009). These authors suggest that the PPA may primarily support perception of the immediate scene, whereas RSC may

support memory retrieval mechanisms that allow the scene to be localized within the broader spatial environment.

To a lesser extent, often noted but seldom discussed (R. A. Epstein, Higgins, & Thompson-Schill, 2005; Hasson, Harel, Levy, & Malach, 2003; Park & Chun, 2009), the Transverse Occipital Sulcus (TOS), a peripheral biased low-level region, also shows selectivity for scenes and buildings.
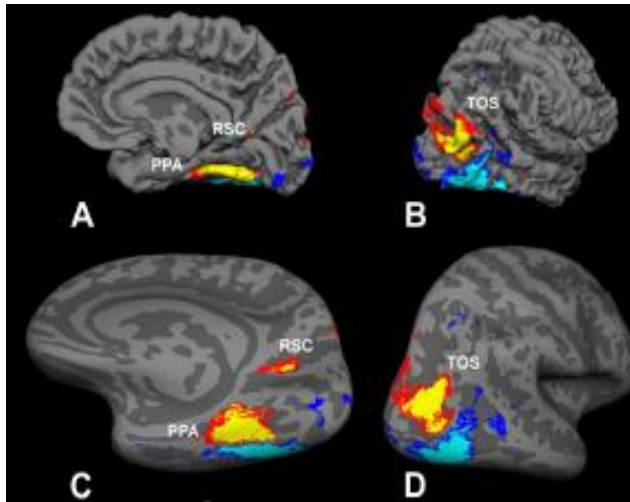
Figure 4.7 - Overall view of scene-selective regions in human visual cortex. Subjects fixated the center of a screen during block-designed presentation of scene versus face localizing stimuli. Relatively higher activity to scenes versus faces is shown in red/yellow versus blue/cyan, respectively. Data are a group average of both the functional and the anatomical data (n=10), in cortical surface format. The right hemisphere is illustrated; data from the left hemisphere were similar. A and B show the medial and lateral-posterior views of folded cortex, respectively. C and D show corresponding views of inflated cortical surfaces. Adapted from (Nasr et al., 2011)

4.2.3 The object-preferring network

Regarding object processing in the visual cortex, neuroimaging studies have focused on an extensive area comprising parts of the inferior temporal and the lateral occipital cortex, globally called the lateral occipital complex (LOC) (R Malach et al., 1995) that responds more to objects than textures or scrambled images. This area can be further divided into a posterior fusiform (pFs or vLOC, v stands for ventral) and a lateral occipital region (LO or dLOC, d stands for dorsal)(K Grill-Spector et al., 1999).

Seminal studies on the LOC have highlighted the role this region has on shape perception (Z Kourtzi & Kanwisher, 2001), favoring 3-D information over 2-D contours (Zoe Kourtzi, Erb, Grodd, & Bülthoff, 2003). Further, representations in the LOC appear to be invariant to some degree to changes in size and position, yet specific to the direction of illumination and the viewpoint of the object (K Grill-Spector, Kourtzi, & Kanwisher, 2001).

Additional experiments suggest that the LOC might contain a hierarchy of shape-selective regions with more posterior regions activated also by object fragments, indicating a coarse spatial coding of shape features in lateral LOC, while anterior regions exhibit stronger activation for whole or half objects, suggesting a more focused coding of the entire shape space within ventral LOC (Drucker & Aguirre, 2009).
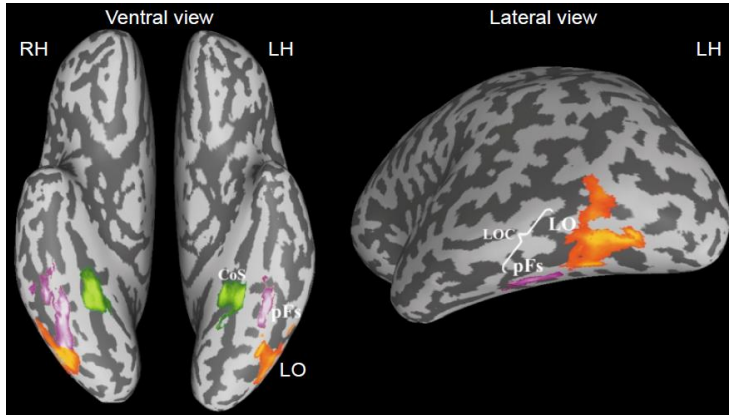
Figure 4.8 - Occipitotemporal object-related areas in the human ventral visual pathway. Location of high-order object areas is shown from a ventral view (left) and posterior–lateral view (right) of 'inflated' hemispheres. The regions include the dorsal lateral-occipital (LO, orange) and the ventral posterior-fusiform (pFs, purple) areas, which together form the lateral occipital complex. More medially, along the collateral sulcus (CoS) and parahippocampal gyrus, the PPA is shown for reference. Results shown are an averaged map of 14 subjects. Reproduced from (Rafael Malach, Levy, & Hasson, 2002)

4.2.4   The body-preferring network

Studies concerning the processing of headless bodies and body parts agreed on two major body-processing clusters: the aforementioned EBA and also the Fusiform Body Area or FBA, which has been shown to be separate from the nearby FFA, given enough spatial resolution. A particular study goes even further as to dissect the EBA into several sub-clusters (Weiner & Grill-Spector, 2011).

Concerning function, Taylor et al (Taylor, Wiggett, & Downing, 2008) propose an analogy of these areas to the nearby face-selective regions occipital face area (OFA) and fusiform face area (FFA). Specifically, they hypothesize that the EBA analyzes bodies at the level of parts (as has been proposed for

faces in the OFA), whereas FBA (by analogy to FFA) may have a role in processing the configuration of body parts and bodies as wholes.
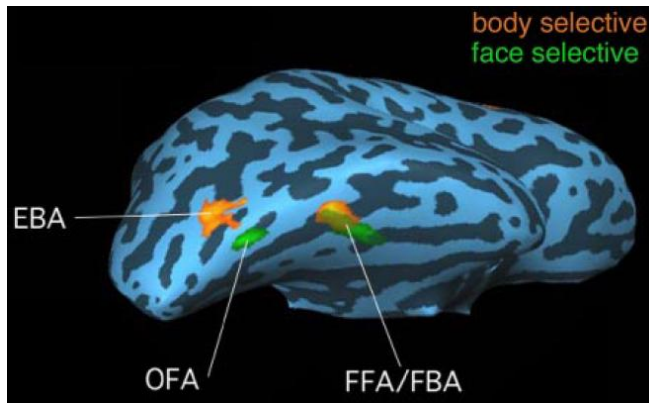
Figure 4.9 - Rendering of the cortical surface of one individual's right hemisphere. Regions of interest are identified for illustrative purposes. Regions were defined by bodies or faces vs. tools, each at a threshold of P < 0.0001. EBA, extrastriate body area; OFA, occipital face area; FFA, fusiform face area; FBA, fusiform body area. Reproduced from (Taylor, Wiggett, & Downing, 2007).

4.3   Visual localizers as a clinical mapping tool in epilepsy

As highlighted throughout the thesis, fMRI is increasingly being used to evaluate children and adolescents who are candidates for surgical treatment of intractable epilepsy. It has the advantage of being noninvasive and well tolerated by young people. By identifying important functional regions within the brain, including unpredictable patterns of functional reorganization, it can aid in surgical decision-making (Liégeois, Cross, Gadian, & Connelly, 2006).

Used in conjunction with conventional investigative methods such as neuropsychological assessment, MRI, and electrophysiology, it can 1) help to improve functional outcome by enabling resective surgery that spares functional cortex, 2) guide surgical intervention by revealing when reorganization of function has occurred, and 3) show when abnormal cortex is also functionally active, and hence that surgery may not be the best option.

Currently, fMRI mapping studies for neurosurgery have focused on language, motor and memory networks (for a review see (Tharin & Golby, 2007)). Although category-specific tasks are included in the memory assessment, we believe that the evaluation of the whole category-preferring visual networks is an important addition to this battery of tests.

Cases that would most directly benefit with the inclusion of these tests are cases of reflex visual seizures not induced by flicker but due to complex visual stimuli such as patterns or round objects (Brockmann, Huppke, Karenfort, Gärtner, & Höger, 2005), or cases where pre-ictal or post-ictal symptoms include visual manifestations, such as prosopagnosia following noncolvusive seizures (Wright, Wardlaw, Young, & Zeman, 2006). Although the visual word form area (selective for words, pseudowords and letter strings) was not included in this discussion, localizers for this area would also be an important tool for epilepsy patients with manifestations of pure alexia, a subset of reading epilepsy.

However, the aforementioned cases are rare manifestations of epilepsy, and thus the main application is in localizing epileptic foci in posterior brain epilepsy. This task remains a difficult exercise in the evaluation for epilepsy surgery because none of the available methods, including reports of clinical manifestations, neurological examination, EEG assessment and neuropsychological evaluations, provides sufficient information about the area of onset, and the fast spread of paroxysms often produces mixed features of occipital, temporal and parietal related symptoms (Lopes et al., 2011). A number of authors have shown that the characterization of EEG category-selective VEPs concerning magnitude and symmetry can prove informative to the localization of the foci (Lopes et al., 2011). Other authors have shown the

impact on visuoperceptual abilities following prolonged seizure activity (Brancati et al., 2012). Following these lines of thinking, and keeping in mind the superior spatial resolution of fMRI in relation to EEG, it is easy to understand the benefit of assessing the topography, asymmetry and magnitudes of activation in category-preferring networks in epileptic patients. Furthermore, this technique is also more adequate to investigate the functioning in the parahippocampal cortices, which can be also impaired in TLE and is difficult to study with EEG due to the distance to the sensors.

However, it is not trivial to achieve robust category-selective signals in individual subjects, and the design of appropriate tight comparisons requires careful optimization of the localizing procedure, as mentioned next.

4.4 Optimizing localization of category-selective networks: impact on topography

There are established general procedures to perform retinotopy, the mapping of low-level visual areas. By using similar checkerboard rotating wedges and expanding rings to identify and delineate boundaries (Engel et al., 1994; Sereno et al., 1995), researchers across groups can build on each others' methods and results to further functionally characterize these areas.

For the localization of higher-level visual areas, such standardization in methodology has not yet been achieved. Methods, and hence results, vary between groups and render the interpretations difficult. There are five factors crucial to the visual localizer methodology in fMRI paradigms: the stimuli used, the overall number of volumes acquired, the control categories used to contrast the experimental category of interest with, the task performed by the subject and the statistical thresholds used. Adding to this the intrinsic anatomical variability in size and location of these areas in different subjects one can understand the difficulty in reaching an agreement upon topography for

category-preferring networks, leading to great differences in the extension and localization of these regions.

Some authors have undergone great efforts to optimize localizer methodology, mainly focusing on the face-preferring network (Berman et al., 2010; Fox, Iaria, & Barton, 2009; Julian, Fedorenko, Webster, & Kanwisher, 2012; Kawabata Duncan & Devlin, 2011; Nieto-Castañón & Fedorenko, 2012; Pitcher, Dilks, Saxe, Triantafyllou, & Kanwisher, 2011). They studied the impact of using static or dynamic stimuli, performing loser vs tighter category comparisons, tasks vs passive viewing and strict vs liberal statistical thresholds.

In addition to these attempts to summarize and homogenize 15 years of localizer variability, other ways to improve reliable single-subject identification of category-preferring networks are being explored.

One such way is to take advantage of the consistent spatial relations to other functionally-defined areas. Although this issue had been established for the spatial relations to low-level retinotopic areas (Halgren et al., 1999), only recently a study used spatial relations and high-resolution functional scanning to refine the organization of face and body-preferring regions of the ventral temporal cortex (Weiner & Grill-Spector, 2010).

This latter author and colleagues focused on the ventral aspect of the occipitotemporal cortex, and, moved by our own findings while conductiong localizers, we conducted a small study on the organization of distinct face-selective areas of the lateral occipitotemporal cortex (LOTC). We aim at showing that, by combining the anatomical location, spatial relations and functional response profile across categories, face-selective patches within LOTC can be refined. Only an approach that maximizes the use of available information can help to the establishment of equivalent regions across studies and ultimately provide a detailed characterization of the topography and properties of category-preferring networks.

4.5 Proof of concept: Face-preferring patches within the LOTC

In this section we focus on face-selective patches along the Lateral OccipitoTemporal Cortex (LOTC). We aim to confirm, as previously stated, that in addition to the anatomy, a way to dissociate these patches is by exploring the spatial and functional relations to other category-preferring regions, namely, the Extrastriate Body Area (EBA).

By doing so, we assess the possibility that faces also belong to a contiguous topographic representation of the human body within the LOTC (in addition to the representation of faces in the inferior occipital gyrus), suggested by Orlov et al (Orlov, Makin, & Zohary, 2010) (see Figure 4.10).
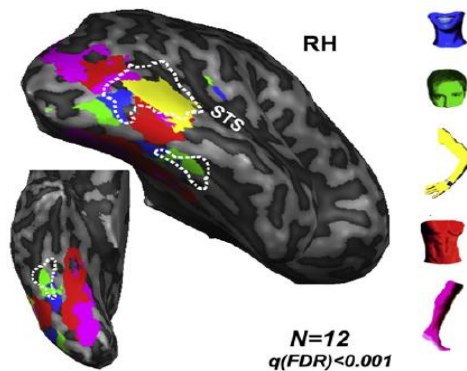
Figure 4.10 – Topographic group map for the preference of body parts in the LOTC. Colors in the group map indicate the preference of each voxel for a certain body part across participants (see icons). These voxels were almost exclusively located in the OTC. The white dashed lines depict the boundaries of EBA and FBA across participants (as defined by an independent localizer). Adapted from (Orlov et al., 2010).

4.5.1   Methods

fMRI data was collected (TR 2secs) from 9 subjects (3 females), ages 20-37 years. All had normal or corrected to normal vision.

The study followed the tenets of the Declaration of Helsinki, informed consent being obtained from all subjects for the protocol, which was approved by our local Ethics Committee.

Images were obtained on a Siemens Tim Trio 3T scanner using a 12 channel head coil. Structural images were collected using a T_1 weighted MPRAGE (magnetization-prepared rapid-acquisition gradient echo) (TR = 2300ms, TE = 2.98ms, flip angle = 9º, matrix size = 256x256 , voxel size = 1mm^3). Standard T_2*-weighted gradient-echo echo planar imaging was used for the functional task runs (TR = 2000ms; TE = 47ms; 2.5x2.5 in-plane resolution ; 3.5mm slice thickness with 0.7mm gap ; flip angle = 90º; matrix size= 102x102; number of slices = 25; 231 measurements). The slices were positioned parallel to the inferotemporal surface of the brain to obtain maximum coverage. All runs were acquired in the same session. Image processing was performed using BrainVoyager QX v2.1 (Brain Innovation, Maastricht, The Netherlands) Pre-processing steps included motion correction, slice scan-time correction, linear trend removal and temporal low and high-pass filtering of 0.00980 Hz (3 cycles in time course).

Our standard localizer stimuli set consists of grayscale images of faces, places (landscapes, buildings, skylines), objects (tools, cars, chairs), bodies (silhouettes, limbs, headless bodies - made available by Christopher Fox in Fox et al (Fox et al., 2009)) and scrambled versions of objects.
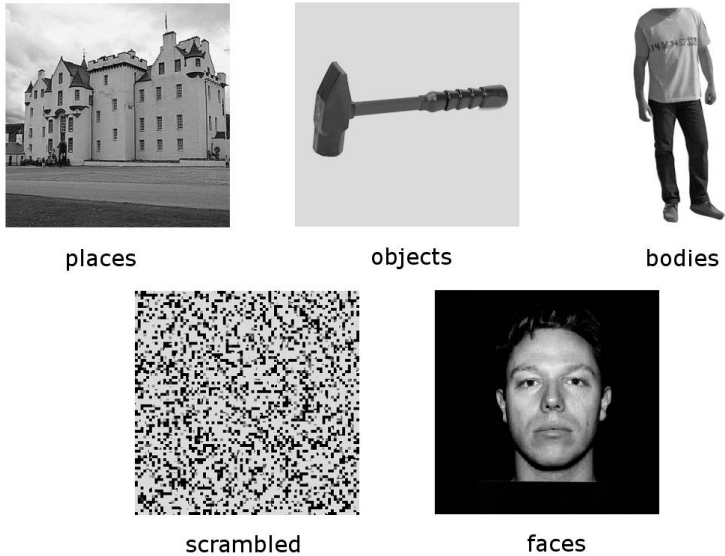
Figure 4.11 – Examples of stimuli used in the localizer task

To quantify activations, assess effects and confirm or reject a hypothesis, a statistical framework is necessary. In the particular case of fMRI, the main statistical instrument is the General Linear Model, also known as GLM (Turner, Friston, Ashburner, Josephs, & Howseman, 1996).

In short, the GLM sets up a model (i.e., a general pattern which you expect to see in the data) and fits it to the data. Such model consists of a set of hypotheses about how BOLD activity might change as a result of the experiment and is used to summarise data in a few parameters that are pertinent to the experiment.

A graphical demonstration is more appealing.

Suppose you have the following timeline, typical of localizers, but only with images of faces and objects:

Images of Faces   Images of Objects   Rest
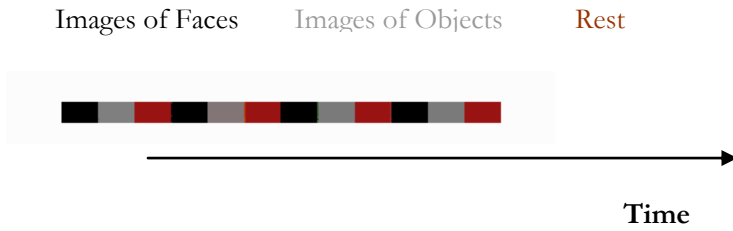
In this case, the model consists of a set of assumptions of the type:

"A voxel that is into face processing might have a time-series looking like this"
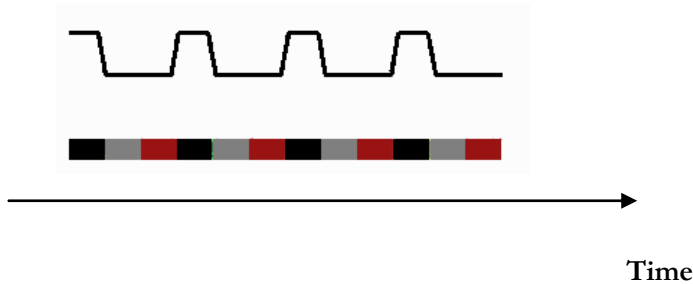
Time

"A voxel that is into object processing might have a time-series looking like this"
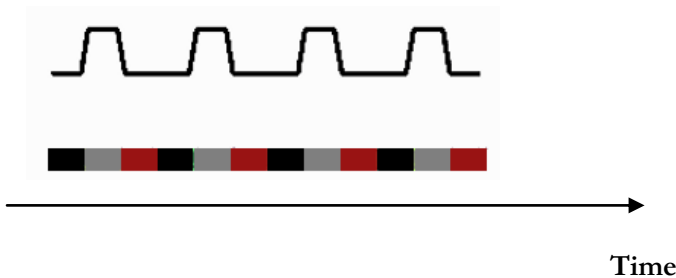
Time

and, "A voxel that is irrelevant to the task might have a time-series looking like this"
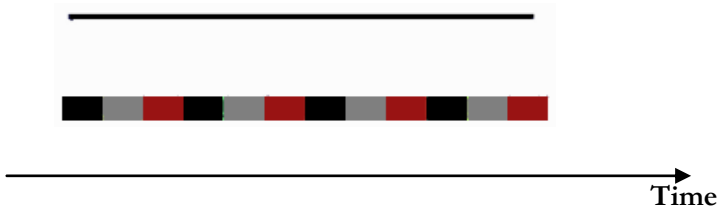
Time

For a given voxel (time-series) the GLM figures out just what type that is by "modelling" it as a linear combination of the hypothetical time-series also named predictors.

The estimation entails finding the parameter values such that the linear combination "best" fits the data. In this case,

Measured   "Known"   "Unknown "parameters"
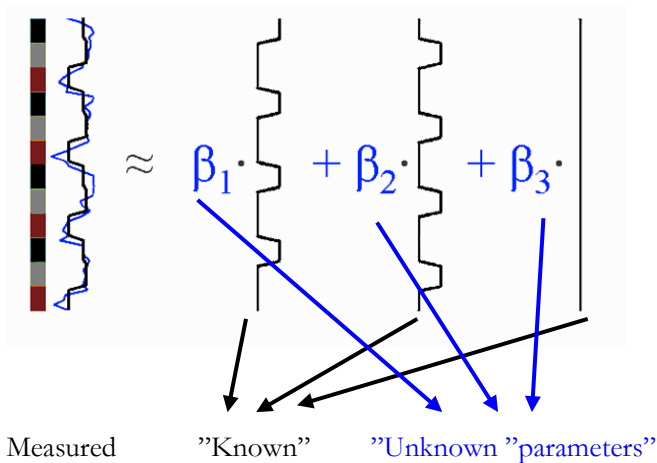
For each voxel or region, the results obtained for these beta values are indicative of how much each condition impacts BOLD activity. Using their values and the statistics of their estimation, they can be combined or compared across conditions in an operation known as a **contrast**. In this case, the output of the contrast beta1 vs beta2 would tells us how much more this voxel responds to faces than to objects, and how signifficant this difference is.

BrainVoyager QX (Brain Innovation, Maastricht, The Netherlands) was the software used for pre-processing the fMRI data, building the GLM and performing statistical tests.

During the localizer subjects performed a 1-back task to keep attention levels stable (they had to perform a button pressing when two consecutive images were equal). 60 volumes were acquired for each condition along two runs. Blocks lasted 20secs (which corresponded to 20 images, 800ms presentation, 200ms inter-stimulus interval) with 10s fixation in between blocks.

Half of the data (the first run of each subject) was used to localize the face and body selective Regions of Interest (ROIs) whilst the other half (second run of each subject) was used to compute contrast values for those ROIs, thus rendering the two analyses independent.

Face selective ROIs were defined as the contiguous patches along the LOTC obeying the criteria Faces>Objects AND Faces>Places AND Faces>Scrambled, p<0.005 uncorrected.

The EBA was defined as the contiguous patch of the Lateral Occipito-Temporal Cortex showing Bodies>Objects AND Bodies>Places AND Bodies>Scrambled, p<0.005 uncorrected.

Given the right-hemispheric dominance in the face-processing literature, and ensuing higher statistical power to detect all relevant regions, analysis was restricted to the right hemisphere.

4.5.2   Results and Discussion

Our localizer unveiled two small face-selective regions in the LOTC (Figure 4.12), one along the posterior STS and another encroached in the anterior/superior boundary of the EBA, near the posterior continuation of the STS and the inferior temporal sulcus.

The first one corresponds to the commonly described STS, while the latter was noted in only a few studies (Pinsk, DeSimone, Moore, Gross, & Kastner, 2005; Pitcher et al., 2011) where it was labelled as pcSTS (posterior continuation of the superior temporal sulcus).
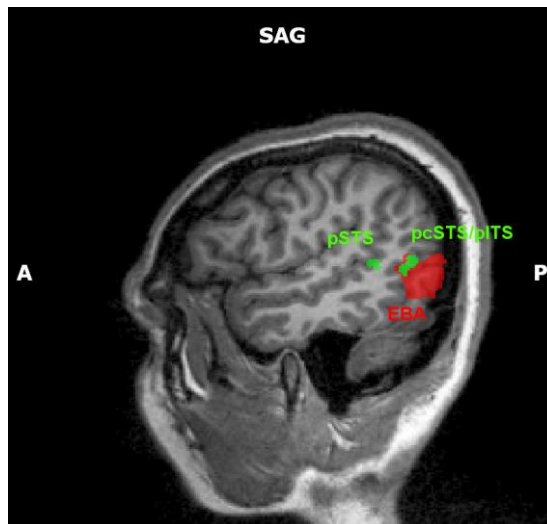
Figure 4.12 - Face-preferring (green) and body-preferring (red) patches in the right Lateral Occipital Temporal Cortex as defined by the localizer (first runs of each subject). Abbreviations: pSTS – posterior Superior Temporal Sulcus; pcSTS/pITS – posterior continuation of the Superior Temporal Sulcus/ posterior Inferior Temporal Sulcus; EBA – Extrastriate Body Area

The coordinates and response profile of these two areas to the shown categories (assessed with independent data) is summarized in Table 4.1. We defend that these are two fundamentally different regions that can be mapped on the majority of subjects.

Notably, the main distinction between these areas, as assessed within the context of this study, besides their anatomical location, is their differential response to the contrast Faces vs Bodies. As hypothesized, while the pcSTS/pITS shows a significantly higher response for bodies than faces, the pSTS shows the inverse relation. It is important to note that, although it may seem paradoxical, saying that a region responds more to bodies than to faces does not invalidate it being technically face-preferring. The contrast faces vs bodies was not used to define the regions. When establishing preference, neuroscientists always assess preference of a category **against** the other categories used to define the region, in this case, faces and objects/places/scrambled. In fact, although highly unlikely, all category-preferring regions known to date may hypothetically yield a higher response to some untested category. We will return to this point in Chapter 6. As an alternative explanation, it may be that the resolution of fMRI has not yet evolved to the point of discriminating between these regions. In the future, studies focused on this region alone may disentangle these patches similarly to the dissociation shown for the FFA and FBA (Schwarzlose, Baker, & Kanwisher, 2005).

pSTS (47, -42, 5)

Predictor	beta	se	t	p
faces	0.346	0.075	4.634	0.000004
objects	-0.114	0.071	-1.598	0.110267
places	0.002	0.071	0.031	0.974976
scrambled	-0.175	0.071	-2.458	0.014056
body	0.112	0.071	1.572	0.116149

Contrast / LF	value	se	t	p
f vs o	0.460	0.091	5.030	0.000001
f vs p	0.344	0.092	3.728	0.000199
f vs s	0.521	0.092	5.665	0.000000
f vs b	0.234	0.092	2.552	0.010780

pcSTS/pITS (46, -57, 5)

Predictor	beta	se	t	p
faces	0.315	0.069	4.538	0.000006
objects	0.084	0.070	1.197	0.231414
places	0.017	0.071	0.246	0.805685
scrambled	-0.067	0.071	-0.948	0.343238
body	0.566	0.071	8.010	0.000000

Contrast / LF	value	se	t	p
f vs o	0.230	0.091	2.541	0.011115
f vs p	0.297	0.091	3.260	0.001130
f vs s	0.382	0.091	4.192	0.000029
f vs b	-0.251	0.091	-2.762	0.005796

Table 4.1 – Talairach coordinates, response profile and contrast values for the defined face-selective ROIs, assessed by independent data (second runs of each subject). Both areas exhibit face-selectivity for all of the categories, except for the contrast faces vs bodies in pcSTS/pITS (negative t-value). f – faces; o – objects; p – places; s – scrambled; b – bodies

With this study we showed that by combining information concerning anatomy, response profile, and spatial relations, category-preferring ROIs can be uniquely identified and studied. However, an attempt to characterize a network that privileges a given category would be incomplete without a study assessing the factors that drive this favoured processing, i.e., endogenous factors depending on the subjective experience rather than the low-level properties of the stimuli. To this goal, we designed decision-making paradigms using ambiguous images, as to highlight such properties and investigate perceptual closure. First, we provide the general architecture as well as our own contributions to the understanding of the neural correlates of perceptual decision-making in the human brain.

References

Atkinson, A. P., & Adolphs, R. (2011). The neuropsychology of face perception: beyond simple dissociations and functional selectivity. *Philosophical transactions of the Royal Society of London. Series B, Biological sciences*, *366*(1571), 1726–38.

Berman, M. G., Park, J., Gonzalez, R., Polk, T. a, Gehrke, A., Knaffla, S., & Jonides, J. (2010). Evaluating functional localizers: the case of the FFA. *NeuroImage*, *50*(1), 56–71.

Brambati, S. M., Myers, D., Wilson, A., Rankin, K. P., Allison, S. C., Rosen, H. J., Miller, B. L., et al. (2006). The anatomy of category-specific object naming in neurodegenerative diseases. *Journal of Cognitive Neuroscience*, *18*(10), 1644–1653.

Brancati, C., Barba, C., Metitieri, T., Melani, F., Pellacani, S., Viggiano, M. P., & Guerrini, R. (2012). Impaired object identification in idiopathic childhood occipital epilepsy. *Epilepsia*, *53*(4), 686–94.

Brockmann, K., Huppke, P., Karenfort, M., Gärtner, J., & Höger, C. (2005). Visually self-induced seizures sensitive to round objects. *Epilepsia*, *46*(5), 786–9.

Calvert, G. A., Bullmore, E. T., Brammer, M. J., Campbell, R., Williams, S. C., McGuire, P. K., Woodruff, P. W., et al. (1997). Activation of Auditory Cortex During Silent Lipreading. *Science*, *276*(5312), 593–596.

Caramazza, A., & Mahon, B. Z. (2003). The organization of conceptual knowledge: the evidence from category-specific semantic deficits. *Trends in Cognitive Sciences*, *7*(8), 354–361.

Damasio, H., Grabowski, T. J., Tranel, D., Hichwa, R. D., & Damasio, A. R. (1996). A neural basis for lexical retrieval. *Nature*, *380*(6574), 499–505.

De Renzi, E. (2000). Disorders of visual recognition. *Seminars in Neurology*, *20*(4), 479–485.

Downing, P. E., Chan, a W.-Y., Peelen, M. V., Dodds, C. M., & Kanwisher, N. (2006). Domain specificity in visual cortex. *Cerebral cortex (New York, N.Y. : 1991)*, *16*(10), 1453–61.

Downing, P. E., Jiang, Y., Shuman, M., & Kanwisher, N. (2001). A cortical area selective for visual processing of the human body. *Science (New York, N.Y.)*, *293*(5539), 2470–3.

Drane, D. L., Ojemann, G. a, Aylward, E., Ojemann, J. G., Johnson, L. C., Silbergeld, D. L., Miller, J. W., et al. (2008). Category-specific naming and recognition deficits in temporal lobe epilepsy surgical patients. *Neuropsychologia*, *46*(5), 1242–55.

Drucker, D. M., & Aguirre, G. K. (2009). Different Spatial Scales of Shape Similarity Representation in Lateral and Ventral LOC, (2), 2269–2280.

Engel, S. A., Rumelhart, D. E., Wandell, B. A., Lee, A. T., Glover, G. H., Chichilnisky, E. J., & Shadlen, M. N. (1994). fMRI of human visual cortex. *Nature*. 369, 525

Epstein, R, & Kanwisher, N. (1998). A cortical representation of the local visual environment. *Nature*, *392*(6676), 598–601.

Epstein, R. A., Higgins, J. S., & Thompson-Schill, S. L. (2005). Learning places from views: variation in scene processing as a function of experience and navigational ability. *Journal of cognitive neuroscience*, *17*(1), 73–83.

Epstein, Russell a, Parker, W. E., & Feiler, A. M. (2007). Where am I now? Distinct roles for parahippocampal and retrosplenial cortices in place recognition. *The Journal of neuroscience: the official journal of the Society for Neuroscience*, *27*(23), 6141–9.

Felleman, D. J., & Van Essen, D. C. (1991). Distributed hierarchical processing in the primate cerebral cortex. (A. T. Smith & R. J. Snowden, Eds.) *Cerebral Cortex*, *1*(1), 1–47.

Fox, C. J., Iaria, G., & Barton, J. J. S. (2009). Defining the Face Processing Network: Optimization of the Functional Localizer in fMRI, *1651*, 1637–1651.

Gainotti, G. (2000). What the locus of brain lesion tells us about the nature of the cognitive defect underlying category-specific disorders: a review. *Cortex*, *36*(4), 539–559.

Gauthier, I., Tarr, M. J., Moylan, J., Skudlarski, P., Gore, J. C., & Anderson, a W. (2000). The fusiform "face area" is part of a network that processes faces at the individual level. *Journal of cognitive neuroscience*, *12*(3), 495–504.

Gerlach, C. (2007). A review of functional imaging studies on category specificity. *Journal of cognitive neuroscience*, *19*(2), 296–314.

Goodale, M. A., Milner, A. D., Jakobson, L. S., & Carey, D. P. (1991). A neurological dissociation between perceiving objects and grasping them. *Nature*, *349*(6305), 154–156.

Grill-Spector, K, Kourtzi, Z., & Kanwisher, N. (2001). The lateral occipital complex and its role in object recognition. *Vision research*, *41*(10-11), 1409–22.

Grill-Spector, K, Kushnir, T., Edelman, S., Avidan, G., Itzchak, Y., & Malach, R. (1999). Differential processing of objects under various viewing conditions in the human lateral occipital complex. *Neuron*, *24*(1), 187–203.

Grill-Spector, Kalanit, & Malach, R. (2004). The human visual cortex. *Annual review of neuroscience*, *27*, 649–77.

Halgren, E., Dale, a M., Sereno, M. I., Tootell, R. B., Marinkovic, K., & Rosen, B. R. (1999). Location of human face-selective cortex with respect to retinotopic areas. *Human brain mapping*, *7*(1), 29–37.

Hanson, S. J., Matsuka, T., & Haxby, J. V. (2004). Combinatorial codes in ventral temporal lobe for object recognition: Haxby (2001) revisited: is there a "face" area? *NeuroImage*, *23*(1), 156–66.

Hasson, U., Harel, M., Levy, I., & Malach, R. (2003). Large-scale mirror-symmetry organization of human occipito-temporal object areas. *Neuron*, *37*(6), 1027–1041.

Haxby, J., Hoffman, E., & Gobbini, M. (2000). The distributed human neural system for face perception. *Trends in Cognitive Sciences*, *4*(6), 223–233.

Hubel, D. H., & Wiesel, T. N. (1968). Receptive fields and functional architecture of monkey striate cortex. *The Journal of Physiology*, *195*(1), 215–243.

Humphreys, G. W., & Riddoch, M. J. (1984). Routes to object constancy: implications from neurological impairments of object constancy. *Quarterly Journal of Experimental Psychology*. 36(3), 385-415

Ishai, A., Schmidt, C. F., & Boesiger, P. (2005). Face perception is mediated by a distributed cortical network. *Brain research bulletin*, *67*(1-2), 87–93.

Julian, J. B., Fedorenko, E., Webster, J., & Kanwisher, N. (2012). An algorithmic method for functionally defining regions of interest in the ventral visual pathway. *NeuroImage*, *60*(4), 2357–2364.

Kanwisher, N., McDermott, J., & Chun, M. M. (1997). The fusiform face area: a module in human extrastriate cortex specialized for face perception. *The Journal of neuroscience: the official journal of the Society for Neuroscience*, *17*(11), 4302–11.

Kanwisher, N., & Yovel, G. (2006). The fusiform face area: a cortical region specialized for the perception of faces. *Philosophical transactions of the Royal Society of London. Series B, Biological sciences*, *361*(1476), 2109–28.

Kawabata Duncan, K. J., & Devlin, J. T. (2011). Improving the reliability of functional localizers. *NeuroImage*, *57*(3), 1022–30.

Kourtzi, Z, & Kanwisher, N. (2001). Representation of perceived object shape by the human lateral occipital complex. *Science (New York, N.Y.)*, *293*(5534), 1506–9.

Kourtzi, Zoe, Erb, M., Grodd, W., & Bülthoff, H. H. (2003). Representation of the perceived 3-D object shape in the human lateral occipital complex. *Cerebral cortex (New York, N.Y.: 1991)*, *13*(9), 911–20.

Kourtzi, Zoe, Tolias, A. S., Altmann, C. F., Augath, M., & Logothetis, N. K. (2003). Integration of local features into global shapes: monkey and human FMRI studies. *Neuron*, *37*(2), 333–46.

Liégeois, F., Cross, J. H., Gadian, D. G., & Connelly, A. (2006). Role of fMRI in the decision-making process: epilepsy surgery for children. *Journal of magnetic resonance imaging: JMRI*, *23*(6), 933–40.

Lopes, R., Cabral, P., Canas, N., Breia, P., Foreid, J. P., Calado, E., Silva, R., et al. (2011). N170 asymmetry as an index of inferior occipital dysfunction in patients with symptomatic occipital lobe epilepsy. *Clinical neurophysiology: official journal of the International Federation of Clinical Neurophysiology*, *122*(1), 9–15.

Lyons, F., Kay, J., Hanley, J. R., & Haslam, C. (2006). Selective preservation of memory for people in the context of semantic memory disorder: patterns of association and dissociation. *Neuropsychologia*, *44*(14), 2887–2898.

Maguire, E. (2001). The retrosplenial contribution to human navigation: A review of lesion and neuroimaging findings. *Scandinavian Journal of Psychology*, *42*(3), 225–238.

Mahon, B. Z., & Caramazza, A. (2009). Concepts and categories: a cognitive neuropsychological perspective. *Annual review of psychology*, *60*, 27–51.

Malach, R, Reppas, J. B., Benson, R. R., Kwong, K. K., Jiang, H., Kennedy, W. a, Ledden, P. J., et al. (1995). Object-related activity revealed by functional magnetic resonance imaging in human occipital cortex. *Proceedings of the National Academy of Sciences of the United States of America*, *92*(18), 8135–9.

Malach, Rafael, Levy, I., & Hasson, U. (2002). The topography of high-order human object areas. *Trends in cognitive sciences*, *6*(4), 176–184.

Martin, A. (2007). The representation of object concepts in the brain. *Annual review of psychology*, *58*, 25–45.

Maunsell, J. H., & Newsome, W. T. (1987). Visual processing in monkey extrastriate cortex. *Annual Review of Neuroscience*, *10*(1), 363–401.

Nasr, S., Liu, N., Devaney, K. J., Yue, X., Rajimehr, R., Ungerleider, L. G., & Tootell, R. B. H. (2011). Scene-selective cortical regions in human and nonhuman primates. *The Journal of neuroscience : the official journal of the Society for Neuroscience*, *31*(39), 13771–85.

Nieto-Castañón, A., & Fedorenko, E. (2012). Subject-specific functional localizers increase sensitivity and functional resolution of multi-subject analyses. *NeuroImage* (in press).

Orlov, T., Makin, T. R., & Zohary, E. (2010). Topographic representation of the human body in the occipitotemporal cortex. *Neuron*, *68*(3), 586–600.

Park, S., & Chun, M. M. (2009). Different roles of the parahippocampal place area (PPA) and retrosplenial cortex (RSC) in panoramic scene perception. *NeuroImage*, *47*(4), 1747–56.

Pinsk, M. a, DeSimone, K., Moore, T., Gross, C. G., & Kastner, S. (2005). Representations of faces and body parts in macaque temporal cortex: a functional MRI study. *Proceedings of the National Academy of Sciences of the United States of America*, *102*(19), 6996–7001.

Pitcher, D., Dilks, D. D., Saxe, R. R., Triantafyllou, C., & Kanwisher, N. (2011). Differential selectivity for dynamic versus static information in face-selective cortical regions. *NeuroImage*, *56*(4), 2356–63.

Puce, a, Allison, T., Bentin, S., Gore, J. C., & McCarthy, G. (1998). Temporal cortex activation in humans viewing eye and mouth movements. *The Journal of neuroscience : the official journal of the Society for Neuroscience*, *18*(6), 2188–99.

Schwarzlose, R. F., Baker, C. I., & Kanwisher, N. (2005). Separate face and body selectivity on the fusiform gyrus. *The Journal of neuroscience the official journal of the Society for Neuroscience*, *25*(47), 11055–11059.

Sereno, M. I., Dale, A. M., Reppas, J. B., Kwong, K. K., Belliveau, J. W., Brady, T. J., Rosen, B. R., et al. (1995). Borders of multiple visual areas in humans revealed by functional magnetic resonance imaging. *Science New York NY*, *268*(5212), 889–893.

Spiridon, M., Fischl, B., & Kanwisher, N. (2006). Location and spatial profile of category-specific regions in human extrastriate cortex. *Human brain mapping*, *27*(1), 77–89.

Tarr, M. J., & Gauthier, I. (2000). FFA: a flexible fusiform area for subordinate-level visual processing automatized by expertise. *Nature neuroscience*, *3*(8), 764–9.

Taylor, J. C., Wiggett, A. J., & Downing, P. E. (2007). Functional MRI analysis of body and body part representations in the extrastriate and fusiform body areas. *Journal of neurophysiology*, *98*(3), 1626–33.

Taylor, J. C., Wiggett, A. J., & Downing, P. E. (2008). Functional MRI Analysis of Body and Body Part Representations in the Extrastriate and Fusiform Body Areas, 1626–1633.

Tharin, S., & Golby, A. (2007). Functional brain mapping and its applications to neurosurgery. *Neurosurgery*, *60*(4 Suppl 2), 185–201; discussion 201–2.

Turner, R., Friston, K., Ashburner, J., Josephs, O., & Howseman, A. (1996). Analysis of fMRI data using the general linear statistical model. *NeuroImage*, *3*(1), S102–S102.

Wandell, B. a, Dumoulin, S. O., & Brewer, A. a. (2007). Visual field maps in human cortex. *Neuron*, *56*(2), 366–83.

Weiner, K. S., & Grill-Spector, K. (2010). Sparsely-distributed organization of face and limb activations in human ventral temporal cortex. *NeuroImage*, *52*(4), 1559–73.

Weiner, K. S., & Grill-Spector, K. (2011). Not one extrastriate body area: using anatomical landmarks, hMT+, and visual field maps to parcellate limb-selective activations in human lateral occipitotemporal cortex. *NeuroImage*, *56*(4), 2183–99.

Wright, H., Wardlaw, J., Young, A. W., & Zeman, A. (2006). Prosopagnosia following nonconvulsive status epilepticus associated with a left fusiform gyrus malformation. *Epilepsy & behavior : E&B*, *9*(1), 197–203.

Xu, Y. (2005). Revisiting the role of the fusiform face area in visual expertise. *Cerebral cortex (New York, N.Y. : 1991), 15*(8), 1234–42.

Chapter 5

Neural correlates of perceptual decision-making in the brain: the multiple functional divisions of the insula

5.1 Open issues and motivation for the study

So far, we have been addressing visual processing in a hierarchical manner which has been strictly bottom-up, starting with the low-level visual system that extracts features from the seen images and feedforwards this information to high level regions. However, to fully understand visual processing we must consider the tasks and goals that drive this feature extraction, i.e., we must consider how top-down processes interact with and shape bottom-up processing. The most relevant concept to take into account in this context is that of perceptual decision-making, which modulates categorization and processing dynamics, especially when presented with ambiguous visual information.

Prior to addressing the influence of perceptual demands on the functional properties of dedicated visual modules and networks, it is vital to identify the neural correlates of decision-making beyond the temporal lobe. Such an elucidation of sensory, perceptual, cognitive control and motor processes in decision making remains an outstanding neuroscientific challenge (Kayser, Buchsbaum, Erickson, & D'Esposito, 2010; Schall, 2001); for review see Heekeren et al, 2008 (Heekeren, Marrett, & Ungerleider, 2008). Although the involvement of multiple interacting modules is consensual (Gold & Shadlen, 2007; Platt, 2002; Salinas, 2008; Wang, 2008), it is hard to infer the exact role of each because of the simultaneous recruitment of distinct cognitive processes. This overlap of cognitive operations gives rise to different theories about the functions of areas thought to be critical in the decision-making architecture, such as the bilateral anterior insula and the adjacent frontal operculum, placed at the core of such processes by a number of studies (Binder, Liebenthal, Possing, Medler, & Ward, 2004; Ho, Brown, & Serences, 2009; Thielscher & Pessoa, 2007). The cognitive role of the insular cortex has received increasing attention and recent evidence highlighting the anatomical and functional

subdivisions of the insula (Cauda et al., 2011; Deen, Pitskel, & Pelphrey, 2010) pave the way for the possibility that this area is not restricted to a single role in the decision-making architecture.

Here, we addressed the role of distinct operculo-insular regions in decision making by using functional Magnetic Resonance Imaging (fMRI) in a neurochronometric face detection task during which the time of perceptual decision was experimentally uncoupled both from time of stimulus onset and from the time of response. This research strategy is relevant to the parsing of a complex mental operation into its components(Sigman & Dehaene, 2005). Such components can be obtained both by means of a widespread data-driven decomposition (ICA, independent component analysis) and standard task-related protocols (GLM, general linear model). Hence, we adapted the accumulator-based decision architecture used by Ploran et al (Ploran et al., 2007; Ploran, Tremel, Nelson, & Wheeler, 2011) (consisting of sensory processors, evidence-accumulation mechanisms and decision-signaling modules) and extended it to investigate a general mechanism concerning the integration of holistic perceptual evidence, decision signaling and response.

We have chosen a dual-task face detection paradigm using Mooney face stimuli (two-tone abstract-like face images) (Mooney, 1957) to investigate these questions. The emergence of the global holistic percept in these images occurs in the absence of change in local saliency cues or sensory signal to noise ratios. In the first task, response is executed upon the moment of perception/detection whilst in the second task the time is color-coded (see Materials and Methods) and the response is delayed. The rationale for including this modified version of the response task was that such procedure abolishes immediate response and minimizes motor planning at the moment of decision whilst keeping information on the detection time.
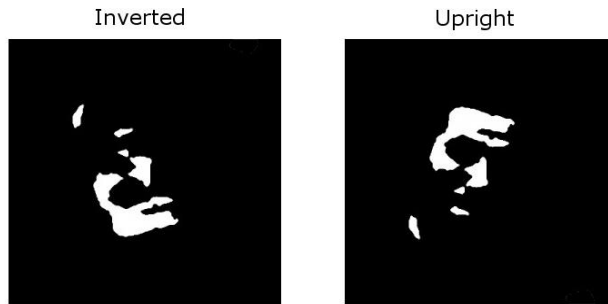
Inverted   Upright

Figure 5.1 - Example of a Mooney image in its inverted and upright versions. Note how the apparently meaningless content becomes readily visible in the upright configuration

This design allowed separation between decision and motor/response processes and by combining the different temporal properties of the tasks we distinguish between sensory regions, motor regions, and those with a broader role in cognitive control and its relation to the holistic decision process.

The combination of these approaches and constraints can help disambiguate the role, or more importantly, roles, of the insular cortex/frontal operculum in the decision-making architecture. Furthermore, we probe the gradient hypothesis proposed by Bud Craig (Craig, 2009) and assessed in the connectivity patterns explored by Cerliani et al (Cerliani et al., 2012) , which suggests that as one moves from posterior to more anterior sites within the insula, the primary interoceptive representations gradually integrate motivational, social and cognitive activity.

5.2. Materials and Methods

5.2.1 Subjects

14 right-handed subjects (8 females, 6 males, ages 21-41 years) participated in the study after providing informed consent. All had normal or corrected to normal vision.

The study followed the tenets of the Declaration of Helsinki, informed consent being obtained from all subjects for the protocol, which was approved by our local Ethics Committee.

5.2.2 Stimuli and Task design

Mooney face stimuli (two-tone images) were chosen because they provide a classical way of generating ambiguous perception (which is enhanced if stimuli are viewed upside down). These stimuli may appear devoid of any recognizable object for several seconds until the observer suddenly becomes aware of the emergence of a holistic face percept. Difficulty levels were adjusted in pilot experiments to render uncertain the presence of a face and to decrease the likelihood of immediate detection. Trials where faces were not perceived can effectively be considered as scrambled controls. These stimuli characteristics were suited to the research goal of uncoupling sensation from object perception for the following reasons:

- sudden global awareness of the face will lead to temporally contained perceptual events that are separable from initial local sensory processing; differential onset of activity on "early" and "late" detection trials is a distinguishing characteristic of a neural encoder of perception processes. This

property can advantageously be used in identifying the perceptual networks involved in the decision process.

- interpretation of the presence of a face relies on holistic perception and cannot easily be achieved through local visual analysis, thereby optimizing the delay between local sensory processing and global perception. Accordingly, the pre-perceptual period of Mooney face stimuli serves as a sensory control/baseline

- further high-level processing of the face (identity, emotion, and other categorical aspects) is deemphasized given stimuli "abstractedness".

5.2.2.1 Simultaneous Decision and Response Task

Mooney images were built by thresholding 60 online images of faces. Online images were favored over databases because they provide more variety in lighting, angle and face sizes, thus maximizing ambiguity.

Difficulty levels were adjusted in pilot experiments to guarantee the desired spread in perception times (% of correct/incorrect answers).

The 120 Mooney images were converted into movies, each lasting 12s, that consist of the rotation of such images. Starting from the inverted position, the image slowly rotates 20º per second until it reaches the upright position where it rests for 3s. There were no repeated movies. Stimuli were presented in a black background and subtended approximately 12.40º of the visual field. Each experimental run consisted of 30 movies interleaved with 8s fixation baseline periods. Subjects were instructed to respond as soon as (but only if) they were confident they were seeing a face. Response was achieved through a response box, by the pressing of a button with a finger of the left hand. This task is referred to as the "Simultaneous Response Task"

5.2.2.2 Color Task: Delayed Response vs. Decision

Stimuli also consisted of 30 movies, each lasting 12s. The movies showed 2-tone (black and white) images of putative faces (Mooney faces) starting in the inverted position and slowly rotating 20º per second until they reached upright position where they rest for 3s. The image foreground changes color every TR (2sec) in the following order (white, blue, yellow, pink, green, light gray). There were no repeated movies (nor within the run nor from the Simultaneous Response Task run). Other stimulus properties were identical to the Simultaneous Response Task. Subjects were instructed to identify the color of the face (in case of detection) at the moment of perception. That color (encoding time of decision) was selected from a list presented only at the end of the trial. Selection was made by using two buttons in one hand to move a cursor up or down until the correct color was highlighted and then pressing a button with the other hand to confirm the choice. When the subject responded the color list disappeared, followed by fixation. This procedure precludes motor responses concomitant to holistic perceptual events and allows one to keep information on the moment of perception by using a color code thereby enabling separation of decision and motor processes. This task is referred to as the "Color Task". Task designs are summarized in Figure 5.2.
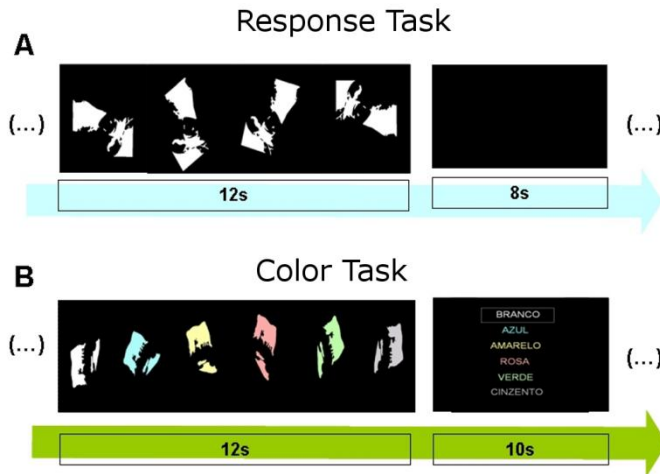
Figure 5.2 - Timeline of the visual recognition task using Mooney stimuli; A – the face rotates from inverted to upright and the subject presses a button when (and only if) a face is detected; B – the "white component" (foreground) of the Mooney face changes color every TR (acquisition volume) and the subject indicates the moment of detection only at the end of the trial by selecting from a list the color that corresponds to detection time.

5.2.2.3 Rationale for the Dual-Task Paradigm

The use of a dual-task paradigm and the complementary nature of the tasks ensure the separation between decision and somatosensory or motor response processes.

Even before directly addressing the decision architecture and ideal activation patterns, let us compare the activity for the two tasks for faces seen, for example, at 4s, i.e., after 4 seconds of rotation. Since the response is delayed in the Color Task (buttons will be pressed only at the end of the trial), areas that are involved merely in the response processes will show a dramatic delay in activity from one task to the other. Accordingly, its activity peak shifts from the time of detection in the Response Task to the end of the trial in the Color

Task. For areas that underlie evidence accumulation or decision signaling this shift will not happen, since the only factor that changes between tasks is the response mechanism.

5.2.3 Image Acquisition parameters and pre-processing

Images were obtained on a Siemens Tim Trio 3T scanner using a 12 channel head coil. Structural images were collected using a T_1 weighted MPRAGE (magnetization-prepared rapid-acquisition gradient echo) (TR = 2300ms , TE = 2.98ms , flip angle = 9º, matrix size = 240x256 , voxel size = 1mm^3). Standard T_2*-weighted gradient-echo echo planar imaging was used for the functional task runs (TR = 2000ms ; TE = 52ms ; 2x2 in-plane resolution ; 3mm slice thickness with no gap ; flip angle = 90º; matrix size= 114x114; number of slices = 23; 455 measurements for the Color Task and 355 for the simultaneous Response Task). The slices were oriented to obtain a brain coverage spanning from the cerebellum to the inferior frontal and parietal lobes, ensuring insular cortex coverage. All runs were acquired in the same session. Image processing was performed using BrainVoyager QX v2.1 (Brain Innovation, Maastricht, The Netherlands) Pre-processing steps included motion correction, slice scan-time correction, linear trend removal and temporal high-pass filtering of 0.00980 Hz (3 cycles in time course).

5.2.4 Data analysis

5.2.4.1 Model-driven approach: RFX-GLM

In order to build an appropriate set of model predictors, we based our analysis (taking into account the specificity of our own design) in the model of Ploran et al (Ploran et al., 2007) and their proposed architecture, with the

important distinction that in our case accumulators do not encode increasing sensory signal to noise levels, since holistic percepts do not necessarily depend on "bottom-up" processes. According to this study, areas relevantly involved in decision-making tasks can be divided into:

- sensory areas, that activate throughout the whole duration of the presented stimulus irrespective of detection times;

- accumulator areas, that reflect gathering of perceptual evidence favoring detection, from stimulus onset up to a moment when the decision threshold is reached (higher accumulation rates imply earlier detection times);

- decision/detection areas which activate transiently around the moment of detection, signaling decision or being recruited by it;

- motor/somatosensory areas, modeled to account for conditions where motor responses coincide with the decision moment but also when they are delayed.

To mimic such modules, 4 regressors (or predictors) were specified:

-Stimulus (S), "on" during the whole period of movie presentation.

- Decision_response (DR) regressor, "on" only on the acquisition volume in which the decision was reported with the button press (Response Task only).

-Decision_color (DC) regressor, "on" only in the time slot in which the face was perceived (based on the color selected at the end of the trial - Color Task only).

-Color_List" (CL), "on" during the period used by the subject to choose the color from the list (Color Task only).

Given that the above specified design (Figure 5.3) features decision regressors that are not orthogonal to the stimulus regressor we performed the standard evaluation of colinearity diagnostics. The standard statistics for this evaluation include the computation of the variance inflation factor (VIF) and its reciprocal, the tolerance, within the set of predictors (Menard, 1995; Myers, 1990). It is generally agreed that VIF values under 10 (and consequently tolerance values above 0.1) are adequate. Our values were all under this and even more conservative thresholds of 5 and 2.5 (Allison, 1999). Thus, the

amount of shared variance in the chosen set of predictors is not a concern. Latency analyses (not shown) confirm the validity of this approach.
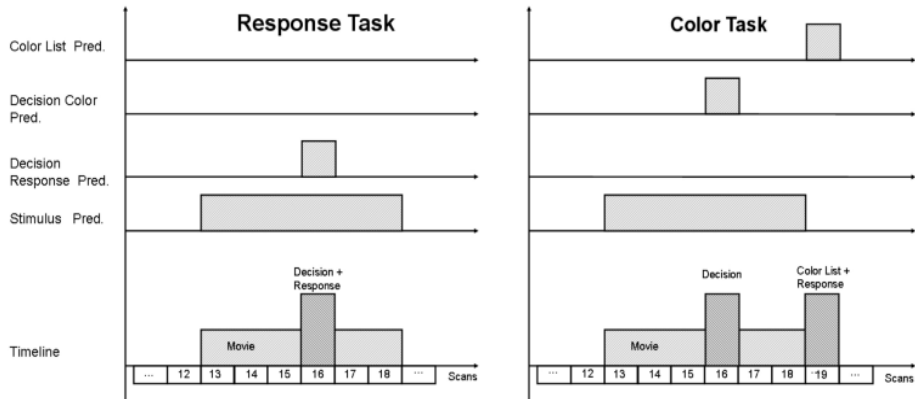
Figure 5.3 - Chronometry of our decision paradigms and respective predictor timelines used in the Random Effects (RFX)-GLM for both tasks (shown before convolution with the haemodynamic response function). Note that decision predictors vary in time from movie to movie favoring predictor decorrelation.

Beta values associated with the regressors could then be contrasted or combined to find candidate areas statistically consistent with the modeled functional properties. In particular, sensory processors can be located by studying the contrast S > (DR + DC), whereas the contrast (DC + DR) > S identifies decision/detection areas. Accumulator areas were analyzed using the contrast S > baseline AND (DR + DC) > baseline (AND denotes conjunction). Motor areas were searched for using the contrast DR > DC. The choice of model and contrasts allows the assessment of the above mentioned decision architecture while allowing the identification of task-relevant areas that exhibit slight deviations to the pre-specified dynamical patterns. This is of

importance and in line with Ploran et al. tenet that "*Although the time course profile predictions are derived from theoretical accounts and empirical findings, we note that BOLD responses need not necessarily show these specific time course patterns because some regions may show combinations of such responses (i.e., both accumulator and moment of recognition patterns, which would preclude dissociation), or show responses not otherwise considered a priori.*".

The contrast set based on the four predictors is summarized in Table 1, where "1" and "0" depict predictor weight as analyzed by the GLM approach. The statistical analysis was based on least-squares estimation with correction for serially autocorrelated observations. BrainVoyager was used to generate the design matrix by convolving a boxcar function with a model for the BOLD response function and a response delay of 6s. Note that the more conservative random effects (RFX) analysis was used in order to provide generalization of effects for the population.

	(S)	(DR)	(DC)	(CL)	Contrast
Sensory Processors	(1)	(0)	(0)	-	S > (DR + DC)
Accumulators/ mixed pattern	(1)	(1)	(1)	-	S and (DR + DC) > baseline
Decision/detection areas	(0)	(1)	(1)	-	DR > S and DC > S
Motor areas	(0)	(1)	(0)	(1)	DR > DC

Table 5.1 - Contrasts for standard Random Effects (RFX)-GLM. Summary of predictor expected type of level (Columns) and classification model for different brain regions (Rows). In the last column, the relevant RFX-GLM contrast to identify the areas for each module in the architecture is shown. (1) means a predictor at "High" state and (0) at "Low" state.

5.2.4.2 Data-driven approach: Independent Component Analysis (ICA)

Data-driven approaches yield model-independent results from the data, which can be used to validate pre-specified model-based hypothesis. In this manner, we have used ICA, a blind source separation algorithm, to investigate if an equivalent functional parcellation of the insula can be obtained without constraints and the inherent limitations of the GLM approach.

The ICA decomposition was performed in BrainVoyager software using the "FastICA" deflation approach, a fixed-point ICA algorithm developed by Hyvarinen and colleagues (see http://www.cis.hut.fi/projects/ica/fastica/). Before applying spatial ICA, we used a spatial mask to restrict the area of interest to the insular/opercular cortex and neighboring regions.

ICA applied to fMRI data prioritizes and maximizes spatial independency, and theoretically produces as many components as there are data points in the processed time course. However, for practicality, the temporal dimension of the data was reduced using Principal Component Analysis (PCA) resulting in 20 components, a number under the advised one-sixth of the number of volumes. The chosen number of ICA components, typically between 20 and 60 is not a strict parameter and depends on the data (Calhoun, Liu, & Adali, 2009). We opted for the former limit because of the lower number of voxels.

ICs were then extracted from both runs for all the 14 subjects, totaling 28 ICA decompositions. These were scaled to spatial z-scores (i.e. the number of standard deviations of their whole-brain spatial distribution). These values express the relative amount a given voxel is modulated by the activation of the component (McKeown et al., 1998). This set was then used as an input to the self-organizing group ICA BrainVoyager algorithm (Esposito et al., 2005) that clusters components across subjects based on their spatial and temporal similarities. The linear correlation coefficient (computed between two spatial

maps and/or two time-course of activity) is adopted as the similarity measure in the present version. The similarity measures are converted to Euclidean distances and these are used to fill a matrix of "distances". Based on the distance matrix, a supervised hierarchical clustering procedure is run, the supervising constraint consisting of accepting just one component per subject in each cluster formed by the hierarchical procedure. We thresholded the input maps at z=1 before spatial similarity comparison to reject noise and used no temporal similarity constraints since each performance timecourse was subject specific.

The statistic for each voxel was calculated as the mean ICA Z-value of that voxel across the individual maps. Maps were thresholded at z= 1.5. We chose clusters of interest according to (1) the clusters with the lowest mean intra-cluster distances, and (2) spatial overlap with the areas of interest. Thus, from the resulting 20 "group" components, the ones representing structured physiological noise were discarded as well as those under 0.1 (10%) mean similarity between subjects.

5.2.4.3 Event-related averages and timecourse parameters

The understanding of "when" and "how" neural processes occur in the brain is just as important as understanding their spatial correlates. Accordingly, event-related average timecourses were calculated for the areas identified with the previous methods.

For each area, seven conditions were defined, each corresponding to a given temporal moment of perceptual decision. In this manner, if the face was detected in the first TR (0-2s after movie onset), this was a different condition than if the face is detected on the second TR (2-4s after movie onset). This yielded six conditions plus one condition where the face was unseen/undetected.

Such dynamics provide valuable information on the putative functional role of the insula parcels (for visualization see Figure 6) by comparing them

against the "ideal" activation patterns for the considered decision architecture, shown in Figure 5.4.
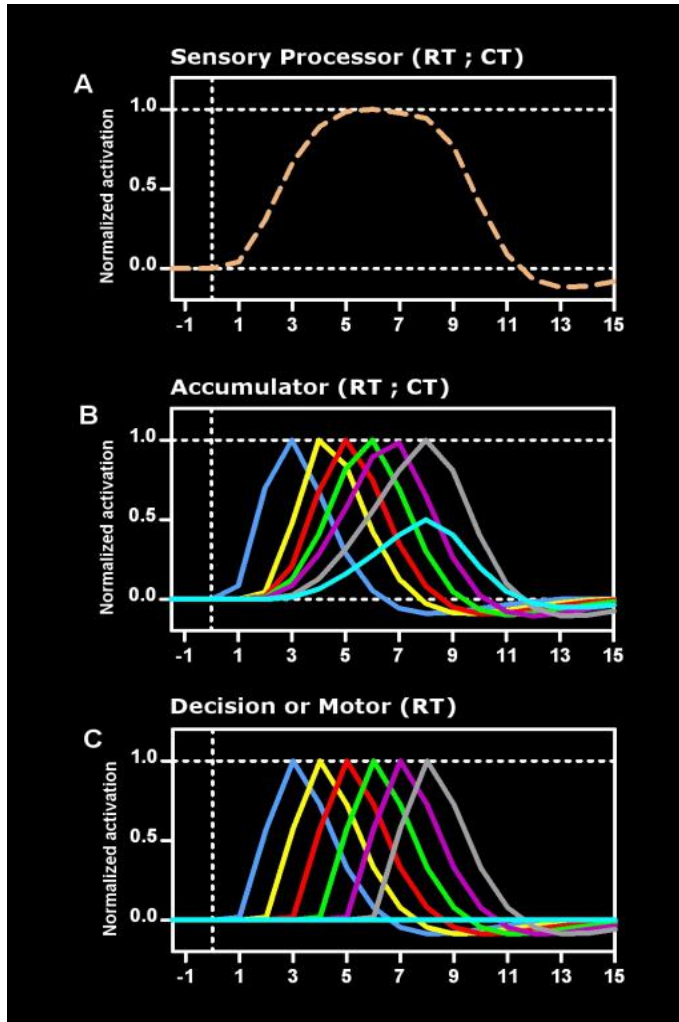
Figure 5.4 (continues on next page)
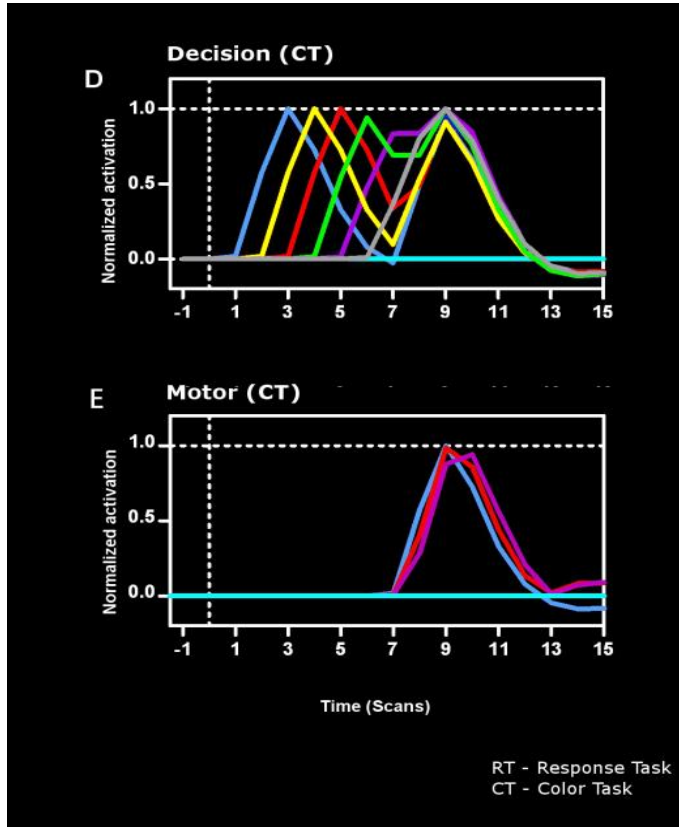
Figure 5.4 (continued) - Ideal activation patterns for the dual-task paradigm concerning the modules in the decision architecture proposed by Ploran et al. 2007. Different colors , i.e., different conditions, correspond to faces detected at different time slots, from movie to movie: blue 0-2s; yellow 2-4s; red 4-6s; green 6-8s; purple 8-10s; gray 10-12s; light blue represents unseen faces. Panel A shows the ideal activation pattern for sensory processors (the same for both tasks) whereas panel B depicts the ideal activation pattern for accumulator areas. From panel C on one can understand the usefulness of the dual-task paradigm in separating decision and motor areas. These areas' patterns will be indistinguishable for the Response Task but motor areas will have its activity shifted towards the end of the trial (button presses) in the Color Task. On the other hand, pure decision areas will maintain the pattern of the Response Task, with the addition of a second peak at the time of button pressing (due to the fact that color selection also implies a decision). In the last panel three plots are not shown to prevent figure cluttering since the missing activations are the same as the depicted conditions.

5.3. Results

5.3.1 Behavioral results

The behavioral results are summarized in Table 2 for the overall data and for each task separately. Relative frequencies of detection were similar across tasks (Chi square test, *ns*). Ranges of time of detection were also similar (Moses Test, *ns*). The choice of difficulty levels for detection stimuli led to spread in decision times (~75% of the stimuli requiring at least a few seconds for detection) and a sizeable number of trials where stimuli were perceived as scrambled.

	Overall	%	Response Task	%	Color Task	%
Face detection interval						
0-2 s	217	26,1	79	19,2	138	32,8
2-4 s	156	18,7	81	19,7	75	17,8
4-6 s	178	21,4	102	24,8	76	18,0
6-8 s	116	13,9	59	14,3	57	13,5
8-10 s	67	8,0	35	8,5	32	7,6
10-12 s	27	3,2	12	2,9	15	3,5
Unseen faces	70	8,4	43	10,4	27	6,4
Total	831	100	411	100	420	100

Table 5.2 - Subject behavioral data. Distribution of face detection times across trials and tasks.

5.3.2 Identification of regions based on the modeled RFX-GLM predictors

We have taken advantage from the segregated chronometry of the decision process enabled by our dual task paradigm, whereby detection times were spread in time, to assign different predictors to key task periods: sensory periods starting prior to perception, decision periods - jittered in time favoring predictor decorrelation - and response periods.

Though our focus is the insular/opercular cortex, Table 5.3 and Figure 5.5 (panels a-d) show regions identified by RFX-GLM contrasts that responded according to the model proposed by Ploran et al.: (sensory areas, decision/detection areas, accumulators and motor areas). While successfully identifying different insular regions with three distinct contrasts, the RFX-GLM shows that "pure" sensory areas are found only in posterior occipital cortex. Intermediate visual areas show a profile sharing both sensory and accumulator features, as well as frontal areas belonging to the cognitive control network.

Concerning the target areas we could identify an anterior accumulator insular cluster and a decision/detection middle cluster. Activity in this middle operculo-insular region was specifically related to the decision regardless of whether a motor response was provided or not (Figure 5.5, contrast c).

Finally, contrast d identified posterior regions of the insular-opercular cortex involved in somatosensory/sensorimotor processing, as well as the cerebellum and the parietal operculum (SII), (Figure 5.5, contrast d).

This refinement of the insular cortex points toward functional segregation: clusters specific to accumulation of evidence, detection signaling mechanisms, and posterior regions purely involved in the motor response components.

Region	Peak X	Peak Y	Peak Z	NrOfVoxels
Contrast a – Stimulus > Decision Color AND Stimulus > Decision Response;				
; putative sensory processors **p0.01 rfx**				
l middle occipital gyrus	-37	-86	-9	1587
r middle occipital gyrus	26	-83	-6	4204
Contrast b – Stimulus AND Decision Color AND Decision Response > baseline;				
accumulators, hybrid patterns **p0.01 rfx**				
r insula	32	16	9	999
r fusiform gyrus	32	-56	-15	2288
l fusiform gyrus	-40	-53	-24	2474
l insula	-31	10	15	821
r precentral gyrus/inferior frontal junction	50	7	24	473
Contrast c - Decision Color AND Decision Response > Stimulus ;				
putative decision/detection areas **p0.01 rfx**				
r insula	38	4	3	94
l insula	-52	10	6	1149
posterior cingulate cortex	-1	-26	24	126
cerebellar vermis	-1	-65	-12	71
Contrast d - Decision Response AND Color List > Decision Color ;				
motor areas **p0.01 rfx**				
l cerebellum	-7	-62	-15	1677
r parietal operculum	50	-26	18	902
r insula	35	-20	6	99
l insula	-43	-5	15	349
r putamen	29	-17	6	95
r globus pallidus	26	-5	18	71
l parietal operculum	-49	-29	21	208

Table 5.3 - Summary of Random Effects (RFX)-GLM contrasts and outputs. X, Y and Z represent Talairach Coordinates. The number of voxels is based on the resolution of the anatomical dataset 1x1x1 mm. r = right; l =left;
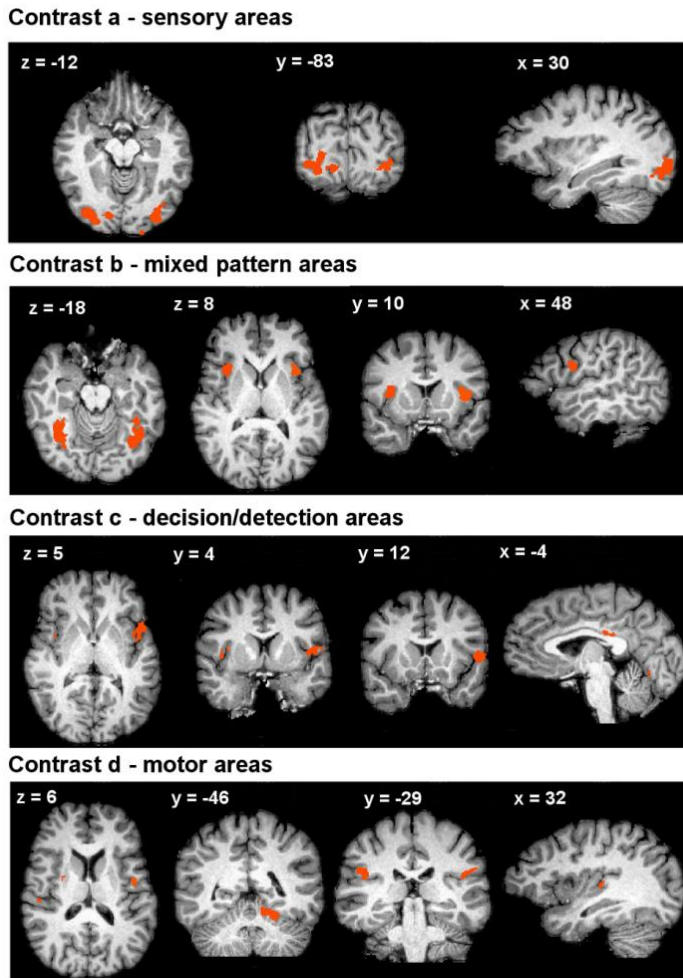
Figure 5.5 - Random Effects (RFX)-GLM output: distinct functional networks of brain regions are identified with contrasts designed to separate processing components in the perceptual decision task. Random effects maps were thresholded at p<0.01

5.3.3 ICA

5.3.3.1 Component selection

Components were sorted according to similarity mean along the 28 decompositions. All clusters under 10% mean similarity were discarded and considered non-structured noise. Eight clusters survived this criterion from among which 5 maps represent structured noise and 3 maps effectively represent task-related BOLD spatial patterns (located in the insula).

In order to relate the component maps to their GLM-defined counterparts, a simple correlation between the component and regressor timecourses is not adequate. This is because the GLM results were obtained through contrasts which imply more than one regressor. In other words, we validated the hypothesized contrasts by finding the same areas with no model constraints.

In addition, since the spatial component pattern needs to be functionally matched with the GLM results, a confirmatory analysis can be used to corroborate this coupling. This was achieved by performing a ROI-GLM using the component maps as the input ROI. As expected, the components exhibit the same significance levels across contrasts as their GLM counterparts.

These results, summarized on Table 5.4 and Figure 5.6 show that the ICA components validate spatially and functionally the parcellation suggested by the GLM analysis.

Predictor	IC2		IC3		IC8	
	t	p	t	p	t	p
S	5.587	0.000119	2.172	0.050618	-2.863	0.014263
DR	9.403	0.000001	6.287	0.000040	3.301	0.006326
DC	5.696	0.000100	5.045	0.000287	-0.248	0.808264

Table 5.4 – RFX-GLM predictor statistics using the task-relevant IC maps as ROIs

The statistical values for the GLM predictors using the component maps as the ROI inputs functionally confirm a similarity in the insular decomposition that was already apparent spatially. IC2, the most anterior and ventral component, shows high t-values for the regressors, consistent with an accumulator pattern, but fails to show increased relevance of both the DC and DR predictors when contrasted to the S predictor. IC3, the middle lateral component, shows the most pronounced difference between both the DR and the DC regressors when compared to the S predictor statistical values. This distribution of values is indicative of a cluster more tightly coupled with decision processes. Finally, The IC8, the most posterior component only exhibits a positive correlation with the DR predictor, pointing towards a pure sensorimotor role.
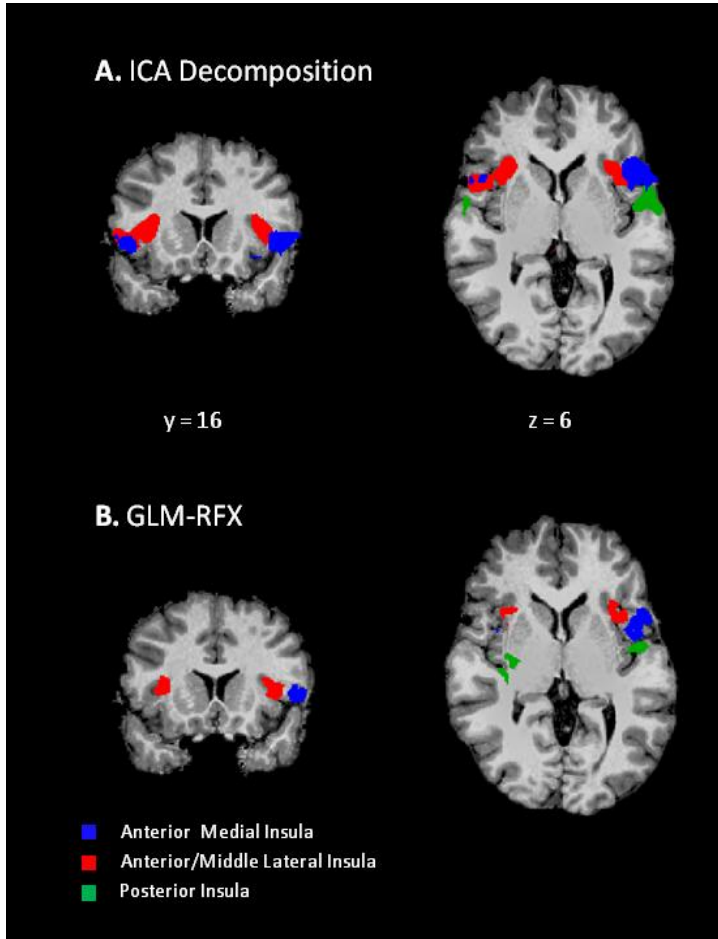
Figure 5.6 - Anterior-to-posterior insular/opercular parcellation achieved with data-driven and model-driven methods. Data-driven IC task-relevant maps are taken from the group clustering after thresholding at z=1,5. Model-driven results are taken from the GLM clusters that overlap the insular/opercular cortex.

5.3.2.3 Event-related averages and timecourse parameters

RFX-GLM analysis provided important insights into the putative functional classification/role of different regions in perceptual decision, which components were segregated in our task.

Event-related averages are important not only to confirm how much the identified areas behave like the ideal modules, but also to investigate to which extent do they deviate, thereby assessing the validity of such an architecture. Critically, they allowed identifying the degree to which regional activation is influenced by decision and its timing.

The value of this approach in the understanding of functional clustering within the insular cortex is depicted in Figure 5.7. Anterior insula dynamics follow the characteristics of an accumulator pattern, increasing activity from stimulus onset to response. Mid-insula and its functionally related frontal operculum (Binder et al., 2004) (Eckert et al., 2009) show a tighter coupling to decision processes, with steep variations and bi-modal activations in the Color Task mimicking the two decision (face detection and color selection) prompted by this task. The sensorimotor/somatosensory processes of the posterior insula are evident from the shift of activation towards the color selection period in the Color Task while not deviating from baseline in the detection periods.
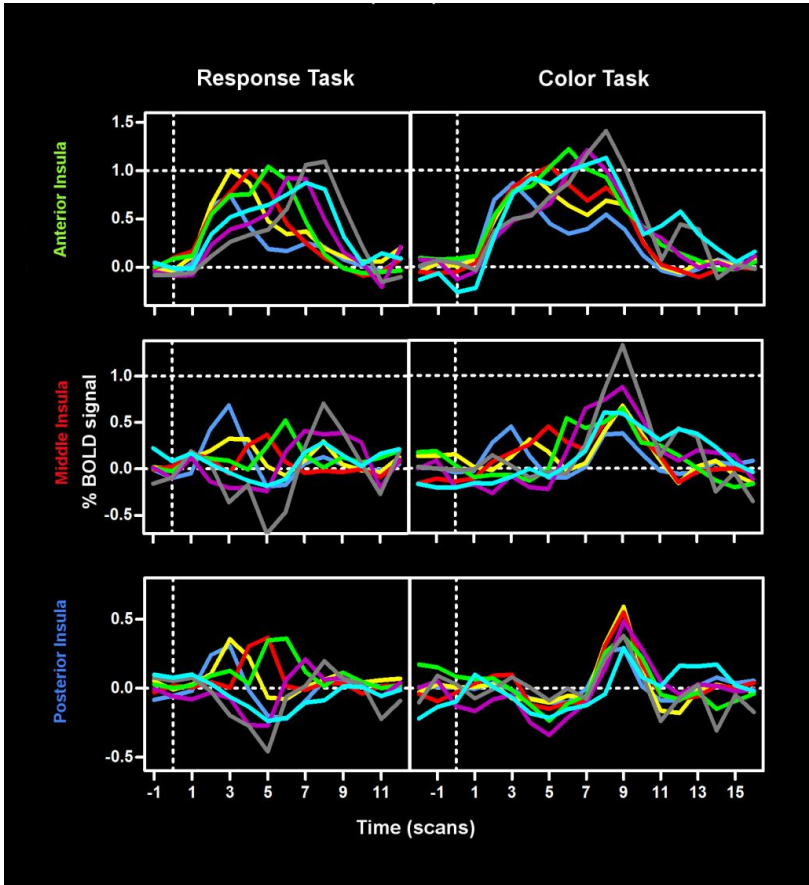
Figure 5.7 - Insular activation patterns for the subregions identified with the different contrasts. Color codes are identical to Figure 5.4 and correspond to different decision times. The dependency of peak activity on decision time and task is clear cut. Error bars not shown for sake of clarity. One can note how the patterns for the Response Task are less complex and how the demands of the Color Task shapes the patterns in ways that elucidate the different roles of the regions.

Anterior insula shows increasing activity from stimulus onset to response, which is more pronouncedly sustained after decision in the Color Task. Mid-insula shows steeper variations and the expected bi-modal activation (two decision times) in the Color Task that retains activity at detection times, suggesting a tighter engagement in "pure" decision processes. On the other hand, the posterior insula dissociable responses in the color and response tasks show that it is involved specifically in the sensorimotor components of the decision.

5.4. Discussion

In this study we were able to use a neurochronometric approach that allowed for the identification of a tripartite functional network in the insular-opercular complex. This was achieved by concomitant separation between sensory and perceptual components in holistic perceptual decision-making. Multiple patterns of activation within this complex were identified in relation to evidence accumulation, decision signaling and sensorimotor functions. These findings are consistent with the anatomical and functional connectivity parcellations of the insula and are relevant to the current discussion concerning the role of insular cortex and adjacent frontal operculum in decision making.

Our neurochronometric approach also allowed to find a distributed decision related network in the visual ventral stream (with a decision component superimposed on a sensory plateau-shaped component).

5.4.1 Relevance of the neurochronometric paradigm in dissecting the cognitive components of decision

Decision is classically considered as the output of an integrative process that comprises sensory processing and accumulating evidence in favor of one perceptual alternative until a given threshold is reached (Gold & Shadlen, 2007; Mazurek, 2003; Ratcliff & McKoon, 2008). This was addressed in our paradigm in the following manner: instead of relying on classical manipulations of signal to noise level we focused on global perceptual integration.

Variation of decision times laid the ground for separability of sensory, detection/recognition areas, accumulators and sensorimotor regions. Initial sensory processing was uncoupled from perception by means of the novel time-varying Mooney perceptual paradigm that delayed the time of decision from stimulus onset through a gradual rotation from inverted to upright

position. This manipulation takes full advantage of the well known bias in holistic processing of Mooney stimuli, by delaying the moment of global integration. Separation of perceptual and motor components was further achieved by comparing a condition that requires a response upon the moment of recognition (response task) to a condition where such action is delayed (color task).

We modeled regional timecourses to identify areas involved in low-level sensory processing (showing sustained activity). Other regions could be modeled as holistic detection triggers whereas in others build-up of activity from stimulus onset was a better descriptor. The color-task paradigm offers a way to separate the computation of a decision threshold, at an abstract level, from the delayed execution of an action, which isolates and provides a better understanding of these processes.

5.4.2 Impact of the current findings on the functional classification of insular regions

The functional role of the insular cortex and neighboring frontal operculum in decision-making has remained elusive. According to Heekeren's et al. (Heekeren et al., 2008) four module hypothesis, the insula belongs to the module that detects perceptual uncertainty/difficulty (Grinband, Hirsch, & Ferrera, 2006) and signals when additional attentional resources are required. Other authors (Binder et al., 2004; Ho et al., 2009; Kayser et al., 2010; Ploran et al., 2007, 2011), have implicated the anterior insular and adjacent frontal opercular cortex with a more important place in the decision hierarchy. This is consistent with a study (Christensen, Ramsøy, Lund, Madsen, & Rowe, 2006) of graded visual perception, where both insular cortex and frontal operculum were listed under the areas which activity modulation obeyed to the rule: clear percept > vague percept > no percept. Other studies have yet implicated these areas on the link between perception and action, (Jiang & Kanwisher, 2003) or

retrieving/activating commands for unexpected shifts of attention (Shulman et al., 2009).

The work of Cole and Schneider (Cole & Schneider, 2007), that includes the anterior insular cortex in the Cognitive Control Network, (see also (Eckert et al., 2009; Sridharan, Levitin, & Menon, 2008; Zysset et al., 2006)) further supports the importance of such structures within and beyond decision-making, though the role of these regions has often remained undebated (Dosenbach et al., 2006, 2007).

The functional diversity of the insula is corroborated by recent studies that show anatomical and connectivity sub-clusters within the insula (Cauda et al., 2010; Deen et al., 2010). In fact, Craig et al (Craig, 2009) suggests a functional gradient in this structure, with more posterior sites subserving primarily interoception and somatosensory representations and more anterior sites gradually integrating motivational, social and cognitive content.

Our study supports this hypothesis and confirms the recent proposal for a general role of the anterior insula in perceptual processes (Sterzer & Kleinschmidt, 2010). Furthermore, it also provides a separation of the role of distinct insular circuits in the decision process, anterior and middle parts being pivotal in perceptual decision and the posterior in somatomotor decision. We hypothesize that the bi-lateral insula/frontal operculum might accumulate sensory evidence irrespective of a motor output, and, upon reaching a given threshold, signals perceptual choice to the rest of the decision network. Von Economo neurons in the insular region (Allman, et al., 2011)(Cauda et al., 2012) , suited for rapid information interchanges, may be privileged neural correlates of such tasks. More specifically, middle insula/frontal operculum takes on decision signaling whereas anterior medial insula handles evidence accumulation.

Though it is not the primary role of this area, we were also able to identify somatosensory/sensorimotor correlates in the posterior insula as already reported by others (Björnsdotter, Löken, Olausson, Vallbo, & Wessberg, 2009; Carey, Abbott, Egan, Bernhardt, & Donnan, 2005; Johansen-Berg & Matthews,

2002; Kurth et al., 2010), markedly dissociated from the response-independent pattern observed in the anterior and middle regions of the insula, providing further clues to the functional anatomy of this structure.

Comparing our results to the studies of Ploran et al (Ploran et al., 2007, 2011) , which established the groundwork to define our set of predictors and decision architecture, there are some differences that need to be addressed. These authors interpreted activity in the bilateral anterior insula as reflecting "commitment to decision". This might at first sight not match our functional classification. However, this is only apparent. The clustering strategy employed by Ploran et al. does indeed emphasize regional cluster means and may reduce sensitivity to detect local functional patterns. The "accumulator"-like pattern seen in their data (see Figure 3d in (Ploran et al., 2011)) is consistent with our own view and may have been collapsed in their analysis by the clustering algorithm into the "decision" group.

5.5. Conclusions

Here we achieved separation of the neural correlates of local sensory (bottom-up) and global gestalt based perceptual decision. We used novel visual recognition/detection tasks with constant signal to noise levels of sensory evidence, enabling the demonstration of perceptual decision representations along local networks in particular within the insular cortex and adjacent frontal operculum. The paradigm also permitted the validation of a distributed hierarchical model of holistic perceptual decision based on the modules commonly accepted on the decision architecture: sensory processors, accumulators and decision/detection regions.

In sum, we have uncovered a pivotal role for bilateral insular cortex / frontal operculum subnetworks in decision making: Activation of anterior and middle insular cortex spans accumulator and pure decisional processes respectively whereas activation of posterior insular cortex is more related to classical sensorimotor/somatosensory processes.

We believe that the functional approach proposed in this study provides a powerful framework to parse the distinct components of cognitive processes in general and global gestalt based decision making in particular.

References

Allison, P. D. *Logistic Regression Using the SAS System: Theory and Application (Vol. 1).* New York, Wiley SAS Institute. (1999).

Binder, J. R., Liebenthal, E., Possing, E. T., Medler, D. A., & Ward, B. D. (2004). Neural correlates of sensory and decision processes in auditory object identification. *Nature neuroscience*, *7*(3), 295-301.

Björnsdotter, M., Löken, L., Olausson, H., Vallbo, A., & Wessberg, J. (2009). Somatotopic organization of gentle touch processing in the posterior insular cortex. *Journal of Neuroscience*, *29*(29), 9314-9320.

Calhoun, V. D., Liu, J., & Adali, T. (2009). A review of group ICA for fMRI data and ICA for joint inference of imaging, genetic, and ERP data. *NeuroImage*, *45*(1 Suppl), S163-72.

Carey, L. M., Abbott, D. F., Egan, G. F., Bernhardt, J., & Donnan, G. a. (2005). Motor impairment and recovery in the upper limb after stroke: behavioral and neuroanatomical correlates. *Stroke; a journal of cerebral circulation*, *36*(3), 625-9.

Cauda, F., D'Agata, F., Sacco, K., Duca, S., Geminiani, G., & Vercelli, A. (2010). Functional connectivity of the insula in the resting brain. *NeuroImage, 55(1),* 8-23.

Cauda, F., D'Agata, F., Sacco, K., Duca, S., Geminiani, G., & Vercelli, A. (2011). Functional connectivity of the insula in the resting brain. *NeuroImage*, *55*(1), 8-23.

Cauda, F., Torta, D. M. E., Sacco, K., D'Agata, F., Geda, E., Duca, S., Geminiani, G., et al. (2012). Functional anatomy of cortical areas characterized by Von Economo neurons. *Brain structure function* (in press).

Cerliani, L., Thomas, R. M., Jbabdi, S., Siero, J. C. W., Nanetti, L., Crippa, A., Gazzola, V., et al. (2012). Probabilistic tractography recovers a rostrocaudal trajectory of connectivity variability in the human insular cortex. *Human Brain Mapping*, *33(9),* 2005-34.

Christensen, M. S., Ramsøy, T. Z., Lund, T. E., Madsen, K. H., & Rowe, J. B. (2006). An fMRI study of the neural correlates of graded visual perception. *NeuroImage*, *31*(4), 1711-25.

Cole, M. W., & Schneider, W. (2007). The cognitive control network: Integrated cortical regions with dissociable functions. *NeuroImage*, *37*(1), 343-60.

Craig, a D. B. (2009). How do you feel--now? The anterior insula and human awareness. *Nature reviews. Neuroscience*, *10*(1), 59-70.

Deen, B., Pitskel, N. B., & Pelphrey, K. a. (2010). Three Systems of Insular Functional Connectivity Identified with Cluster Analysis. *Cerebral cortex , 21(7),* 1498-506

Dosenbach, N. U. F., Fair, D. a, Miezin, F. M., Cohen, A. L., Wenger, K. K., Dosenbach, R. a T., Fox, M. D., et al. (2007). Distinct brain networks for adaptive and stable task control in humans. *Proceedings of the National Academy of Sciences of the United States of America*, *104*(26), 11073-8.

Dosenbach, N. U. F., Visscher, K. M., Palmer, E. D., Miezin, F. M., Wenger, K. K., Kang, H. C., Burgund, E. D., et al. (2006). A core system for the implementation of task sets. *Neuron*, *50*(5), 799-812.

Eckert, M. A., Menon, V., Walczak, A., Ahlstrom, J., Denslow, S., Horwitz, A., & Dubno, J. R. (2009). At the heart of the ventral attention system: the right anterior insula. *Human Brain Mapping*, *30*(8), 2530-2541.

Esposito, F., Scarabino, T., Hyvarinen, A., Himberg, J., Formisano, E., Comani, S., Tedeschi, G., et al. (2005). Independent component analysis of fMRI group studies by self-organizing clustering. *NeuroImage*, *25*(1), 193-205.

Gold, J. I., & Shadlen, M. N. (2007). The neural basis of decision making. *Annual review of neuroscience*, *30*, 535-74.

Grinband, J., Hirsch, J., & Ferrera, V. P. (2006). A neural representation of categorization uncertainty in the human brain. *Neuron*, *49*(5), 757-63.

Heekeren, H. R., Marrett, S., & Ungerleider, L. G. (2008). The neural systems that mediate human perceptual decision making. *Nature reviews. Neuroscience*, *9*(6), 467-79.

Ho, T. C., Brown, S., & Serences, J. T. (2009). Domain general mechanisms of perceptual decision making in human cortex. *The Journal of neuroscience : the official journal of the Society for Neuroscience*, *29*(27), 8675-87.

Jiang, Y., & Kanwisher, N. (2003). Common neural substrates for response selection across modalities and mapping paradigms. *Journal of cognitive neuroscience*, *15*(8), 1080-94.

Johansen-Berg, H., & Matthews, P. M. (2002). Attention to movement modulates activity in sensori-motor areas, including primary motor cortex. *Experimental brain research. Experimentelle Hirnforschung. Expérimentation cérébrale*, *142*(1), 13-24.

Kayser, A. S., Buchsbaum, B. R., Erickson, D. T., & D'Esposito, M. (2010). The functional anatomy of a perceptual decision in the human brain. *Journal of neurophysiology*, *103*(3), 1179-94.

Kurth, F., Eickhoff, S. B., Schleicher, A., Hoemke, L., Zilles, K., & Amunts, K. (2010). Cytoarchitecture and Probabilistic Maps of the Human Posterior Insular Cortex. *Cerebral Cortex*, *20*(6), 1448-61.

Mazurek, M. E. (2003). A Role for Neural Integrators in Perceptual Decision Making. *Cerebral Cortex*, *13*(11), 1257-1269.

McKeown, M. J., Makeig, S., Brown, G. G., Jung, T. P., Kindermann, S. S., Bell, a J., & Sejnowski, T. J. (1998). Analysis of fMRI data by blind separation into independent spatial components. *Human brain mapping*, *6*(3), 160-88.

Menard, S. (1995). *Applied Logistic Regression Analysis*. (M. S. Lewis-Beck, Ed.)*Online* , 106, 111.

Myers, R. H. (1990). *Classical and modern regression with applications*. (N. Ed, Ed.)*The Duxbury advanced series in statistics and decision sciences* (Vol. 2nd, p. 488). Duxbury.

Platt, M. L. (2002). Neural correlates of decisions. *Current opinion in neurobiology*, *12*(2), 141-8.

Ploran, E. J., Nelson, S. M., Velanova, K., Donaldson, D. I., Petersen, S. E., & Wheeler, M. E. (2007). Evidence accumulation and the moment of recognition: dissociating perceptual recognition processes using fMRI. *The Journal of neuroscience: the official journal of the Society for Neuroscience*, *27*(44), 11912-24.

Ploran, E. J., Tremel, J. J., Nelson, S. M., & Wheeler, M. E. (2011). High Quality but Limited Quantity Perceptual Evidence Produces Neural Accumulation in Frontal and Parietal Cortex. *Cerebral Cortex*, *21*(November), 2650-62.

Ratcliff, R., & McKoon, G. (2008). The diffusion decision model: theory and data for two-choice decision tasks. *Neural Computation*, *20*(4), 873-922.

Salinas, E. (2008). So many choices: what computational models reveal about decision-making mechanisms. *Neuron*, *60*(6), 946-9.

Schall, J. D. (2001). Neural basis of deciding, choosing and acting. *Nature reviews. Neuroscience*, *2*(1), 33-42.

Shulman, G. L., Astafiev, S. V., Franke, D., Pope, D. L. W., Snyder, A. Z., McAvoy, M. P., & Corbetta, M. (2009). Interaction of stimulus-driven reorienting and expectation in ventral and dorsal frontoparietal and basal ganglia-cortical networks. *The Journal of neuroscience: the official journal of the Society for Neuroscience*, *29*(14), 4392-407.

Sigman, M., & Dehaene, S. (2005). Parsing a cognitive task: a characterization of the mind's bottleneck. *PLoS biology*, *3*(2), e37.

Sridharan, D., Levitin, D. J., & Menon, V. (2008). A critical role for the right fronto-insular cortex in switching between central-executive and default-mode networks. *Proceedings of the National Academy of Sciences of the United States of America*, *105*(34), 12569-74.

Sterzer, P., & Kleinschmidt, A. (2010). Anterior insula activations in perceptual paradigms: often observed but barely understood. *Brain structure & function*, *214*(5-6), 611-22.

Thielscher, A., & Pessoa, L. (2007). Neural correlates of perceptual choice and decision making during fear-disgust discrimination. *The Journal of neuroscience : the official journal of the Society for Neuroscience*, *27*(11), 2908-17.

Wang, X.-J. (2008). Decision making in recurrent neuronal circuits. *Neuron*, *60*(2), 215-34.

Zysset, S., Wendt, C. S., Volz, K. G., Neumann, J., Huber, O., & von Cramon, D. Y. (2006). The neural implementation of multi-attribute decision making: a parametric fMRI study with human subjects. *NeuroImage*, *31*(3), 1380-8.

Chapter 6

Selectivity dynamics before and after perceptual closure: novel insights into the functional profile of category-preferring visual networks

6.1 Open issues and motivation

The cortical topography of object, scene and face selective regions in the visual ventral stream has been extensively studied, and general principles of organization have been discussed earlier in this thesis. Classically, the characterization of these areas is investigated through the manipulation of the low-level properties of the stimuli and quantifying the associated changes in activity within the network of regions that are category preferring.

However, as mentioned in Chapter 4, visual processing involves a balance between bottom-up and top-down processes, i.e., between saliency of stimulus features and their relevance for the task goals. In order to emphasize the study of perceptual mechanisms instead of low level sensory processing, and to favor the emergence of top-down influence, we have designed perceptual decision-making paradigms using ambiguous impoverished images, the advantages of which are detailed in Chapter 5. Through these, we can assess perceptual closure on category-preferring networks and study how selectivity changes in time as a function of these events. Perceptual closure refers to the well known Gestalt principle of perceptual organization that reflects the ability to perceive an incomplete pattern or object as complete or whole. In other words, it refers to the coherent perception of an image content under circumstances when the visual information is incomplete (Grützner et al., 2010).

The impact of perception demands on dynamic selectivity is an important unresolved issue because it provides a window to understand the computations occurring before and after perceptual closure.

Moreover, by studying whole networks, the contribution of each region-of-interest (ROI) to the overall perception of preferred and non-preferred categories reveals how dedicated or distributed this processing actually is in the visual cortex.

A few previous studies have also generated perceptual ambiguity through the use of impoverished images, namely pure noise images which change throughout time into a coherent object or face (Jiang et al., 2011) (Ploran et al., 2007). In turn, McKeef and Tong (McKeeff & Tong, 2007) used Mooney stimuli with a specific focus on the FFA and OFA's role in perceptual decision. They conclude that the "activity in the FFA (as well as the OFA of some subjects) corresponded to both the perceptual content and the timing of the subject's decision about faces". Another study by Andrews et al (Andrews & Schluppeck, 2004) found a similar link between perception and the FFA, but noted that "in contrast, there was no difference in magnetic resonance response between face and no-face perceived events in either the face-selective voxels of the STS, PPA or LOC".

These studies are very relevant and insightful by studying these phenomena although they substantially differ from ours both in aim and focus. Concerning the latter they address short time scales (Andrews & Schluppeck, 2004) small subsets of regions (McKeeff & Tong, 2007) and in the former they used more restricted stimulus conditions, focusing on preferred stimulus categories, such as faces and their scrambled controls.

In this study we followed a different approach, as we were specifically interested in the temporal dynamics of selectivity before and after perceptual closure. This was not possible in the study of Andrews & Schluppeck, 2004. We did therefore use long time scales, to dissect selectivity along time and its dependence on category and perceptual closure. Here we also departed from previous studies by including responses to non-preferred stimulus categories. Moreover, this approach was extended to a broader range of regions, most importantly PPA and STS. We did therefore extend our paradigm by building long trials (12s) of rotating Mooney images of objects, in addition to faces, to assess the dynamics of activity and selectivity in previously localized category-preferring networks. By investigating whole networks with faces and objects, we could assess BOLD activity in distributed regions of interest (ROIs) in response to expected preferred or non-preferred categories.

6.2. Methods

6.2.1 Subjects

13 right-handed subjects (6 females, 7 males, ages 22-33 years) participated in the study after providing informed consent. All had normal or corrected to normal vision.

The study followed the tenets of the Declaration of Helsinki, informed consent being obtained from all subjects for the protocol, which was approved by the Ethics Committee of the Faculty of Medicine of the University of Coimbra.

6.2.2 Stimuli

The stimuli for the main experimental paradigm (see 6.2.4 for localizer scans) comprised two sets of Mooney images of faces or objects. The first set consisted of the 60 Mooney images of faces described and used in the study reported in Chapter 5.

The second set was built by thresholding 60 online images of objects. Online images were favored over databases because they provide more variety in lighting, angle and object sizes, thus maximizing ambiguity. Due to the broader span of the object category, images of objects were restricted to three sub-categories: utensils, means of transportation and musical instruments.

Mooney stimuli (two-tone images) were chosen because they provide a classical way of generating ambiguous perception (which is enhanced if stimuli are viewed upside down). These stimuli may appear devoid of any recognizable content for several seconds until the observer suddenly becomes aware of the emergence of a holistic percept. These stimuli characteristics were suited to the study's goals because the sudden global awareness of the content will lead to

temporally contained perceptual events, separable from initial local sensory processing and ideal to induce abrupt changes in selectivity. Also, differential onset of activity on "early" and "late" detection trials is a distinguishing characteristic of a neural encoder of perception processes, a property that can advantageously be used in identifying the perceptual visual networks involved.

Finally, interpretation of the image content cannot be easily achieved through local visual analysis, and renders high-level processing impossible in the pre-perceptual period, which serves as a sensory control/baseline.

Difficulty levels were adjusted in pilot experiments to guarantee the desired spread in perception times (% of correct/incorrect answers, see behavioral results).

The 120 Mooney images were converted into movies that consist of the rotation of such images. Starting from the inverted position, the image slowly rotates 20° per second until it reaches the upright position where it rests for 3s. There were no repeated movies. Stimuli were presented in a black background and subtended approximately 12.40° of the visual field.

6.2.3 Task: the dual categorical paradigm

Subjects performed the same dual-task paradigm described in 5.2.3, consisting of the "Simultaneous Response Task " and the "Color Task".

Each of the tasks now comprised a run with faces and a run with objects. In each experimental run subjects were informed on the stimuli to search for, i.e., faces or objects. In the case of objects, runs were divided into three blocks, before which a cue was presented centrally for 4s with the sub-category to search for: tools, means of transportation and musical instruments. Task design is summarized in Figure 6.1

The dual-task paradigm was chosen as it ensures the separation between decision (or commitment to a decision) and somatosensory/motor processes of the response as previously observed (Rebola, Castelhano, Ferreira & Castelo-Branco, 2012).

Activity in high-level visual ROIs was pooled across tasks. This pooling approach is theoretically valid for non-motor regions, and was verified by direct comparison of response profiles for both tasks.
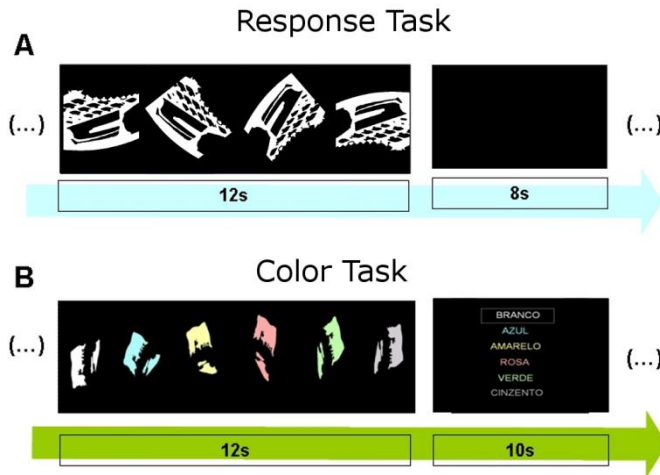
Figure 6.1 - Timeline of the perceptual closure paradigm using ambiguous Mooney stimuli; A – the image rotates from inverted to upright and the subject presses a button when (and only if) the content is detected; B – the "white component" (foreground) of the Mooney image, changes color every TR (acquisition volume) and the subject indicates the moment of closure only at the end of the trial by selecting from a list the color that corresponds to perception time. This last task precludes simultaneous processes of perceptual closure and motor response. The two tasks were carried out using both Mooney faces and objects, in separate runs.

6.2.4 Localizer Scans to map selective regions for ROI analysis

Localizer stimuli consisted of greyscale images of faces, places (buildings; landscapes; skylines), objects (tools; cars; chairs), and scrambled versions of

objects. Stimuli were presented in a black background and subtended approximately 9.48º of the visual field.

Localizer scans consisted of two runs of alternatively viewed blocks of stimuli from a given class (faces, places, objects, scrambled images). Each run had 12 blocks and each block lasted 20s (30 images, 800ms each), separated by 10s fixation baseline intervals. During each block subjects performed a 1-back task to keep stable attention levels. Three repetitions per block were employed. The definition of contrasts to identify distinct brain regions (ROIs) can be seen in Table 6.2, which also presents details of the localized areas.

6.2.5 Image Acquisition parameters and pre-processing

Images were obtained on a Siemens Tim Trio 3T scanner using a 12 channel head coil. Structural images were collected using a T_1 weighted MPRAGE (magnetization-prepared rapid-acquisition gradient echo) (TR = 2300ms, TE = 2.98ms , flip angle = 9º, matrix size = 256x256 , voxel size = 1mm³). Standard T_2*-weighted gradient-echo echo planar imaging was used for the functional task runs (TR = 2000ms ; TE = 47ms ; 2.5mm x 2.5mm in-plane resolution ; 3.5mm slice thickness with 0.7 gap ; flip angle = 90º; matrix size= 102x102; number of slices = 25; for faces, 455 measurements were acquired for the Color Task and 335 were acquired for the simultaneous Response Task; for objects, due to the cue that signals the sub-categories, 476 measurements were acquired for the Color Task and 356 were acquired for the simultaneous Response Task). The slices were positioned parallel to the inferotemporal surface of the brain to obtain maximum coverage. Runs were acquired across two sessions. Image processing was performed using BrainVoyager QX v2.1 (Brain Innovation, Maastricht, The Netherlands). Pre-processing steps included motion correction, slice scan-time correction, linear trend removal and temporal high-pass filtering of 0.00980 Hz (3 cycles in time course).

6.2.6 Data analysis

6.2.6.1 Trial sorting: Timing of Perceptual Closure

Perceptual closure, the moment in which the subject makes sense out of a seemingly meaningless image, could occur anytime during the movies. It could also not occur at all. In this manner, trials were sorted into different post-hoc "perceptual closure conditions" according to the moment of the emerging percept. The distribution of face and object trials according to the moment of perceptual closure is shown on Table 6.1. Responses within the same TR were binned together, thus yielding seven conditions for each category, six "perceived" conditions plus one condition where the categorical content was "unperceived". As an example, if the content was perceived in the first TR (0-2s after movie onset), this is a different condition than if it was perceived on the second TR (2-4s after movie onset), and so on until the sixth "perceived" condition (10-12s).

Conditions 1 (faces perceived in the interval 0-2s) and 6 (faces perceived in the interval 10-12s) were excluded from analysis of contrasts because in the former case there is no pre-perceptual period while in the latter there is no post-perceptual period.

6.2.6.2 GLM contrasts

Due to the nature of our paradigm, and the different ROI's sensitivity to sensory and perceptual processes, we opted for a deconvolution approach (Glover, 1999), which poses no constraints on the shape of the haemodynamic response function (HRF). Deconvolution approaches are generally used in rapid-event-related designs, as a means of separating overlapping responses to individual trials. Since we used a slow-event-related design, allowing the BOLD

signal to return to baseline before the subsequent stimulus presentation, this approach is equivalent to an event-related-average. It does, however, have an added benefit. By using a deconvolution approach the generated output for each type of trial is a succession of beta values (in our case 10) and its inherent statistics along the whole timecourse, starting from stimulus onset. This output is superior to the succession of mean and standard-deviation values obtained with the event-related average, since it provides the data needed to perform contrast statistics.

A flexible use of contrasts could then focus on categorical selectivity and perceptual dynamics, constructed to reflect the impact of each of these factors before, during and after perceptual closure. This could only be achieved by basing the contrasts not on whole conditions but on specific time-points of conditions, according to their relation to the perceptual closure moment.

Three sets of analysis were computed.

The first one evaluates the impact of perceptual closure on ongoing BOLD activity.

To this end, the most straightforward procedure is to contrast, across the 'perceived' conditions, the moment of perception to its non-perceptual predecessor (accounting for the haemodynamic lag). These contrasts are better understood by their graphical explanation, shown on Figure 6.2.

The evaluation of this contrast for faces and objects within a given ROI, shows how much perceptual closure of a given category shapes the BOLD response within that ROI. Furthermore, the difference between the values obtained for faces and objects reflects if the impact of perception is significantly different between categories.

The second type of contrasts assesses categorical selectivity dynamics. Thus, this time, the logic is in contrasting one category versus the other within each ROI.

By evaluating this contrast prior, during, and after perceptual closure (across the 'perceived' conditions), one can inspect how the dynamics of selectivity change between and within the different category-preferring networks. Graphical examples of these contrasts are shown on Figure 6.3.

The third and last type of contrasts analyses perceptual closure versus non perceptual closure (unperceived categories) for the same moment in time. It opposes, across conditions, the activity of perception time to its corresponding moment in the 'unperceived' condition, pure search trials where a gestalt is not formed during the whole time o stimulus presentation. In this manner, the contrast represents how activity differs between perceived and unperceived content of the same category, albeit having been exposed to the stimuli for the exact same time. This knowledge can prove insightful to the computations that distinguish unsuccessful search and perception in each ROI. Graphical examples of these contrasts are depicted on Figure 6.4

6.3 Results

6.3.1 Behavioral Results

The behavioral results are summarized in Table 6.1 for the overall data and for each category separately. Relative frequencies of detection were similar across categories (Independent Samples Mann-Whitney U-test, p=0.286). The adequate choice of difficulty levels for detection stimuli led to the desired spread in decision times (~75% of the stimuli requiring at least a few seconds for detection) and ~13% of trials where stimulus content was not perceived.

	Faces	%	Objects	%
Time of Perception (conditions)				
0-2s	117	15	147	19
2-4s	132	17	162	21
4-6s	166	21	125	16
6-8s	168	22	126	16
8-10s	92	12	80	10
10-12s	21	3	27	3
Unperceived	84	11	113	14
TOTAL	**780**		**780**	

Table 6.1 – Trial distribution, sorted by time of perceptual closure (absolute and relative frequencies), for faces and objects. Bins are two seconds in length (matching the TR).

6.3.2 Localization of object, scene and face selective regions

The present study focused on three category-preferring networks: the face network, the object network and the place network. From the face network we consider only the core system: FFA, OFA and pSTS. The object network is represented by the LOC, partitioned into the segregate areas vLOC and dLOC. The analysed place-preferring areas comprise the PPA, RSC and TOS.

Table 2 shows mean Talairach coordinates and mean number of voxels for the localized regions.

		X	Y	Z	Nr of Voxels
Faces>Objects AND Faces>Scrambled					fdr<0.01
FFA	L	-39	-48	-20	462
	R	37	-48	-21	621
OFA	L	-43	-73	-5 (8)	236
	R	44	-67	0 (5)	745
pSTS	L	-47	-56	9 (3)	392
	R	45	-48	8 (6)	300
Objects>Scrambled					fdr<0.01
vLOC	L	-33	-54	-17	1052
	R	30	-51	-18	673
dLOC	L	-40	-79	-2 (7)	2926
	R	36	-79	-3 (9)	1376
Places> Objects AND Places>Faces AND Places>Scrambled					fdr<0.01
PPA	L	-25	-44	-10	710
	R	23	-42	-11	883
RSC	L	-16	-55	6 (5)	678
	R	16	-54	8 (6)	642
TOS	L	27	-86	13 (7)	1081
	R	-28	-87	11 (9)	1045

Table 6.2 – Contrasts, mean Talairach coordinates and mean number of voxels for the localized ROIs. Numbers in parenthesis represent standard deviation. L=Left; R= Right

6.3.3 Selectivity dynamics across the ventral stream

For each of the ROIs considered above, three sets of analyses were conducted that highlight different aspects of perceptual closure and selectivity dynamics within the regions.

- The impact of perceptual closure on ongoing brain activity

We first analyzed the impact that perceptual closure has on ongoing activity. Such activity, starting from stimulus onset, encompasses sensory processing of impoverished image content. Activity changes when the subject finally forms a gestalt. This change should therefore be accounted for by the perceptual closure process. We tested whether such step differs significantly between categories (see Figure 6.2, arrows depict moment of closure, see Table 6.3 for statistical tests).
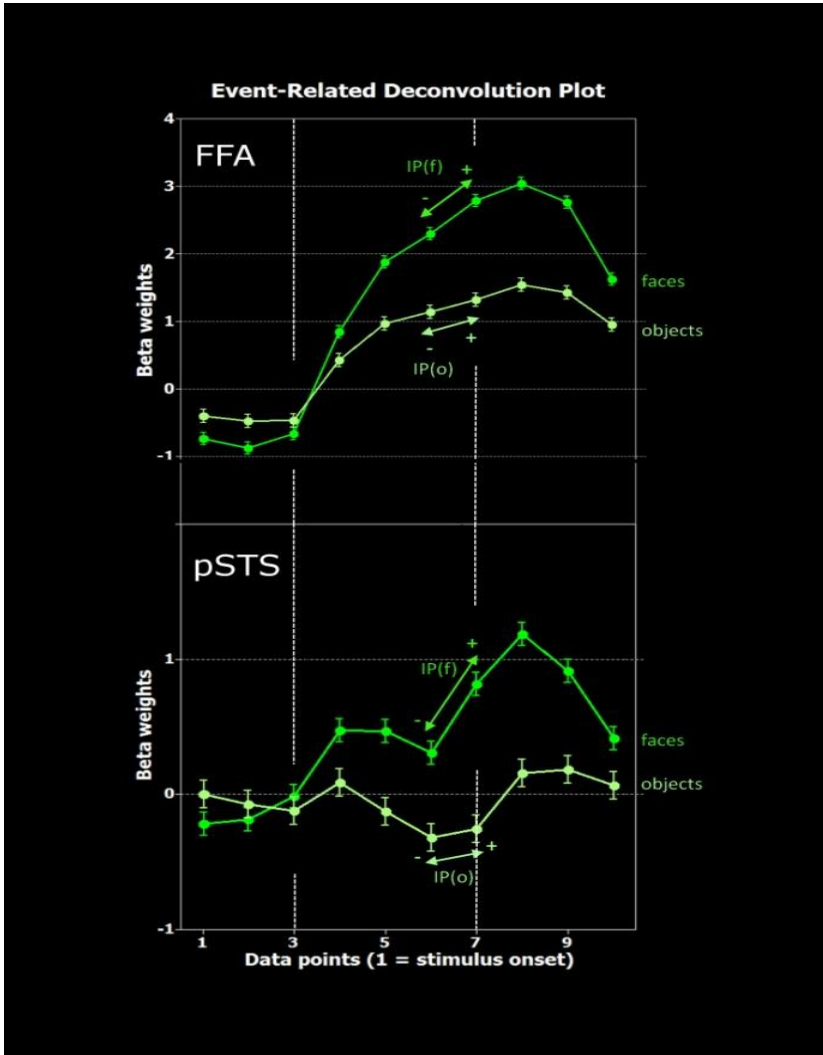
Figure 6.2 - Impact of perceptual closure on ongoing activity as measured by the first defined set of contrasts in the fMRI data. Changes in BOLD activity (see arrows) reflected perceptual closure for both preferred and non-preferred categories. Though this effect was calculated across perceived conditions 2, 3, 4 and 5, these examples depict closure condition 4, where faces and objects are seen from 6 to 8s. The left dashed line represents stimulus onset, after the haemodynamic lag, whereas the right dashed line represents time of perception

for this condition, after the same lag. By contrasting, for each category, the moment of perception to its predecessor, one can statistically quantify the impact of perception of faces – IP(f) - and objects – IP (o). Graphs are shown for the FFA and the pSTS. The former shows a significant impact for both categories (see Table 6.3) and the latter only for faces.

		Faces			Objects			Diference	
		t	p		t	p		t	p
Area									
FFA		8.624	0.000		4.538	0.000		2.586	0.009
OFA		6.042	0.000		2.957	0.003		1.969	0.048
pSTS		4.653	0.000		0.142	0.887		3.076	0.002
vLOC		4.422	0.000		5.359	0.000		-0.892	0.372
dLOC		6.185	0.000		5.146	0.000		0.469	0.638
PPA		1.337	0.181		4.490	0.000		-2.364	0.018
RSC		-2.456	0.014		-0.085	0.931		-1.616	0.106
TOS		2.406	0.016		3.630	0.000		-0.961	0.336

Table 6.3 – Categorical dependence of the impact of closure on ongoing brain activity (post-hoc t contrasts computed across all closure conditions).

Within the face-preferring network, we found the expected significant impact of perceiving faces, but there was also a highly significant impact of perceiving objects in the FFA and the OFA. In other words, forming a gestalt of the non-preferred category changes brain activity for all the face-preferring regions with the notable exception of pSTS. Accordingly, in the pSTS, only the perception of faces has a significant impact on ongoing activity.

Scene-selective regions exhibited different activity patterns. The PPA is impacted by object perception but not faces (see table 6.3 for statistical tests). The RSC is negatively impacted by perceiving faces (deactivation) but not by objects, the difference being once again significant.

Object areas show significant impact of perceiving both objects and faces.

- Dynamic changes in categorical selectivity induced by perceptual closure

The difference in activity elicited by the two tested categories (faces and objects) was evaluated before, during and after perception. This analysis investigates how the selectivity is shaped by the perceptual closure process. Figure 6.3 illustrates how the difference in response to different categories is modified by the closure process (see arrows). Statistics are shown in Table 6.4.
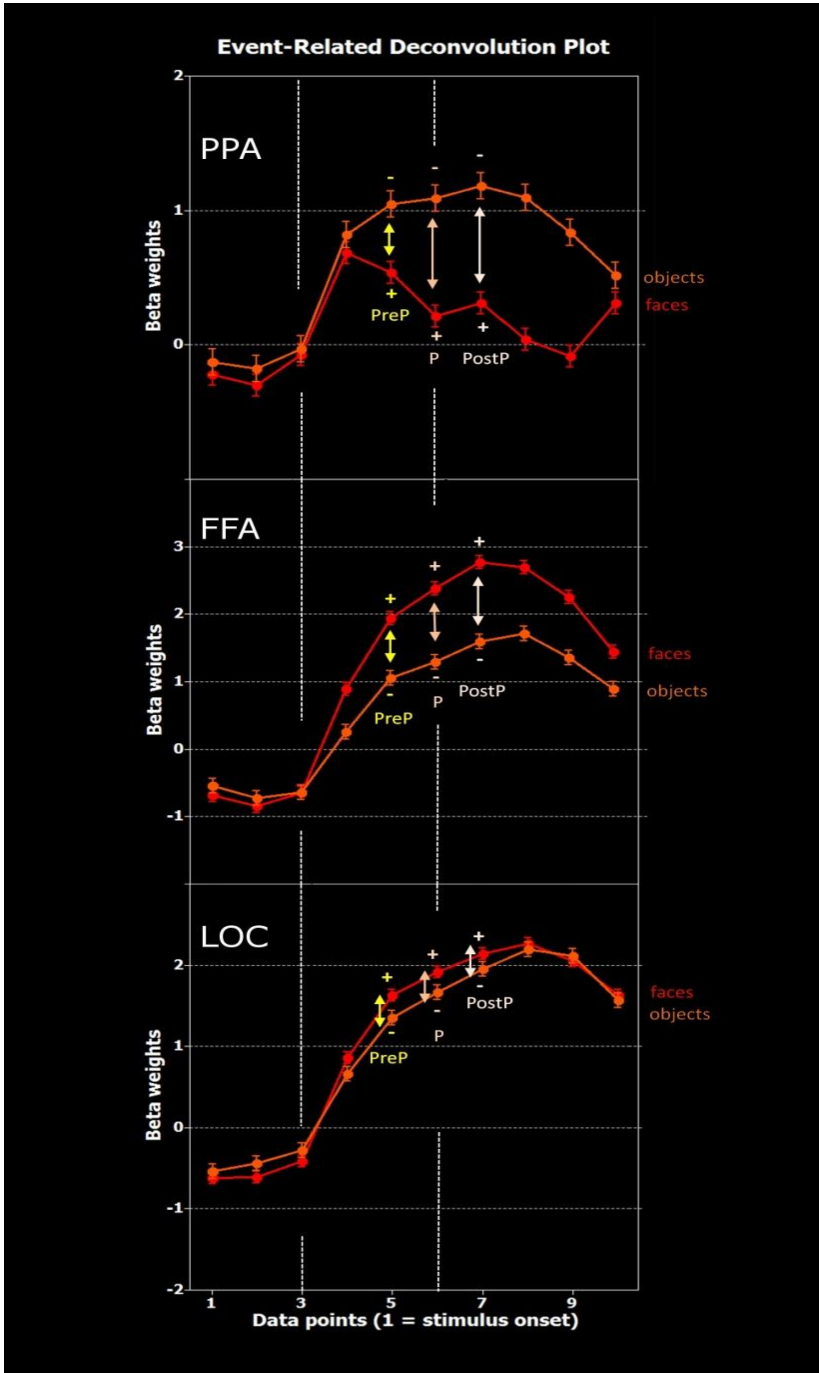
Event-Related Deconvolution Plot

Figure 6.3 - Distinct dynamics of category selectivity before, during and after perceptual closure, across ventral stream regions. The panels illustrate closure condition 3, i.e., faces and objects seen from 4 to 6s. In this panel, the left dashed line represents stimulus onset, after the haemodynamic lag, whereas the right dashed line represents time of perception for this condition, after the same lag. As in Figure 2, though only depicted for one closure condition (3), contrasts are calculated across conditions 2, 3, 4 and 5.Graphs are shown for the PPA, FFA and dLOC. Face selectivity increases over time, until after closure, for FFA. Object selectivity follows the same rule in ventral LOC (vLOC) and scene preferring regions, but not in the dorsal part of LOC. For PPA a pattern of deactivation occurred for the non preferred category.

Area	Pre-Percept(f-o)		Percept (f-o)		PostPercept(f-o)	
	t	p	t	p	t	p
FFA	10.151	0.000	13.452	0.000	13.390	0.000
OFA	8.100	0.000	10.616	0.000	10.879	0.000
pSTS	7.038	0.000	10.969	0.000	11.990	0.000
vLOC	-0.530	0.595	-1.669	0.095	-2.192	0.028
dLOC	3.684	0.000	4.283	0.000	3.170	0.001
PPA	-7.772	0.000	-10.793	0.000	-13.033	0.000
RSC	-1.647	0.099	-3.712	0.000	-4.969	0.000
TOS	-5.285	0.000	-6.514	0.000	-8.500	0.000

Table 6.4 – Dynamics of ROI selectivity (faces – objects, f-o) as a function of the perceptual closure process (before, during and after). Values were assessed through post-hoc t contrasts

All face-preferring areas exhibit a large selectivity even in pre-perceptual periods. This selectivity is enhanced with perceptual closure, and increases in the post-perceptual period, suggesting that additional processing steps kick-in.

The ventral part of the LOC exhibits an ambiguous response pattern, with higher responses to objects than faces from the start but only showing significantly higher activity to objects in the post-perceptual period. The dorsal LOC is even more intriguing, by responding more to faces than objects during the overall process of perceptual closure.

In sum, face selectivity increases over time, until after closure, for all regions of the core face network (OFA, FFA and STS). Object selectivity obeys to the same rule in vLOC and also scene preferring regions, but not in dLOC.

The scene network responds generally more to objects than faces in a significant manner for all periods, with selectivity increasing with closure and even further into the post-perceptual period.

- Differences in brain activity under closure vs non closure (failure to perceive and categorize)

Finally, we asked whether dynamics of perceptual search are different when comparing closure vs non closure for the same category at the same time point. We compare, across conditions, the activity at the perceptual closure times to its corresponding moments in the condition in which the stimulus remains 'unperceived' throughout the whole trial. Perceived and unperceived stimuli are thus equated in terms of elapsed time from stimulus onset. This allows exploring and comparing the computational trade-offs between perceptual closure and perceptual search that does not culminate in the forming of a gestalt (see arrows in Figure 6.4, and statistics in Table 6.5).
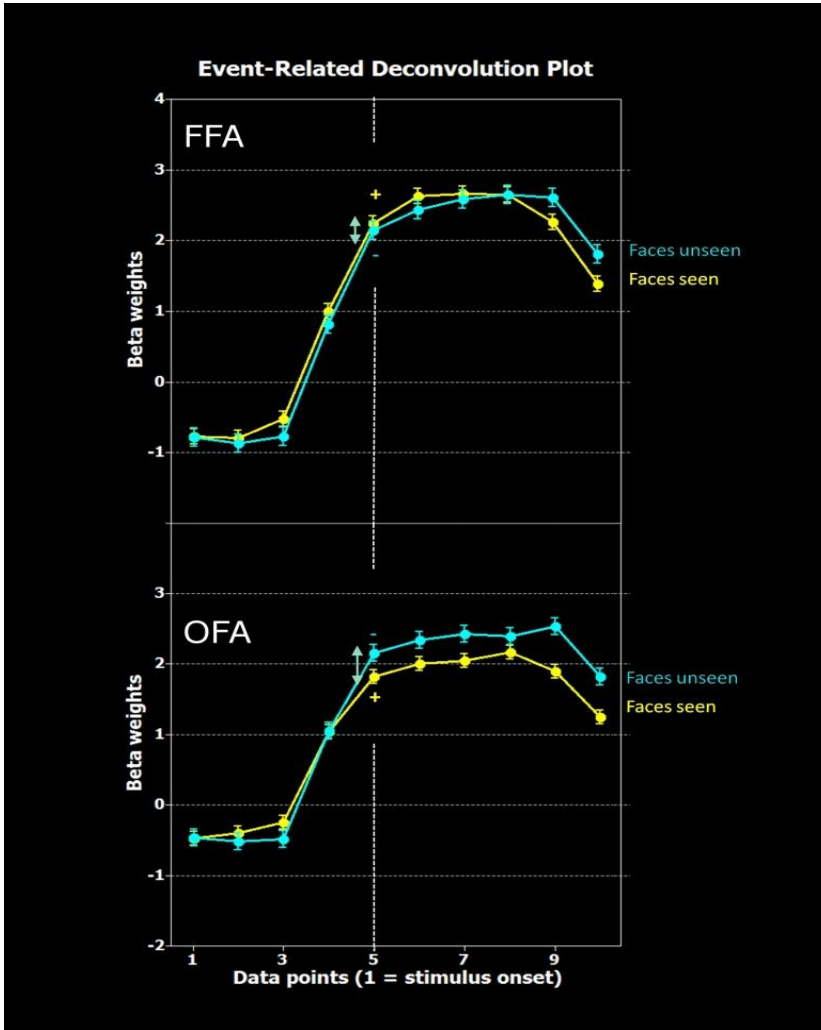
Figure 6.4 – Differences in activity between the time of perception for the 'perceived' conditions (in this case closure condition 2, i.e., faces seen from 2 to 4s.) and the same time point for the 'unperceived condition (no closure), in which a gestalt is not formed throughout the whole trial. The contrast represents how activity differs between seen and unseen content of the same category, albeit having been exposed to the stimuli for the exact same time. As in previous Figures, though only shown for condition 2 faces, this contrast is calculated across conditions 2, 3, 4 and 5, and also for the object category. The graphs show dissociation between FFA and OFA. OFA shows a pattern that matches object and scene selective regions (see text), with larger activity for

unseen faces, in contrast with FFA. These data suggest that OFA is related to the search process and FFA to the perceptual and post-perceptual mechanisms elicited by closure.

		P vs U (f)			P vs U (o)		
		t	p		t	p	
Area							
FFA		1.032	0.301		0.734	0.462	
OFA		-3.014	0.002		-3.344	0.000	
pSTS		4.095	0.000		0.569	0.569	
vLOC		-2.998	0.002		-1.455	0.145	
dLOC		-6.522	0.000		-2.596	0.009	
PPA		-3.047	0.002		1.786	0.074	
RSC		-0.662	0.508		2.086	0.036	
TOS		-2.079	0.037		1.066	0.286	

Table 6.5 – Brain activity under closure vs non-closure (perceived vs unperceived, P vs. U) for all equivalent time points as shown graphically in Figure 6.4. Values were assessed through post-hoc t contrasts for faces (f) and objects (o) (t contrasts).

In the striking cases of the OFA and dLOC, ROIs located posteriorly in the networks, BOLD activity associated with 'unperceived' stimuli is larger than the activity elicited by the perceptual intervals in the remaining conditions, for faces and objects. This effect of increased response to the unperceived content in unsuccessful search, is shown for faces in OFA is not present in FFA, and suggests an interesting functional uncoupling between these two regions.

In pSTS the inverse pattern (increased response to the perceived content) was significant specifically for faces, suggesting a particular role for this region in the face processing network. A noteworthy finding of this analysis is this dissociation between the OFA and the rest of the face-preferring network.

Regarding the scene-preferring cortex, only the PPA shows a highly significant effect and only for the face-category, being more responsive during non-closure search than perception.

Note that this last analysis compares perception closure processes to the special case of search processes that do NOT culminate in closure (unsuccessful perception).

6.4 - Discussion

We set out to study the selectivity dynamics within the face, object and scene-preferring networks using a delayed perceptual closure paradigm. This design uses a gestalt rule whereby a percept is constructed from incomplete physical information. To this end, we first localized category selective ROIs. Then, we used long presentation trials of ambiguous faces and objects images, to assess activity and selectivity dynamics prior to, during and after perceptual closure.

- The Impact of perceptual closure on ongoing brain activity

We addressed the impact of perceptual closure on ongoing BOLD activity, for each ROI, for the preferred and non-preferred categories. All category-preferring ROIs, with the exception of RSC, show a significant closure-induced increase in activity when perceiving the preferred-category (face selective regions: FFA > OFA > pSTS ; object selective regions: dLOC > vLOC ; scene selective regions: PPA > TOS). Furthermore, all of these areas also show in their BOLD activity a significant increase with perceptual closure of the non-preferred category, with the notable and relevant exceptions of the pSTS when viewing objects (showing evidence for highly specific responses to faces) and the PPA when viewing faces. This suggests a particular and opposing pattern of functional specificity in these two regions, in terms of responsiveness to face stimuli.

Apart from the two noteworthy cases described above our results are in general more in favor of a distributed vs modularized system for perceptual closure. All the remaining high-level visual areas participate in the perceptual closure of faces AND objects, thus confirming the label of category-preferring rather than truly category-selective. These findings suggest that some of the computations of these specialized modules are shared by the non-preferred categories.

As mentioned, the PPA shows a highly significant impact of perceiving objects while being unaffected by the perception of faces. Scene-selective regions were localized against faces AND objects AND scrambled images. This suggests that face processing is uncoupled from scene analysis, unlike object categories that can convey spatially invariant information used for context building and spatial relations. However, during the pre-perceptual period, the PPA is significantly engaged even by faces, which means that the ongoing computations during this phase can be advantageously used for the categorization process. Note that in the runs with face stimuli, subjects know to expect faces, and therefore the pre-perceptual activity cannot be elicited by the expectancy to see the preferred category. In turn, the failure of the pSTS to respond to object perception

points to its hypothesized role of extracting social and emotional meaning from the stimuli (Puce, Allison, Bentin, Gore, & McCarthy, 1998). Contrary to the PPA for faces, the pSTS does not deviate from baseline in the pre-perceptual period when presented with object stimuli. The strict non-responsiveness to perceptual closure in objects in contrast to faces points to an important role in the social cognition network.

- Dynamic changes in categorical selectivity induced by perceptual closure

We explicitly confirmed selectivity changes before, during and after the perceptual closure process. If the brain activity within a ROI is modulated differently to the perception of faces and objects, then an impact on selectivity should be found.

For all the face-preferring areas, the already highly significant selectivity in the pre-perceptual search period increases during the perceptual interval with a further boost in the post-closure period. A similar pattern, albeit with inverse selectivity (higher for objects than faces), is present in the scene-preferring areas, with the important observation of face perception inducing deactivation.

As for the LOC, we found spatially distinct patterns. The fusiform part, vLOC, showed a moderate trend towards higher object-related activity during search, extends this trend with perceptual closure of the content, but only reaches significance in the post-perceptual interval. In contrary, vLOC showed surprisingly significantly higher activity to faces than objects in the pre-perceptual period, a significance even widened in particular during closure.

This apparent lack of selectivity may be explained by the standard criteria to define the LOC, which simply opposes objects to scrambled objects, and thus not constraining the area's face-response. This standard way to localize "object-selective" areas influences the way selectivity is inferred, and alternative approaches are necessary. It remains to be tested whether parts of LOC

contribute to early face processing, but there might be object-specific processes worth studying that require a stricter definition of object areas, contrasting them against several sets of other stimuli. As an example of this reasoning, if we were simply to identify face areas with the contrast faces>scrambled objects (see (Ishai, 2008) but also (Wiggett & Downing, 2008)) we would see large clusters of face-responding regions which properties would be less-informative about actual face-selective mechanisms.

- Differences in brain activity under closure vs non closure (unsuccessful perception)

Our analysis of the impact of perceptual closure vs non closure at comparable time points may provide a new way to disentangle search vs. closure mechanisms. For the preferred-category, only the FFA and pSTS exhibited positive values (higher for seen faces). This means these are the only areas for which perceived activity is above its unperceived counterpart, for the same time of exposure to the stimuli. All the other areas, most notably the occipital ones, showed higher BOLD activity for the unperceived condition.

The heightened activity to stimuli that remain unperceived can be related to an increase of computations and resources, tightening the link of the OFA and other occipital areas to the search processes and pre-categorization computations. This suggests the notion that such areas privilege and process primary features necessary for classification of their preferred categories which are then fed forward to the rest of the network. A similar reasoning can be carried for the dLOC.

It is revealing to note the absence of this effect in FFA and pSTS, suggesting a fundamentally different processing nature. This reinforces the crucial role of the OFA during the analysis/search phase, where templates generated by top-down processes (Fenske, Aminoff, Gronau, & Bar, 2006) may be confronted against the demanding stimulus for a possible match.

The opposing pattern in FFA and pSTS confirms the difference in computations that may be carried in the different ROIs of the face-network, and thereby their functional dissociation, as the additional processing for seen faces may include subordinate categorical processing in the FFA or face emotional and social processing within the pSTS.

As suggested by (Atkinson & Adolphs, 2011), these findings point to an "interactive model in which higher-level face perception abilities depend on the interplay between several functionally and anatomically distinct neural regions". However, our results seem to challenge the claim that "lower-level face categorization abilities, such as discriminating faces from objects, can be achieved without OFA".

6.5 – Conclusion

We found that categorical selectivity changes before, during and after perceptual closure, suggesting that the nature of visual computations evolves across time in ventral regions as a function of perceptual demands. This dynamical view helped shed light on the relative functional properties of regions such as FFA, OFA, PPA, LOC and pSTS. By comparing perceptual closure vs. non-closure we found that OFA is dominantly recruited during demanding search and FFA after closure. The lack of selectivity for objects vs faces found in the LOC, as classically defined, calls for a revision of localizing criteria. We also found evidence for distributed computations during perceptual closure. PPA and the pSTS were notable exceptions, in the sense that they failed to be modulated, or they even deactivated, for non preferred categories. These observations suggest a link between the pSTS region, which cannot be engaged by object stimuli, and high level social face processing networks.

References

Andrews, T. J., & Schluppeck, D. (2004). Neural responses to Mooney images reveal a modular representation of faces in human visual cortex. *NeuroImage*, *21*(1), 91–98.

Atkinson, A. P., & Adolphs, R. (2011). The neuropsychology of face perception: beyond simple dissociations and functional selectivity. *Philosophical transactions of the Royal Society of London. Series B, Biological sciences*, *366*(1571), 1726–38.

Fenske, M. J., Aminoff, E., Gronau, N., & Bar, M. (2006). Top-down facilitation of visual object recognition: object-based and context-based contributions. *Progress in brain research*, *155*(4), 3–21.

Glover, G. H. (1999). Deconvolution of impulse response in event-related BOLD fMRI. *NeuroImage*, *9*(4), 416–29.

Grützner, C., Uhlhaas, P. J., Genc, E., Kohler, A., Singer, W., & Wibral, M. (2010). Neuroelectromagnetic correlates of perceptual closure processes. *The Journal of neuroscience: the official journal of the Society for Neuroscience*, *30*(24), 8342–52.

Ishai, A. (2008). Let's face it: it's a cortical network. *NeuroImage*, *40*(2), 415–9.

Jiang, F., Dricot, L., Weber, J., Righi, G., Tarr, M. J., Goebel, R., & Rossion, B. (2011). Face categorization in visual scenes may start in a higher order area of the right fusiform gyrus: evidence from dynamic visual stimulation in neuroimaging. *Journal of neurophysiology*, *106*(5), 2720–36.

McKeeff, T. J., & Tong, F. (2007). The timing of perceptual decisions for ambiguous face stimuli in the human ventral visual cortex. *Cerebral cortex (New York, N.Y.: 1991), 17*(3), 669–78.

Ploran, E. J., Nelson, S. M., Velanova, K., Donaldson, D. I., Petersen, S. E., & Wheeler, M. E. (2007). Evidence accumulation and the moment of recognition: dissociating perceptual recognition processes using fMRI. *The Journal of neuroscience: the official journal of the Society for Neuroscience, 27*(44), 11912–24.

Puce, a, Allison, T., Bentin, S., Gore, J. C., & McCarthy, G. (1998). Temporal cortex activation in humans viewing eye and mouth movements. *The Journal of neuroscience : the official journal of the Society for Neuroscience, 18*(6), 2188–99.

Rebola, J., Castelhano, J., Ferreira, C., & Castelo-Branco, M., "Functional parcellation of the operculo-insular cortex in perceptual decision-making: An fMRI study. *Neuropsychologia* (in press)

Wiggett, A. J., & Downing, P. E. (2008). The face network: overextended? (Comment on: "Let's face it: It's a cortical network" by Alumit Ishai). *NeuroImage, 40*(2), 420–422.

Chapter 7

Discussion and Conclusions

The aim of this thesis was to address methodological, clinical and cognitive neuroscience challenges with a focus on perceptual decision and categorization in the human brain and potential applications and implications for functional brain mapping in epilepsy.

Methodologically, we focused on an alternative pipeline for EEG source localization of interictal spikes. The combination of an efficient source separation algorithm (ICA) with an approach to the inverse problem that combines the advantages of high and low-resolution current density reconstructions (SSLOFO) proved an adequate solution to the problem of non-independent sources that propagate fast from site to site. Furthermore, we confirmed the clinical hypothesis of the involvement of the Frontal Lobe in Temporal Lobe Epilepsy, as suggested by previous literature. Similar approaches can be used in the surgical planning of refractive epilepsy or adapted for the investigation of other hypotheses on the pathophysiological meaning of interictal data.

A potential non-invasive tool in the course of epilepsy surgery planning and evaluation of outcome is that of brain mapping. In this procedure neuroimaging techniques are commonly used to map crucial functions to the patient and make sure that those areas will not be affected by the resection, or at least have a realistic and as accurate as possible prediction of how they will be impaired. Though more commonly used to such purpose, clinical neuroscientists are starting to use this tool to assist in the localization of the epileptic foci, in particular when combining simultaneous EEG/fMRI for functional brain mapping, which is an area where we also gathered some relevant experience (Marques et al., 2009).

The current mapping batteries are grounded on motor, language and memory tasks, and we defend that localization of high-level visual modules, such as areas dedicated to face or object processing, is an important addition that can prove informative both to foci localization and assessment of surgical outcome, in particular but not exclusively in occipital and temporal neocortex.

Accordingly, cases that would benefit the most of this inclusion are the ones of non-lesional posterior brain epilepsies, as well as rare cases of patients with visual reflex seizures not induced by flicker. Occipital and posterior temporal epilepsies are more common in pediatric cohorts, an area where our work might be of greatest clinical benefit.

Future work should include monitoring of patients throughout the whole surgical planning, procedure and outcome, for confrontation of non-invasive high-level visual brain mapping localizers with actual data from electrocorticography. Furthermore, when possible, recording electrocortigraphic data of patients carrying out the visual localizer tests will also provide answers on the cognitive neuroscience side for better pruning and validation of the category-selective network topography and characterization. This is an area of clear cross talk and benefit between basic and clinical research.

The precise localization of high-level visual areas nonetheless remains a highly debated topic. We have contributed to the elucidation of some relevant issues in this debate. Presently, the lack of homogeneity and standards in the localizer procedures hamper the interpretation of results which are at times inconsistent. Different choices of stimuli, contrasts, tasks and statistical thresholds are the reason for these discrepancies. Apart from standardization of methodology, some authors have highlighted alternative ways to minimize the subjectivity in area identification and delineation that arises from the natural anatomical variability from subject to subject. One such criterion is through the spatial relationships to other functionally-defined areas in the ventral occipitotemporal cortex. We extended this reasoning to the lateral occipitotemporal cortex and in combination with the analysis of the functional profile of responses to the non-preferred categories, we identified a region in the posterior end of the Superior Temporal Sulcus bordering the EBA which is dissociable from the classical face-preferring pSTS activation. A similar systematization of criteria should be applied in the future to the other category-preferring networks for a more objective map that helps research groups build on each other's results in a productive and incremental manner.

In addition to the bottom-up flow of information in the visual system, no characterization of an area is complete without analyzing the influence of top-down processes on its functional properties. Goal-related and cognitive control processes are known to play an important role even on lower-level areas, since the hierarchical organization of the visual system does not imply a strict feed-forward model. Feedback from higher cognitive processes is crucial, especially in conditions where exogenous sensory information is scarce. We studied the interplay between exogenous and endogenous factors with paradigms of perceptual decision-making under ambiguous conditions. These allowed us to assess the intrinsic properties of the regions, driven by the task-related constraints, and evaluate their interactions with exogenous properties, driven in a bottom up manner by the stimuli category, local features and saliency. However, to understand these interactions, a clear picture of the neural correlates of perceptual decision-making was needed. Although decision-making architectures have been proposed, the role of some of the modules, namely the insular cortex/frontal operculum was still highly controversial and elusive. We assessed the role of this cluster in decision-making and achieved a novel proposal for the functional parcellation of this anatomical complex, thereby isolating the multiple roles of the insular cortex and frontal operculum. The anterior part of the insula relates to evidence accumulation, while the middle part of the insula and adjacent frontal operculum shows a tight link to the decision signaling process. Posterior parts of this cluster participate in the planning and motor execution of the responses. This explains the disparate roles that have been assigned to the insular/opercular complex in literature. In the future, an identical approach should focus on the role of the dorsolateral prefrontal cortex, an equally important structure in the same architecture that has been regarded differently in separate studies.

Using the same paradigm, we moved from studying this sensory and cognitive hub to the characterization of its high-level visual counterparts. Extending the paradigm to include objects as well as faces, we addressed response properties to the preferred and non-preferred categories of regions within these specialized networks. By doing so, we explored, across networks, the dynamics

of selectivity with perceptual closure. We also confirmed that most specialized networks significantly contribute to the perception of the non-preferred categories, which makes them category-preferring than truly category-selective, and provides a significant challenge to the concept of specialization because it shows that information about non preferred categories is also present in areas believed to be dominated by particular categories. Our results thereby agree with the perspective presented by Haxby and colleagues (Haxby et al., 2001; Hanson, Matsuka, & Haxby, 2004) , extending it to the recruitment of specialized areas by top-down processes and not merely bottom-up feature extraction. The magnitude of such contribution reflects the extent to which the computations for the preferred category can be recruited by exemplars of the non-preferred categories. Notable exceptions to this pattern are the pSTS and the PPA, which fail to be recruited by objects and faces, respectively. In the case of the former, this exception tightens the link of this region to emotional and social processing that is inherent to the analysis of faces, and cannot be elicited by object images. Regarding the latter, the PPA is known to extract visual features from a scene than can build contextual and spatial relations for navigation within an environment. Although objects (especially large non-movable ones, that may provide spatial landmarks for navigation) can provide such information, faces typically cannot and thus do not engage this area. Intriguingly, unlike the pSTS for objects, the PPA significantly deviates from baseline during the pre-perceptual period for faces, which suggests that to some extent PPA computations can be advantageously used for face detection and categorization, an issue that may be explored in future work.

Finally, by comparing perceptual closure to non-closure (failure to reach perceptual categorization under ambiguous conditions) in the category selective regions of interest, in equivalent time points, we found subtle but significant functional dissociations. Some regions, such as the OFA and dLOC, are more involved during demanding perceptual search processes and others, such as the FFA and vLOC, during the processing that kicks in after successful categorization.

In sum, we believe that this thesis, by exploring methodological, basic cognitive neuroscience, and brain mapping issues with a potential for clinical application, has contributed to shorten the gap that still exists between fundamental and applied biomedical science.

References

Hanson, S. J., Matsuka, T., & Haxby, J. V. (2004). Combinatorial codes in ventral temporal lobe for object recognition: Haxby (2001) revisited: is there a "face" area? *NeuroImage*, *23*(1), 156–66.

Haxby, J. V., Gobbini, M. I., Furey, M. L., Ishai, A., Schouten, J. L., & Pietrini, P. (2001). Distributed and overlapping representations of faces and objects in ventral temporal cortex. *Science New York NY*, *293*(5539), 2425–2430.

Marques, J. P., Rebola, J., Figueiredo, P., Pinto, A., Sales, F., & Castelo-Branco, M. (2009). ICA decomposition of EEG signal for fMRI processing in epilepsy. *Human Brain Mapping*, *30*(9), 2986–2996.

List of publications

Peer-reviewed publications

-J. Rebola, J.Castelhano, C. Ferreira, M. Castelo-Branco, "Functional parcellation of the operculo-insular cortex in perceptual decision-making: An fMRI study. Neuropsychologia (in press)

-J.P. Marques, J. Rebola, P. Figueiredo, A. Pinto, M. Castelo-Branco, "ICA decomposition of EEG signal for fMRI processing in epilepsy.", Hum Brain Mapp. 2009, 30(9), 2986-96.

Conference Proceedings

Communications

-J. Rebola, J.P. Marques, F. Sales, M. Castelo-Branco, "Avaliação do envolvimento do lobo frontal na epilepsia do lobo temporal em EEG com um método de decomposição de dados", 19º Encontro Nacional de Epileptologia

-J. Rebola, J. Castelhano, A. Pinto, M. Castelo-Branco, "Separating the sensory, perceptual and motor components of visual decision making", Human Brain Mapping, 2010 (Trainee Abstract Award)

-J. Rebola, J. Castelhano, A. Pinto, M. Castelo-Branco, "Perceptual Decision Making: from snapshots to movies in the human brain", IBILI Meeting 2009;

Posters

-J. Rebola, M. Castelo-Branco, M. Van Asselen, "Implicit contextual learning is mediated by the basal ganglia in the healthy brain", Society for Neuroscience (2012) (accepted for nanosymposium)

-J. Rebola, J. Castelhano, A. Pinto, M. Castelo-Branco, "Face-selective patches within the Exstrastriate Body Area and LOTC ", Human Brain Mapping, 2011

-J. Rebola, J. Castelhano, A. Pinto, M. Castelo-Branco, "Separating the sensory, perceptual and motor components of visual decision making", Human Brain Mapping, 2010 (also E-Poster)

-J. Castelhano, J. Rebola, E. Rodriguez, M. Castelo-Branco, "Neural synchronization in the gamma frequency range is tightly associated with detection of ambiguous face stimuli", Human Brain Mapping 2009

-J. Rebola, J. Castelhano, A. Pinto, M. Castelo-Branco, "Beyond the Fusiform Face Area (FFA):dissection of neural circuits involved in identification of ambiguous faces", Society for Neurosciences, 2008

-J. Rebola, F. Sales, M. Castelo-Branco, J.P. Marques, "EEG source localization and timecourse reconstruction with a combined ICA-SSLOFO method: Principles and simulation", Human Brain Mapping (13), S114, 2007

-J. Rebola, F. Sales, M. Castelo-Branco, J.P. Marques, "EEG source localization and timecourse reconstruction with a combined ICA-SSLOFO method: Preliminary application in temporal lobe epilepsy", Human Brain Mapping (13), S125, 2007

-N. Raposeiro, J. Rebola, F. Sales. M. Castelo-Branco, "Análise de Geradores na Epilepsia Temporal Mesial com Dipolo Equivalente", 19º Encontro Nacional de Epileptologia

Curriculum vitae

José Rebola was born on July 10, 1982 in Coimbra, Portugal. In 1999 he completed his secondary school education at Escola Secundária de Jaime Cortesão, after which he studied Electrical and Computer Engineering at the University of Coimbra, graduating in 2004. After doing research for seven months in the Institute of Systems and Robotic of the University of Coimbra he moved to the Centre of Ophthalmology and Visual Sciences of IBILI, part of the Faculty of Medicine of the same university, where after a nine months research he started working on his Ph.D. project in February 2007.